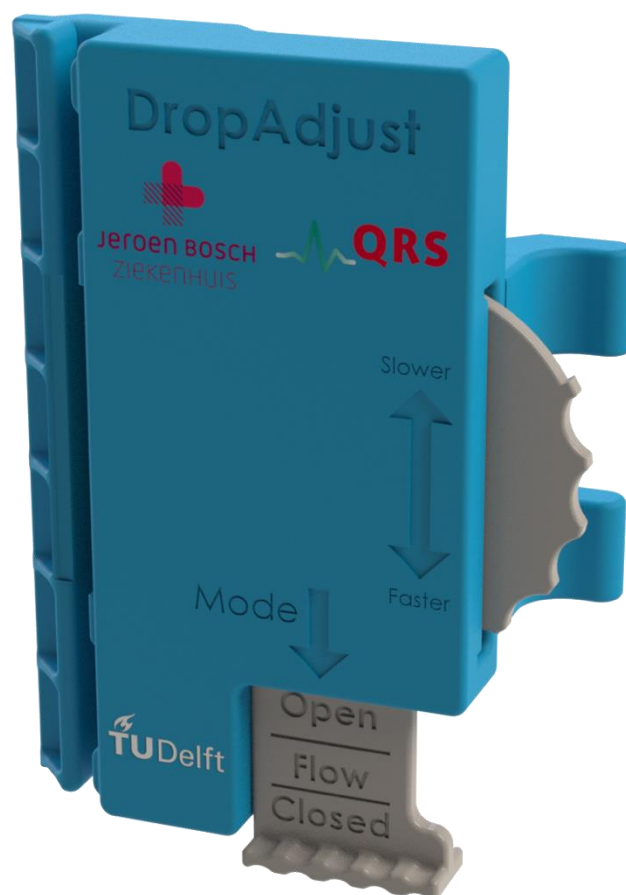


DropAdjust: infusion flow regulator

Design and development of a precise and accurate manually controlled over-line flow regulator for gravity-driven infusion.

Wouter E.C. Donders

Master of Science Thesis



DropAdjust: infusion flow regulator

Design and development of a precise and accurate manually controlled over-line flow regulator for gravity-driven infusion.

By

Wouter E.C. Donders

in partial fulfilment of the requirements for the degree of

Master of Science

in Mechanical Engineering:
BioMechanical Design (track)

at the Delft University of Technology,
to be defended publicly on the 14th of September, 2021 at 1:00 PM.

Student number:	4288025	
Supervisors:	dr. ir. A.J. Loeve, dr. ing. M. van Velzen, E. Kooijman,	TU Delft, Dept. BioMechanical Engineering Jeroen Bosch Ziekenhuis QRS
Thesis member:	prof. dr. J. Dankelman,	TU Delft, Dept. BioMechanical Engineering

An electronic version of this thesis is available at <http://repository.tudelft.nl/>.

Preface

During this project, I had the chance to apply the acquired knowledge of Mechanical Engineering and contribute to a solution for a relevant healthcare problem. The assignment provided the right balance between theory and practice, and underlined the relevance of the connection between those. This master, and even more this project, were challenging but all the more very educational. Although it was sometimes hard, also given the COVID-situation, my supervisors always kept me motivated throughout the process. I am pleased with the steps I have made and curious about the follow-up of the project.

I would like to express my gratitude to my supervisors Arjo Loeve, Marit van Velzen and Ewoud Kooijman, for granting me the opportunity to work on this exciting challenge. I also want to thank them for all the meetings, motivation, guidance and valuable feedback. Moreover, I appreciate the unparalleled accessibility of Arjo, who was always (online) available to provide quick feedback to ensure the project's continuity. Additionally, I would like to thank Jenny Dankelman for her participation in the final part of my graduation process. Furthermore, I wish to thank my roommates for their patience and support, especially in the more challenging times. In particular, I appreciate the assistance of Olivier during the entire design process. Finally, I am very grateful to my parents and family for their unconditional support and for making it possible to finish my masters.

I am looking forward to the public defence on September 14, 2021, at 1:00 PM.

Wouter Donders

Rotterdam, September 1, 2021

Abstract

Worldwide 70-90% of hospitalised patients receive intravenous infusion at some stage during their stay. In many situations, a high degree of infusion accuracy is essential as deviation from the intended dose can quickly become dangerous and moreover costly. Electronic infusion pumps provide the most accurate way of infusion, but they require programming and frequent maintenance. Furthermore, they are unsuitable for austere environments, costly, and could even become scarce in times of a pandemic. Gravity infusion combined with a drop counter could pose an interesting alternative. However, this method appears to be inaccurate over time and setting an accurate flow rate is challenging. The typically used flow regulator, a roller clamp, is the cause of these complications.

This study aimed to design and develop a precise and accurate manually controlled over-line flow regulator for gravity-driven infusion.

The design process consisted out of three design phases: analysis, synthesis and evaluation. During the analysis, the design requirements were set up. The synthesis phase consisted of generating a morphological overview and several pincher experiments. A pincher is used to clamp the tubing to regulate the flow rate. Then, promising partial solutions were selected, and through rapid prototyping, a final design and prototype were developed. In the evaluation phase, the flow regulator prototype was evaluated based on the set requirements.

The developed DropAdjust prototype demonstrated a major performance increase in terms of mean flow rate accuracy and regulation control compared to the roller clamp.

In conclusion, the DropAdjust satisfies all tested design criteria and outperformed the roller clamp in terms of accuracy and precision. Moreover, it even showed a mean flow rate accuracy error comparable to the infusion pumps. Thus, the DropAdjust combined with a drop counter provides a more affordable and accessible alternative to the infusion pumps.

The prototype is already practice-ready, but several steps are still needed to realise a market-ready device. For instance, conducting endurance tests and acquiring injection moulding advice from an experienced specialist are advised. Also, additional tests are necessary to verify its safety and functionality to qualify for a CE marking.

Nomenclature

Accuracy, closeness of the measurements to the target value

Catheter, a thin, flexible tube that is inserted into the patient

Drop counter, a device that use an optical sensor to count the drops to compute and visually display the flow rate

Drip chamber, chamber between the fluid bag and the flow regulator which provides a way to estimate the flow rate by drip counting

Gravity infusion (GI), drug administration by making use of gravity as driving force

In-line flow regulator, flow regulator which is permanently placed in the infusion lines

Infusion, delivery of a substance other than blood into the bloodstream

Intravenous (IV) administration, substance delivery into a vein

IV therapy, a medical technique to provide intravenous drug infusion (see intravenous (IV) administration)

Over-line flow regulator, flow regulator which can be placed over the infusion lines

Precise, closeness of the repeated measurements to each other

Tubing, the hollow, plastic tube between the patient and the fluid bag

Table of Contents

1	<i>Introduction.....</i>	<i>1</i>
1.1	Intravenous infusion.....	1
1.2	Thesis objective	2
2	<i>Background on gravity infusion.....</i>	<i>4</i>
2.1	Gravity infusion sets	4
2.2	Factors influencing flow rate.....	5
2.3	Factors influencing flow rate over time	6
2.4	Fluid mechanics	7
3	<i>Design analysis</i>	<i>9</i>
3.1	Methods.....	9
3.1.1	Design requirements.....	9
3.1.2	System architecture	9
3.2	Results	9
3.2.1	Design requirements.....	9
3.2.2	System architecture	10
4	<i>Design synthesis.....</i>	<i>11</i>
4.1	Methods.....	11
4.1.1	Generation of partial solutions	11
4.1.2	Evaluation of partial solutions	13
4.1.3	Selection of partial solutions	16
4.1.4	Prototyping and final design	16
4.2	Results	17
4.2.1	Generation of partial solutions	17
4.2.2	Evaluation of partial solutions	20
4.2.3	Selection of partial solutions	22
4.2.4	Prototyping and final design	24
5	<i>Design evaluation</i>	<i>27</i>
5.1	Methods.....	27
5.1.1	FEM Analysis	27
5.1.2	Validation experiments.....	27
5.1.3	Prototype evaluation	29
5.2	Results	29
5.2.1	FEM Analysis	29
5.2.2	Validation experiments.....	30
5.2.3	Prototype evaluation	32
6	<i>Discussion</i>	<i>33</i>
7	<i>Conclusion</i>	<i>36</i>
	<i>Bibliography.....</i>	<i>37</i>

<i>Appendix A – Fluid Mechanics.....</i>	<i>43</i>
<i>Appendix B – Technical Data Sheet of Volumed infusion set</i>	<i>46</i>
<i>Appendix C – Free flow rate experiment Volumed infusion set.....</i>	<i>48</i>
<i>Appendix D - SolidWorks flow simulations results</i>	<i>49</i>
<i>Appendix E - Experiments for evaluation of partial solutions</i>	<i>52</i>
<i>Appendix F - Granta Edupack 2020 material analysis</i>	<i>62</i>
<i>Appendix G - Prototyping iterations and final design.....</i>	<i>67</i>
<i>Appendix H – Technical drawings.....</i>	<i>71</i>
<i>Appendix I – Protolabs inquiry</i>	<i>77</i>
<i>Appendix J – DropAdjust pincher force experiment.....</i>	<i>84</i>
<i>Appendix K – Formlabs Grey Photopolymer Resin</i>	<i>85</i>
<i>Appendix L – Design evaluation experiments</i>	<i>86</i>

1 Introduction

1.1 Intravenous infusion

Worldwide 70-90% of hospitalised patients receive intravenous infusion at some stage during their stay [1-3]. Yearly, over one billion infusion lines are used by hospitals worldwide [2]. In many situations (e.g., critical medicine, elderly, children), a high degree of infusion accuracy is essential, as deviation from the intended dose can quickly become dangerous [4-16]. Besides the safety of the patients, medication administration errors also have a financial impact. In 2006 medication administration errors cost the USA \$380 million for the healthcare system [17]. Infusion can be done using gravity infusion (GI), volumetric infusion pumps (VIP), or syringe pumps (SP) (Figure 1).



Figure 1 – Methods of infusion. Left: gravity infusion, adopted from [18]. Middle: volumetric infusion pump, adopted from [19]. Right: syringe pump, adopted from [20].

The VIPs and SPs use electronic-driven motors to regulate the flow rate [21]. These pumps are the most accurate means for infusing fluids, with a mean flow rate accuracy error of 0.5-6% over one hour [22, 23]. However, pumps require training and programming for setting the desired flow rate, and frequent maintenance is mandatory [21]. The pumps are also less suitable for use in austere environments, where access to electrical power could be limited or unreliable [24]. Another disadvantage of pumps is the cost price of over €1800 [25, 26], above the variable cost of €1 for each infusion set [27]. This additional expense makes pumps often unavailable for low-income countries (LICs) [28]. Nevertheless, even in high-income countries (HICs), the availability of pumps could become a problem. During pandemics, like the current COVID-19, demands of infusion pumps increase significantly [29], and the first signs of scarcity appeared [30-32].

Because of these problems related to infusing fluids using pumps, GI could pose an interesting alternative in specific applications. GI uses gravity as the driving force for fluid flow. A flow regulator, typically a roller clamp [33], regulates the flow rate. The healthcare provider manually counts the drops passing the drip chamber, converts this to a flow rate, and adapts the roller clamp accordingly. GI only has the variable cost of €1 for each infusion

set [27], as the roller clamp is already included. The simplicity in usage and implementation [21, 34, 35], its great mobility, and the lack of need for electric power make it particularly suitable for austere environments and prehospital settings [36]. However, setting up and checking the GI flow rate is a slow and cumbersome process [21, 37]. Using the wrong infusion rate is moreover the most common type of medication error (40%), often caused by miscalculations of the flow rate [38, 39]. Furthermore, many studies showed that the GI method with the roller clamp is inaccurate over time [9-12, 15, 34, 37, 40-50], with a flow rate accuracy error of 23.7-60% over one hour [37, 49, 51]. Because of this low accuracy, frequent manual checks and adjustments are necessary [52, 53].

A solution for the above-described downsides of GI could be a drop counter, like the Monidrop [56] or DripAssist [57] (Figure 2). These devices use an optical sensor to count the drops to compute and visually display the flow rate. Additionally, alarms can be set to alert healthcare providers when the flow rate becomes out of the prescribed range. Couperus et al. showed that healthcare providers from various levels rate the DripAssist as easier to use than manually counting the drops [6]. Buonora found improvements in flow rate setting speed, drop counting accuracy, and monitoring [24]. The prices range from €290-€330 for the DripAssist [6, 24] and €495 for the Monidrop [51].

The downsides of the GI method remaining unresolved with the drop counters are the inaccuracy over time and the difficulty of accurately setting the desired flow rate. These problems are mainly caused by the roller clamp's regulation step size and inaccuracy over time [10, 49]. Recent unpublished reports from Lie et al. showed that using the Monidrop with a regular roller clamp indeed did not improve the accuracy error over time [51].



Figure 2 – Drop counters. Left: Monidrop, adopted from [54]. Right: DripAssist, adopted from [55].

Problem statement

The use of GI combined with a drop counter, like the Monidrop or DripAssist, could provide several benefits over infusion pumps. However:

“A manual flow regulator which is more accurate and has a finer regulation step size than the typically used roller clamp is needed to use drop counters, like the Monidrop or DripAssist, to their full potential.”

1.2 Thesis objective

The way the problem was approached is illustrated and described in Figure 3. The nine steps mentioned in this engineering process model were grouped into three design phases: analysis, synthesis and evaluation [58]. The analysis phase is covered in Chapters 1, 2 and 3.

The synthesis phase is discussed in Chapter 4, and lastly, the evaluation phase is covered in Chapters 5, 6 and 7.

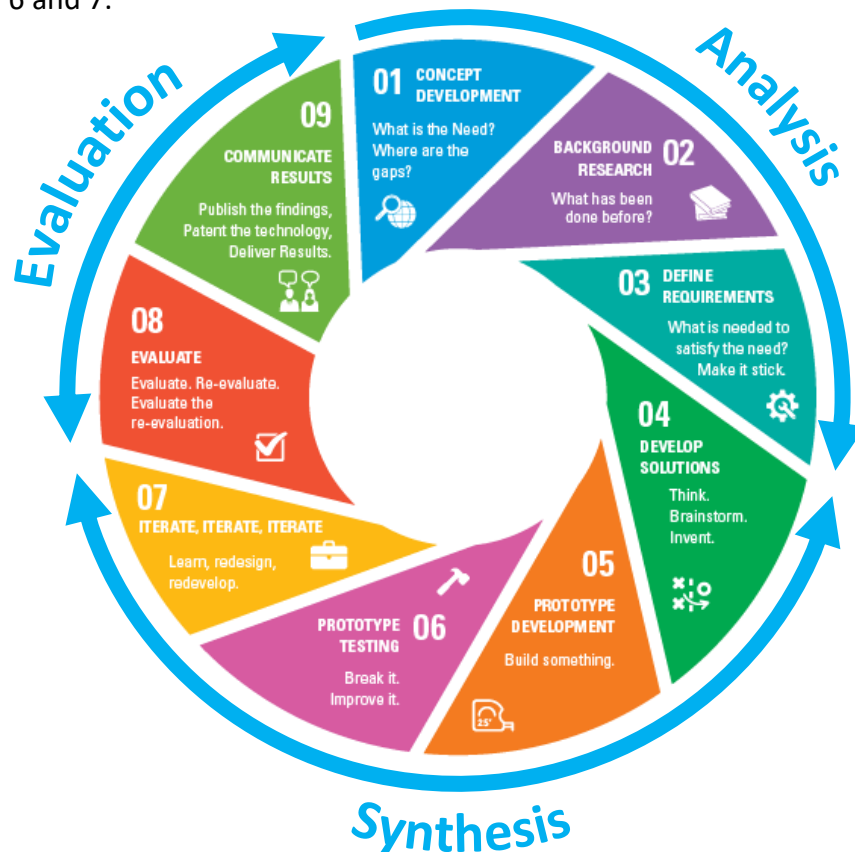


Figure 3 - Engineering Process Model and the three iterative design phases: analysis, synthesis and evaluation. Adapted from [59].

Prior to this thesis, a literature research was conducted [60], covering the first two steps and partly the third step of the analysis phase. This research provided the needed background information and helped to identify the actual research gap: there is a need for a precise and accurate flow regulator variant. This research gap provided the following thesis objective:

“Design and develop a precise and accurate manually controlled over-line flow regulator for gravity-driven infusion.”

2 Background on gravity infusion

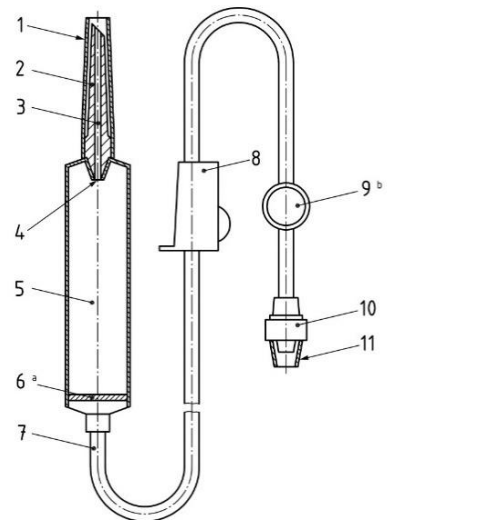
2.1 Gravity infusion sets

Gravity infusion uses hydrostatic pressure drop to generate a fluid flow by creating a height difference between the fluid bag and the patient. A gravity infusion set is placed in between the fluid bag and the patient-inserted catheter. The standardised gravity infusion set is described in ISO 8536-4 by the International Organization for Standardization [61] (Figure 4).

The drip chamber (5) is directly inserted into a fluid bag. Fluid will come in through the fluid channel and enter the transparent drip chamber. By visually counting the number of fluid drops over time, healthcare providers can calculate the flow rate and adjust the flow regulator accordingly. There are two different types of drip chambers: macrodrip and microdrip. Macrodrip chambers provide 20 drops per millilitre, and microdrip chambers provide 60 drops per millilitre [21].

The hollow tubing (7) is made of flexible, transparent material to provide the opportunity to detect possible gas bubbles. Typically plasticised (soft) PVC is used as the material [62-64].

A flow regulator (8) is placed in between the drip chamber and the patient to regulate the fluid flow. Typically, a roller clamp (Figure 5) is used [33] in standard infusion sets. The roller clamp consists of a housing (yellow) and a roller wheel (white). The tube is placed between the housing and the wheel. By rolling the wheel towards the tube, the pressure drop is regulated. A more detailed explanation of how this pressure drop is realised is provided in Section 2.4. The flow rate depends on this pressure drop. The sensitivity of the roller clamp is emphasised by Flack & Whyte [44]. They found that for a range of 0-30 drops/min (90mL/h), a change in obstruction diameter of only 0.0076 cm and high forces are required. The reason for these needed high forces is illustrated in Figure 6: when the middle part is closed, two small



Key

- | | |
|--|---|
| 1 protective cap of closure-piercing device | 7 tubing |
| 2 closure-piercing device | 8 flow regulator |
| 3 fluid channel | 9 injection site |
| 4 drip tube | 10 male conical fitting |
| 5 drip chamber | 11 protective cap of the male conical fitting |
| 6 fluid filter | |
| a The fluid filter may be positioned at other sites, preferably near the patient access. | |
| b The injection site is optional. | |

Figure 4 – Gravity infusion set described by the International Organization for Standardization. Adopted from [61].

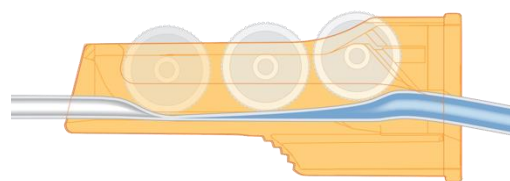


Figure 5 – Section view of a roller clamp where the roller (white) moves from open (right) to a closed (left) position. Adopted from [65].

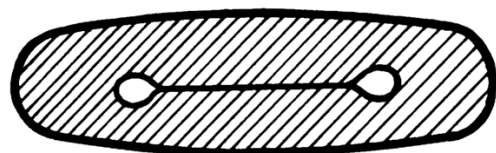


Figure 6 – Cross-section view of a tube clamped by a roller clamp. Adopted from [44].

openings remain. To also close these narrow openings the whole tube needs to be squeezed together, so higher forces are required.

To validate the findings of Flack & Whyte, a SolidWorks [66] non-linear Finite Element Analysis (FEA) for a similar setup was conducted using a hyperelastic Blatz-Ko model [67]. The results indeed confirm the claims of Flack & Whyte (Figure 7).

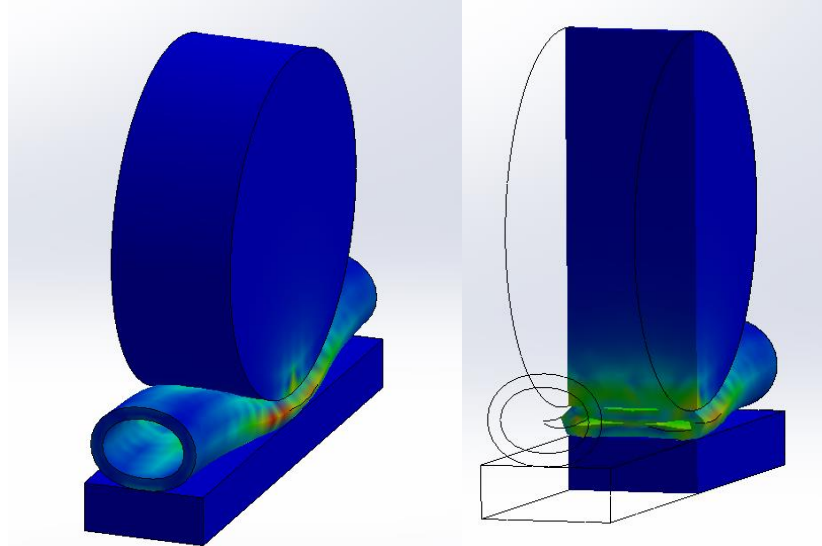


Figure 7 – Results of the SolidWorks [66] non-linear study for clamping a plasticised (flexible) PVC tube using an ABS wheel. The colours indicate the amount of stress relative to other sections, where red is the highest and blue is the lowest. Left: full view of simulation results, right: section view of simulation results.

2.2 Factors influencing flow rate

Using Hagen-Poiseuille's equations and assuming laminar flow, Steenhoek derived Equation 1 for the flow rate Q in the tube [m^3/s] [9]. This equation holds for a tube with a constant cross-section and using an incompressible fluid [68].

$$Q = \frac{\pi * \Delta p * D^4}{128 * \mu * L} \quad \text{Equation 1}$$

D is the tubing inner diameter [m], μ is the fluid's dynamic viscosity [$\text{Pa}\cdot\text{s}$], and L is the tubing length [m]. Δp is the pressure drop [Pa] over the infusion set and is computed as shown in Equation 2.

$$\Delta p = \rho * g * \Delta h - p_{\text{venous}} \quad \text{Equation 2}$$

ρ is the fluid's specific mass [g/cm^3]. The influence of this specific mass is typically opposed by a rise of the dynamic viscosity [40]. Because the increase of dynamic viscosity usually dominates, the flow rate generally decreases with increasing specific mass. g is the gravitational acceleration [m/s^2]. The venous pressure p_{venous} [Pa] depends on the patient's injection site [9] and the body position [44]. Δh is the bag-cannula height difference [m], so the difference between the fluid bag level and the site of injection of the patient. This Δh is the gravity infusion's driving force.

2.3 Factors influencing flow rate over time

Unfortunately, not all the parameters mentioned above are constant over time, resulting in an inaccurate flow rate over time for gravity infusion. Table 1 shows these time-sensitive parameters.

Table 1 – The flow rate parameters that are changing over time and their cause.

Parameters	Affected by
Venous pressure p_{venous}	<ul style="list-style-type: none"> • Body posture [44, 46] • Coughing, breathing rate and depth [44, 46]
Bag-cannula height difference Δh	<ul style="list-style-type: none"> • Infusion bag deflation [45, 49] • Body posture [12]
Tubing inner diameter D	<ul style="list-style-type: none"> • Creep (also known as cold flow) of the tube [37, 43-45, 49]

Creep

Most of the mentioned parameters of Table 1 are inherent to the method of gravity-driven infusion and difficult to control using an over-line regulator. A parameter that could be influenced is the creep of the plastic tubing. This creep results in an undesirable flow rate decrease over time.

Creep is a phenomenon where the material slowly deforms over time when a constant, below yield strength load is applied. So, this creep deformation is above load dependant, also time-dependent. Furthermore, creep is strongly temperature dependant; creep increases exponentially with temperature [69]. Creep occurs when the material approaches its melting point [70], which is not the case at room temperature for most materials. However, crystalline polymers with melting temperatures of 150-200°C tend to slowly creep when loaded at room temperature. The same holds for glassy (amorphous) polymers with a glass transition temperature of 50-150°C. For metals, creep becomes apparent when exceeding a temperature of $0.35 * T_m$, where T_m is the melting temperature [69]. Ceramics start creeping when approaching $0.45 * T_m$.

Creep is divided into three stages: primary creep, secondary creep and tertiary creep (Figure 8). Primary creep increases quickly but exists only for a short period of time. The secondary creep is seen as the steady-state creep, because of its constant strain rate $\dot{\epsilon}_{ss}$. At the tertiary creep stage, the creep rate increases exponentially until rupture. Metals, polymers and ceramics follow these stages when creep occurs, but the exact shape differs per material. Empirical data is needed for each specific material to compose the concerning creep curve.

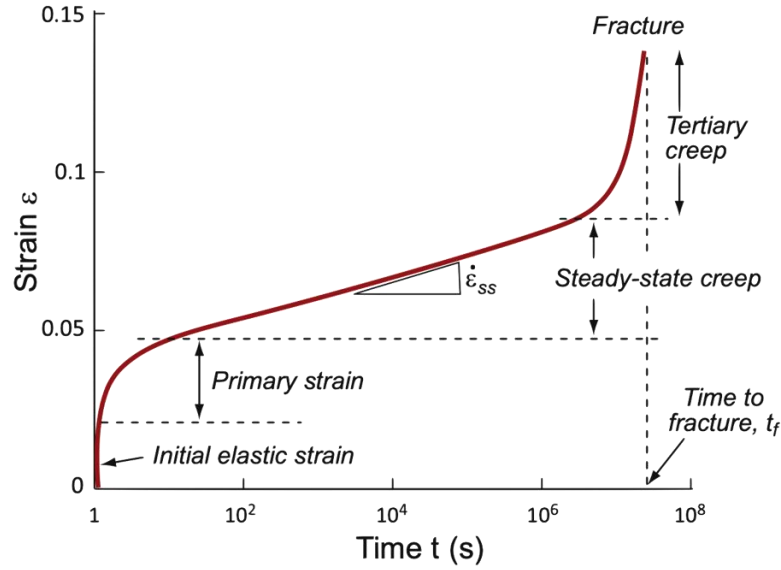


Figure 8 – Typical creep curve for a material at constant load and temperature. $\dot{\epsilon}_{ss}$ is the steady-state creep rate. The stages are explained in the text. Adapted from [69].

The above theory on creep confirms the findings of researchers testing the tubing sets [37, 43-45, 49]. Most of this creep occurs in the first fifteen minutes [45], corresponding to the primary creep stage. In addition, the amount of flow rate deviation over time when compressing a tube is indeed strongly temperature-dependent [44]. In theory, also creep of the plastic roller clamp itself could be of influence. This impact was researched by Flack & Whyte, and they claim it to be negligible in practice [44]. However, to check their claim, experiments are described in Section 4.1.2.

2.4 Fluid mechanics

Steenhoek explains the flow rate regulation with the pincher through Equation 1 [9]: by pinching the tube, the diameter decreases and a lower flow rate establishes. However, this equation was made under the assumption of constant cross-section. Consequently, his reasoning only holds if the diameter of the entire tubing length decreases. This is not the case as only an estimated 2mm [71] of the (minimal) 1.5m tubing [61] is pinched.

Interestingly, when ignoring the friction and minor losses, a contraction would not even affect the volume flow rate at all. As according to Bernoulli [68], the flow velocity increases at the contraction; one would also, wrongly, expect an increase in volume flow rate. Nevertheless, as the cross-sectional area also decreases proportionally, the volume flow rate stays constant. This is endorsed with the use of a simplification of the pinching configuration (Figure 9). As conservation of mass holds [68], Equation 3 applies here. Thus, the volume flow rate must be the same at each section of the tubing.

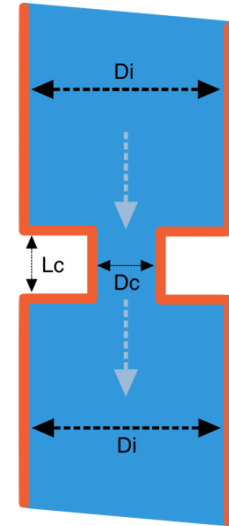


Figure 9 – Simplification of the pinching configuration with inner diameter D_i , contraction diameter D_c and contraction width L_c .

$$Q = V_1 * A_1 = V_2 * A_2 = V_3 * A_3$$

Equation 3

Where V is the flow velocity, A is the cross-sectional area, and Q is the volume flow rate. Some assumptions are: steady flow; one-dimensional inlets and outlets; incompressible fluid (density constant); subsonic flow; and no (friction) losses.

The presence of friction (major) and minor losses in the actual tubing is why compressing the tube reduces the flow rate. This reduction is due to the additional friction (Moody) losses at the elevated flow velocities at its contraction [68]. The Moody-type friction losses due to the viscosity of the fluid exist in the entire tube. However, as the friction in the tubing is velocity-dependent, the increase in flow velocity at the contraction causes added friction losses. These additional friction losses result in a decrease in volume flow rate [68].

The longer the pinched section, the larger the extra friction losses. Thus, the volume flow rate decrease depends on the width as well as the depth of the contraction. Appendix A can be consulted for a more detailed explanation and corresponding computations.

The transition between the inner diameter D_i and contraction diameter D_c of Figure 9 is greatly exaggerated. Nevertheless, even in this case, the minor losses due to this sudden contraction and expansion can be neglected compared to the friction losses (see computations Appendix A).

3 Design analysis

3.1 Methods

3.1.1 Design requirements

To manufacture and distribute the flow regulator in Europe, it has to comply with the European Union Medical Device Regulation (EU MDR) 2017/745 [72]. Over-line flow regulators are classified as risk class IIa: low to medium risk. To comply with the EU MDR requirements and receive the obligatory CE marking, the producer of the flow regulator needs to verify its safety and functionality. This verification can be done by meeting the designated ISO 8536-14 standard requirements for flow regulators without fluid contact [33].

ISO 8536-14 distinguishes clamps for on/off-function and a flow regulator to control the fluid flow. It is desired to satisfy both the clamp and flow regulator requirements of the standard to make the improved flow regulator even more versatile.

Besides complying with the ISO 8536-14, additional design requirements were set up founded on insights from the priorly conducted literature research [60] and meetings with user's delegates.

3.1.2 System architecture

Based on the earlier set requirements, a system architecture of the desired flow regulator was set up. This architecture is an overview of what features the flow regulator should have and which component is responsible for this.

3.2 Results

3.2.1 Design requirements

The entire list of design criteria is shown in Table 2. The target performance for each requirement is also stated and concisely explained. In Section 5, these criteria were also used to evaluate the performance of the developed design.

Table 2 – Design requirements for an improved manually controlled flow regulator for gravity-driven infusion.

Criterion	Value	Reason
Mean flow rate accuracy error over one hour without prior settling	$\leq 23.7\%$	Better than most accurate roller clamp [51] found in the priorly conducted literature research [60].
Flow rate deviation over 6 hours after 15 min settling time	$< 10\%$	To comply with the A.2 flow regulator test of ISO 8536-14 [33].
Fine regulation step size possible	$\leq 1\%$ of desired flow rate	This way it, is easier to set the correct desired flow rate. The minimum needed step size is depending on the prescribed flow rate.
Cost price	$\leq \text{€}50,-$	Competitive price compared to its accuracy. Furthermore, because it is reusable, the long-term costs are lower.
User-friendly	-	Easy and intuitive to operate.
Compatibility range of external tubing diameters	3.0-4.5 mm	To comply with flow regulator requirement of ISO 8536-14 (6.1) [33].

Safe in use and no puncture or damage to the flexible tubing	-	To comply with flow regulator requirement of ISO 8536-14 (4) [33]. This includes, as little as possible exterior moving components are used, and fluid spillage cannot enter the mechanism.
Number of needed movements of subcomponents to disconnect the flow regulator	≤ 2	To comply with clamp requirements of ISO 8536-14 (6.3) [33].
Number of movements of subcomponents in a single plane to lock the flow regulator's position	≤ 1	To comply with clamp requirements of ISO 8536-14 (6.3) [33].
Modular prototypes, but end product impossible to disassemble by customers	-	Easy to (dis)assemble for design iterations. However, the customers should not be able to take apart the end product.
Compatible with the Monidrop [73]	-	To achieve the full potential of both the Monidrop and improved flow regulator.
Open-close time	≤ 2 s	It needs to be possible to quickly open or close the flow regulator.
Maximum dimensions	$\leq 15 \times 10 \times 5$ cm	A balance between providing design freedom but still maintaining mobility.
No line modifications are necessary	-	No direct fluid contact, so no sterile issues and can be used multiple times. Besides the financial benefits, this is also more sustainable. Furthermore, it is compatible with all infusion lines and not depending on a preassembled infusion set.

3.2.2 System architecture

In Figure 10, the system architecture can be found. The flow regulator was subdivided into two main components: the regulation mechanism and the housing. Each component has its own features and function.

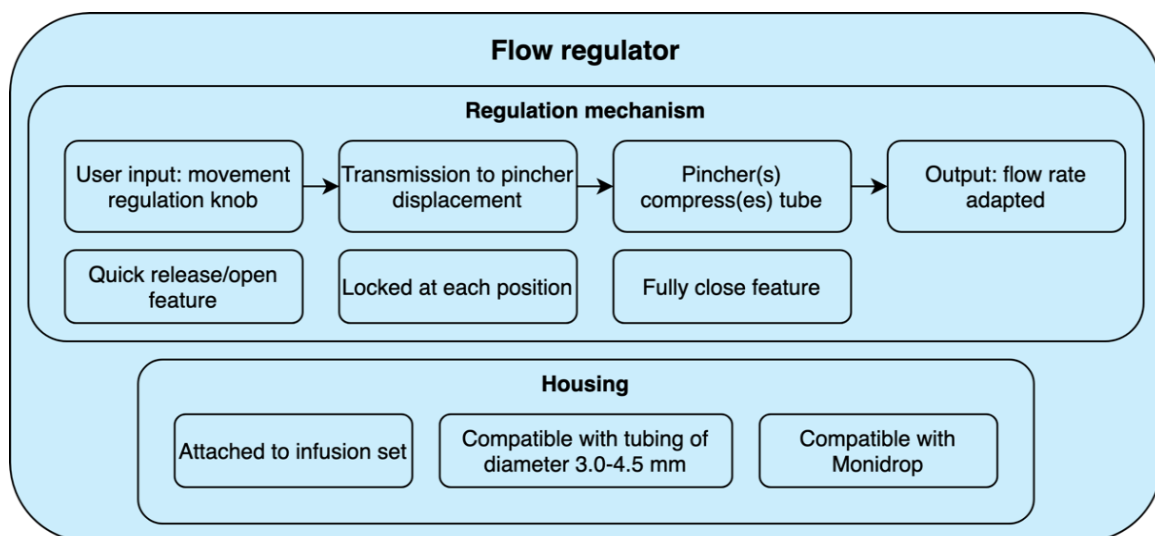


Figure 10 – System Architecture of the flow regulator. The essential features were assigned to two separate components: regulation mechanism and housing.

4 Design synthesis

A design framework was set up to approach the design synthesis phase in a structured way (Figure 11). This framework consists of multiple process steps: generation, evaluation and selection of partial solutions, and to conclude prototyping. Each process step has its own result, or 'product', which was input for the next step.

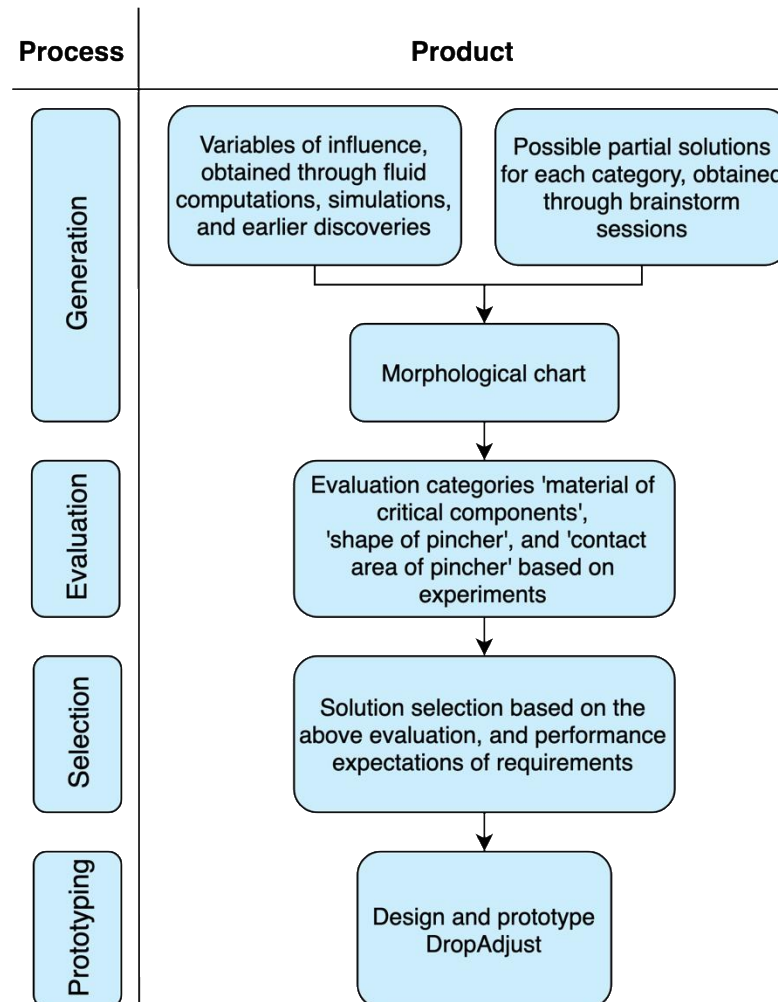


Figure 11 – Design framework of synthesis phase. For each process step the product is mentioned.

4.1 Methods

4.1.1 Generation of partial solutions

Different categories were created to comply with the set feature requirements, as provided in the system architecture. These categories are components or properties to consider and for which various possible partial solutions were generated. The corresponding possible partial solutions for the categories were then merged into one morphological overview. Most of the categories and partial solutions were established during multiple brainstorm sessions and based on knowledge acquired from literature. The categories mentioned below, in bold headlines, were generated through computations or earlier discoveries.

Material of critical components

As mentioned in Section 2.3, the creep of the tubing is one of the main factors influencing the flow rate over time. The tube's material is fixed, but there is design freedom regarding the flow regulator's material. Flack & Whyte claim that the influence of this regulator's material is negligible in practice [44]. However, new tests were done given the lack of detailed experiment setup and experimental data to support the claim. So, by setting a minimum melting and glass temperature, different materials can be chosen which do not tend to creep at room temperature ($\approx 21^\circ\text{C}$). Besides avoiding creep, properties as price, stiffness, strength and density were also considered in this analysis. The provisional material selection was made with the use of Granta Edupack 2020 [74]. For each of the three major material classes (polymers, metals and ceramics) [69], one or two high potential materials were chosen to include. This material analysis was meant for all components where the high stresses occur due to squeezing the tube and therefore is prone to creep.

Shape of pincher

Section 2.4 already showed that the flow rate depends on the width and depth of the contraction. Fluid mechanic computations were carried out to examine if this pincher's width also influences the precision of regulation. The model for pinching the tube was found on multiple assumptions and simplifications (Figure 9). This model was based on the experiment setup of Section 4.1.2 and Section 5.1.2, and the Volumed infusion set (Appendix B). Due to space limitations, this infusion set was shortened to 1.5m. The free flow rate (without pinching) was measured in Appendix C and set at 19,000 mL/h. The flow was assumed to be at steady state (fully developed) and laminar.

Furthermore, the pinching was assumed to create a circular constriction at the centre of a round pipe of inner diameter D_i . In practice, pinching the tube will however change the constriction's shape (Section 2.1). Nevertheless, the exact behaviour is hard to predict and implement in a simple model for fluid mechanic calculations. As it is just to show the influence of specific variables, for now, this simplification suffices. The fluid mechanic calculations can be found in Appendix A.

Besides the fluid mechanic calculations, several finite element analyses (FEA's) were performed to confirm the earlier findings. The FEA's were made by using the internal Flow Simulation add-in of SolidWorks [66].

A model of the tubing (Appendix B) was created using the provided material and dimensions. A tubing of 150mm was used instead of 1500mm to reduce the simulation time of the flow simulation. Figure 12 shows the model for one pinching area. First, the free flow rate of 19,000 mL/h was imposed without pinching ($D_c=D_i$) to find the pressure drop over this shortened tubing part. Then, the measured pressure drop was used as input for the difference between the inlet and outlet. Subsequently, using a parametric study, the pinching diameter D_c was varied in 14 steps. The flow rate data at each stage was then imported into MATLAB [75] (Appendix D) for visualisation of the data. This process was repeated for four different pinching widths $L_c=10$ mm, $L_c=20$ mm, $L_c=40$ mm, $L_c=80$ mm. One simulation stage is presented in Figure 13 to provide some insight in the SolidWorks flow simulation.

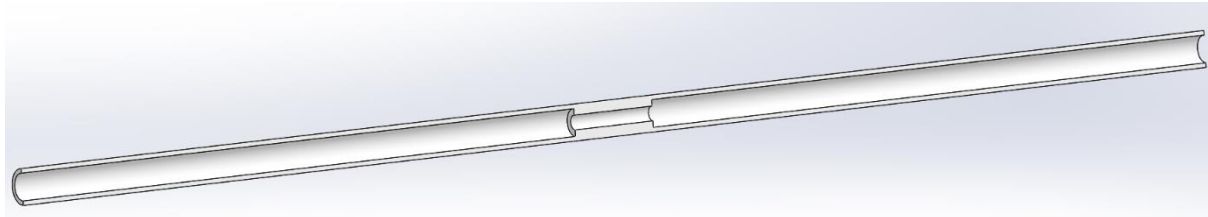


Figure 12 – Section view of the 150mm long 3x4.1 mm PVC tubing model with one pinching area. Created with SolidWorks [66].

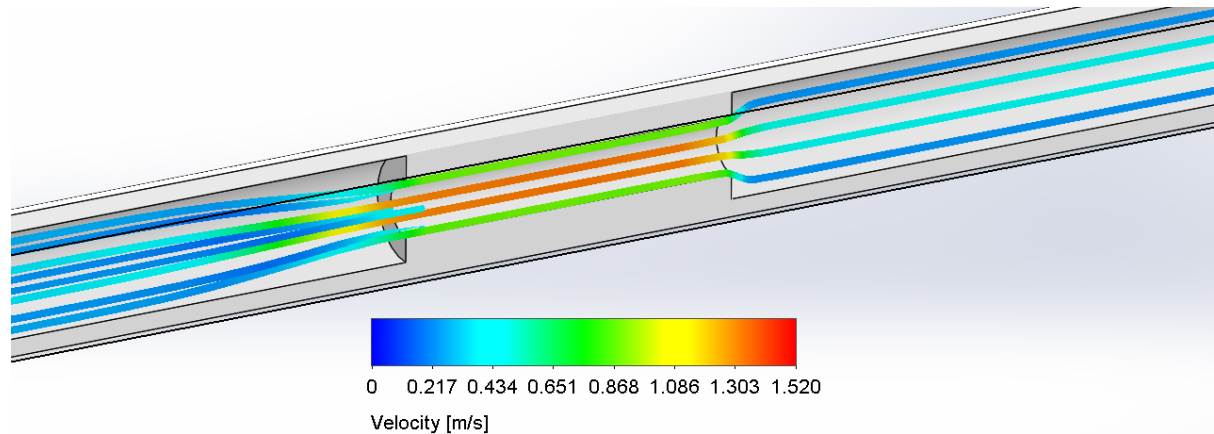


Figure 13 - Close-up section view of a flow simulation for the model of Figure 12 for pinching diameter $D_i=1.6$ mm. The colours indicate the fluid velocity [m/s], and the legend is shown below the model. Created with SolidWorks [66].

Two additional models were created to predict the influence of multiple pinching areas on the flow rate. One model existed of two pinching areas of width $L_c=5$ mm, simulated with a 10 mm and 40 mm distance in between. The other model existed of three pinching areas of $L_c=3.33$ mm with a 40 mm space in between. These models were again simulated for 14 different pinching diameters D_c using a parametric study. The section views of these two models and flow simulations can be found in Appendix D.

Contact area of pincher

During the priorly conducted literature research [60], an overview of over-line flow regulators was created. In this overview, one over-line flow regulator stood out in terms of flow rate accuracy over time. The Adelberg roller clamp showed a 3-10% flow rate accuracy error over one hour [37, 40] against 23.7-60% of the conventional roller clamps [37, 49, 51]. Because of the clamp's ingenuities multiple patents were granted [76-79]. These patents and research articles were analysed, and insights were gained into possible reasons for its standout performance. Based on this analysis, potential configurations are suggested.

4.1.2 Evaluation of partial solutions

The material of the critical components and the configuration of the pincher seems to be of influence on the performance of the pincher (Section 4.2.2). However, several assumptions were made at setting up these calculations and simulations. Experiments were conducted to check these relations in practice before selecting the partial solutions for the design.

The experiment setup is shown in Figure 14 and 15. Conform ISO 8536-4 (purified) water was used for testing [61]. The water flows from the reservoir (A) through the ball valve (C) into the infusion set with the Monidrop attached (D). A linear stage, with a



Figure 14 – Pinching setup. The setup existed of a Thorlabs PT1/M linear stage [80] (black) mounted on a configuration of aluminium extrusion profiles combined with connection elements (grey). The infusion line (transparent) was clamped in between the vertical profile and the pincher (white) with a load cell (red). This Futek LSB200 S-Beam jr. 2.0 111N [81] load cell was mounted on the linear stage.

calibrated load cell attached, variably pinched the tube and thus controlled the flow rate. The pincher used to clamp the infusion line differed per experiment. The fluid flows from the infusion set in the measuring cup, placed on another calibrated load cell. That load cell acted as a scale to measure the fluid volume. The millivolt analogue signals of both the 4.5N [82] and 111N [81] load cell were amplified by an analogue signal conditioner [83]. This amplifier was connected to an analogue-to-digital converter [84] to load the signals to LabVIEW 2018 [85] on a laptop (Dell Latitude 5570 [86]). By converting the voltage of the 4.5N load cell to a force, the flow volume was computed. Because the flow was dripping into the measuring cup, this data consisted of repeatedly high peaks that settled afterwards. However, there was a clear overall trendline in the increase of the volume. A polynomial was fitted to obtain this trendline. Using the elapsed time also the flow rate [mL/h] was found. MATLAB [75] was used for this data processing. The Monidrop was consulted for the initial flow rate setting and as an extra check if the 4.5N load cell (G) values were reasonable.

During the experiments, a total of 28 runs were performed. The specific experiments are concisely explained below (see Appendix E for the extensive experiment method, setup, list of materials, and measurement protocols).

Material experiment

A plastic- and steel pincher with equal dimensions (Figure 16) were tested and compared to verify whether the material choice indeed influences the flow rate accuracy over time. As steel is more creep-resistant than plastics (Appendix F), an improved mean flow rate accuracy over time was expected. During the experiment, the flow rate was initially set at 100 mL/h with the help of the Monidrop [87]. Then, the flow rate was recorded for 60 minutes. This experiment was repeated four times for both pinchers.

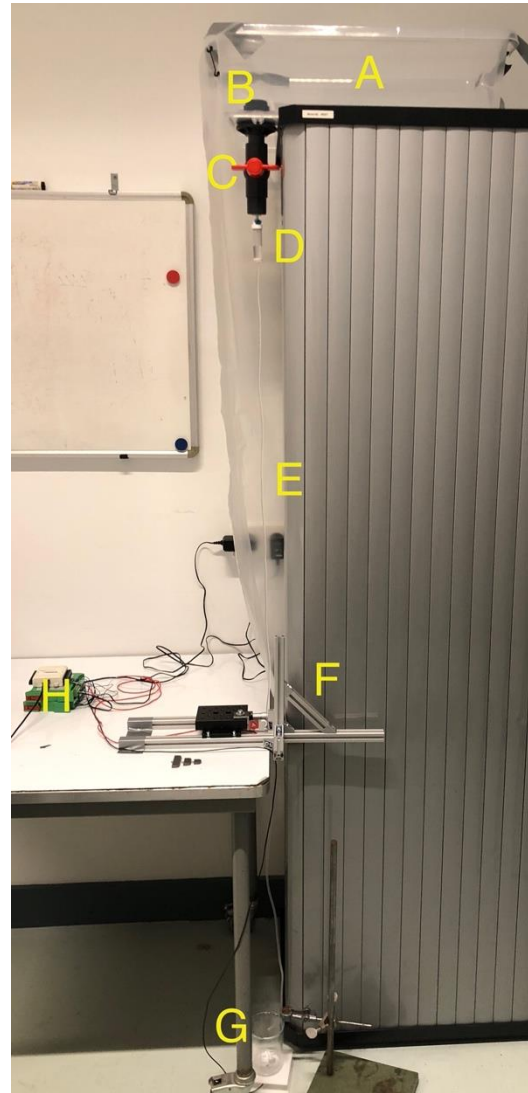


Figure 15 – Experiment setup. A: water reservoir, B: PVC flange feedthrough, C: PVC ball valve, D: drip chamber and optional Monidrop, E: tubing, F: pinching setup (Figure 14), G: measuring cup on a Futek LSB200 S-Beam jr. 4.5N load cell [82], H: Scaime CPJ Rail amplifier [83] and National Instruments NI USB-6008 converter [84].

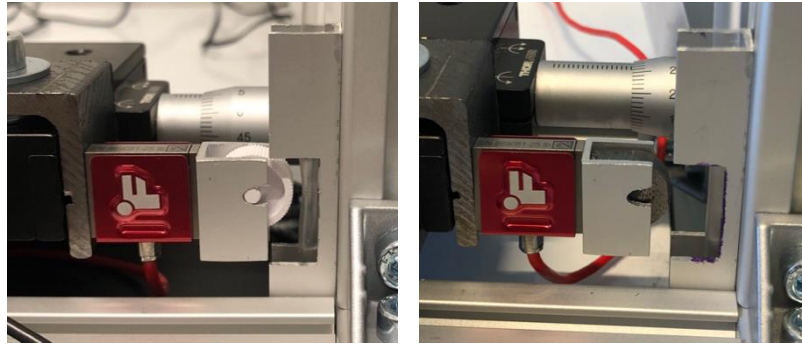


Figure 16 – Material experiment pinchers. Left: 14mm wide plastic pincher, right: 14mm diameter steel pincher. Both pinchers have the same rounding radius.

Shape experiments

The pincher's shape was expected to affect the regulation control. Based on the earlier findings (Section 4.2.2), three different steel pinchers were tested: a 14mm wide pincher (Figure 16 right), a 44mm wide pincher (Figure 18 left), and a pincher that combines two 14mm wide pinchers with a 14mm distance in between (Figure 18 right). The smallest pincher was expected to provide the least gradual flow control and the lowest pinching force. During the experiment, the pincher was moved 0.01mm away from a closed tube, and the fluid volume was recorded for 30-seconds subsequently to obtain a reliable flow rate. This process was repeated until the measuring cup was full.

An additional experiment was arranged to investigate whether a wider pincher also causes an increased flow rate deviation over time. Because, an increased pinching force was expected for a wider pincher, and creep is load-dependant. However, since this pinching force is also distributed over an increased area, it induces smaller stress peaks. The method and measurement protocol were equal to those used in the material experiment, except that now the 44mm wide steel pincher was used.

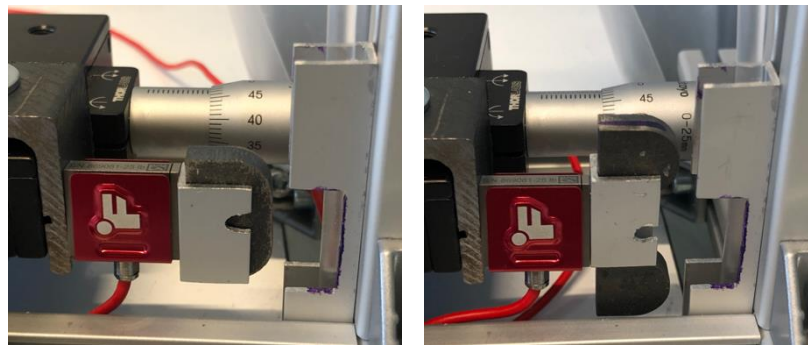


Figure 18 – Shape experiment 1 pinchers. Left: 44mm wide steel pincher. Right: double 14mm wide pinchers with a 14mm distance in between. Both pinchers have the same rounding radius.

Contact area experiment

As the Adelberg's European patents are expired [88], the tapered groove shows up in roller clamps of several other brands. The roller clamp, as described in Appendix B, also contains this feature (Figure 17). The material experiment was repeated to investigate the degree of influence of this feature, but now using this roller clamp instead of the pinching setup (Figure 14). The same plastic wheel was exactly the same as used during the material experiment.

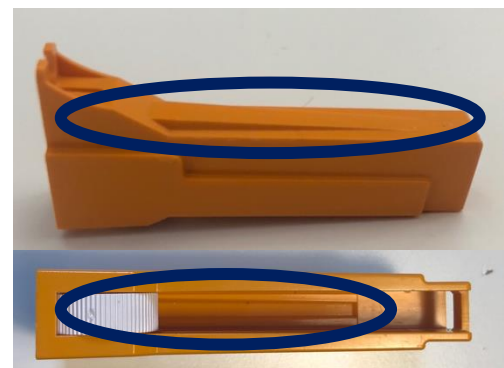


Figure 17 – Contact area experiment. Plastic roller clamp. The blue ellipse indicates the tapered groove.

4.1.3 Selection of partial solutions

Every category of the morphological chart (Section 4.2.1) is independent of partial solution choices made for other categories. For this reason, the partial solution with the most potential was chosen for each particular category. The choices were based on the results of the evaluation of the partial solutions above, and the expected performance of the applicable design requirements.

4.1.4 Prototyping and final design

The selected partial solutions were combined into one all-encompassing embodiment: the final design. A 3D computer-aided-design (CAD) model was created using SolidWorks 2020 [66], and renders were made using the Visualize plug-in [89]. Many potential (practical) complications were already solved during this creation, before they would manifest themselves in the actual prototype. However, some issues only emerge when actually building the prototype. For this reason, rapid prototyping using fused deposition modelling (FDM) was used to quickly verify relevant properties as form, fit, and function of the design at an early stage. This allowed fast building, reviewing, and iteratively refining the design.

During these iteration steps, design recommendations for plastic injection moulding [90-94] were already considered. In this manner, most potential defects at injection moulding (and consequently increased designing costs) are prevented. The most relevant aspects taken into account were:

- Smooth transition between features, through fillets or chamfers
- Constant wall thickness and less than or equal to 3mm for most materials
- Undercuts (Figure 19) should be avoided, as these require additional actions and therefore costs during moulding
- Ribs and gussets for reinforcement: recommended dimensions are shown in Figure 20
- Fillets on adjoining walls: recommended dimensions are shown in Figure 20



Figure 19 – A snap-fit which causes an undercut (hatched area).

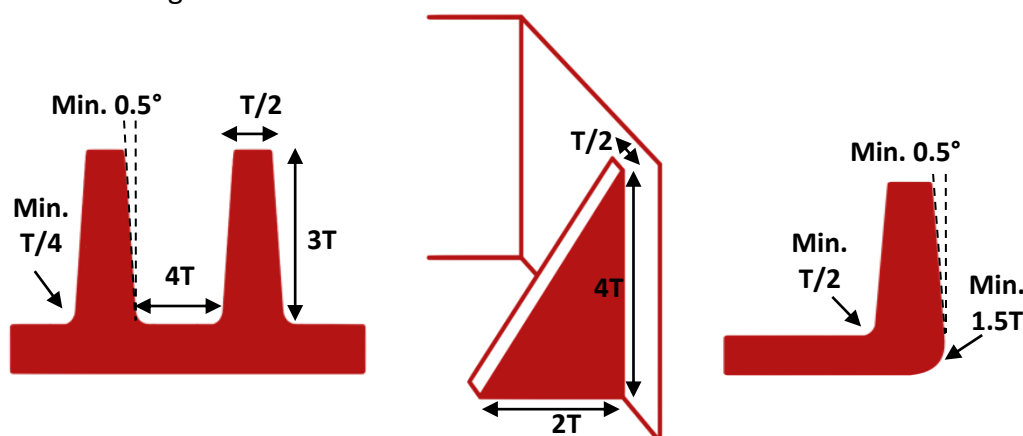


Figure 20 – Recommended dimensions of ribs (left), gussets (middle) and adjoining walls (right). All the dimensions are the maximum recommended sizes, except when indicated otherwise. T : wall thickness.

For a rough cost estimation of the plastic components of the DropAdjust, a provisional quote was requested at Protolabs [95]. This company provides injection moulding for functional prototyping, low-volume production, and pilot runs.

4.2 Results

4.2.1 Generation of partial solutions

Table 3 presents the possible solutions for each category in a morphological overview.

Table 3 – Morphological chart. The partial solutions enclosed by a green rectangle are the selected ones as described in Section 4.2.3. In the illustration, yellow indicates the movements, orange the tubing, red the pincher or mechanism, blue the fluid and black the fixed supports.

Categories ↓	Partial solutions →			
Regulation mechanism for non-uniform pinching	Initial fixed coarse setting with spring-release mechanism 	Drop cam 	Lever 	Non-uniform ramp
	Coarse and fine adjustment 	Eccentric cam lever 		
Attach flow regulator to infusion set	Connect to drop counter	Clamp on tubing	Connect to IV pole	
Fix tube in place	Form-fitting pincher and/or house 	Lock up/close entry 	Slide over line 	Push through/bend
Number of pinchers	1 	2 	3 	∞
Shape of pincher	Round 	Wider 	Multiple 	Pointy
Contact area of pincher	Straight 	Groove 	Ribbons 	
Material of critical components	Polymers (PET, UP) 	Metals (Al-alloy, Mg-alloy) 	Ceramics (silicon) 	

Material of critical components

The materials with the highest potential in terms of creep resistance, price, stiffness, strength, and density for each material class are provided below (see Appendix F for the detailed material selection overview):

Polymers: polyethylene terephthalate (PET) and polyester (UP).

Metals: aluminium alloy or magnesium alloy.

Ceramics: silicon.

Shape of pincher

Figure 21 shows a graph of the volume flow rate in the tubing [mL/h] versus pinching depth [mm] for the investigated pinching widths [mm]. As provided by the cooperating hospital (Jeroen Bosch Ziekenhuis [96]), drugs are usually infused at flow rates below 200 mL/h. For this reason, only the range of 0-200 mL/h is shown in the figures. The results of the FEAs are displayed in Figure 22, 23 and 24.

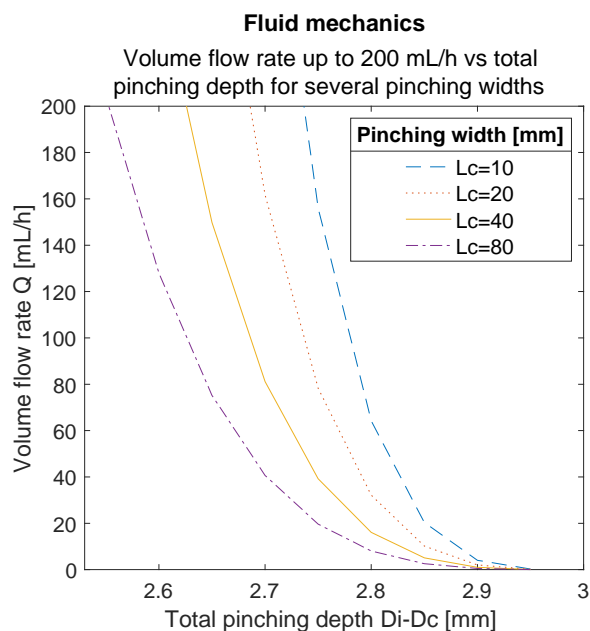


Figure 21 – Fluid mechanics: volume flow rate [mL/h] up to 200 mL/h versus total pinching depth [mm] for several pinching widths.

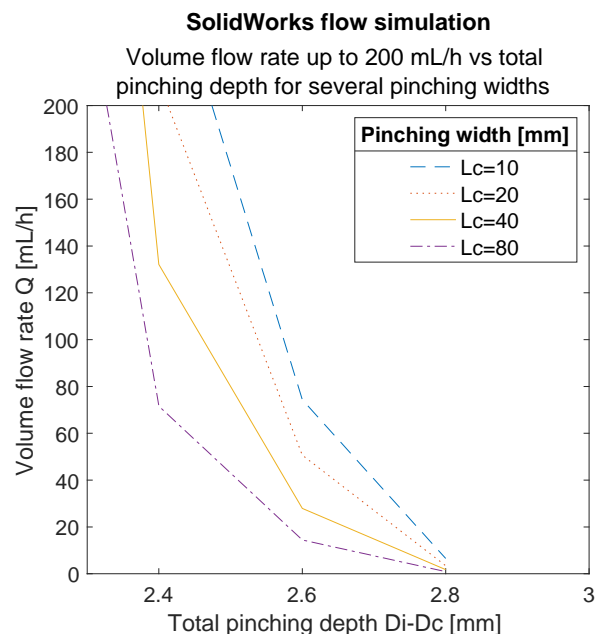


Figure 22 – SolidWorks flow simulation: volume flow rate [mL/h] up to 200 mL/h versus total pinching depth [mm] for several pinching widths.

The figures of the fluid mechanic model (Figure 21) and the FEM model (Figure 22) are similar and reveal a clear relation between the width of the pincher and the flow rate. These simulations show that wider pinchers allow for more gradual control of the fluid flow.

Figure 23 and 24 illustrate that an increase in the number of pinchers or space in between the pinchers also positively influence the regulation control.

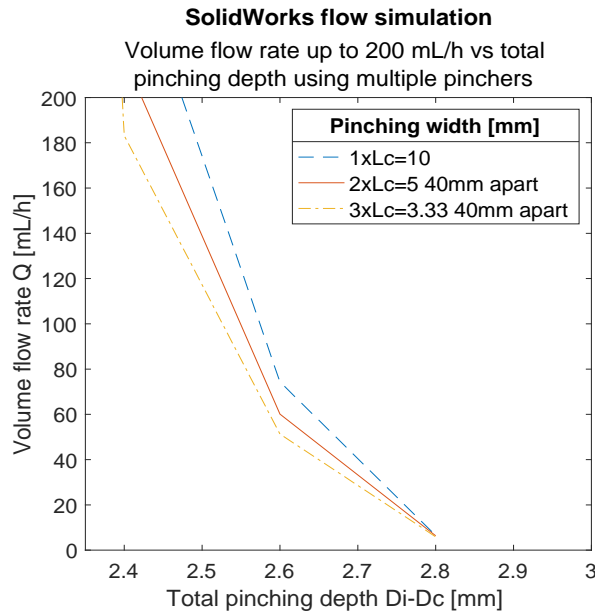


Figure 23 – SolidWorks flow simulation: volume flow rate [mL/h] up to 200 mL/h versus total pinching depth [mm] for a 10mm wide pincher, two 5mm wide pinchers with 40mm in between and three 3.33mm wide pinchers with 40mm in between.

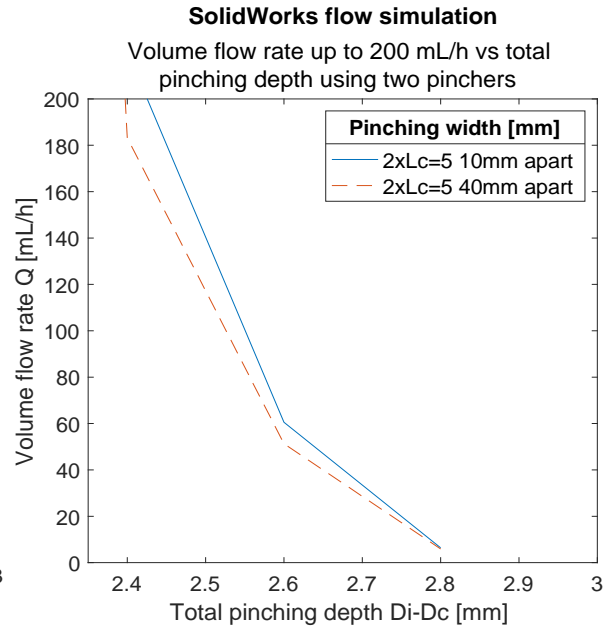


Figure 24 - SolidWorks flow simulation: volume flow rate [mL/h] up to 200 mL/h versus total pinching depth [mm] for two 5mm wide pinchers with 10mm and 40mm in between.

Although the above models were made with specific assumptions, e.g. pinching creates a round orifice in the middle of the tube, the same or similar relations are expected in practice. In Section 4.1.2, experiments to verify this are described.

Contact area of pincher

In the middle of Figure 25, the first improved version of the Adelberg clamp [79] is shown. This version owes its improved performance to the tapered groove (D) at its centre. Due to this groove, the fluid channel remains at the centre while clamping. The highest stresses are concentrated at the outer sides. For this reason, most of the creep takes place at these outer sides and has less influence on the fluid channel's size. According to Adelberg, the second version of Figure 25 (right) is even slightly better [77, 78]. This one contains ridges (E) to grip the tube and was claimed to result in a slight additional reduction of creep (Figure 26).

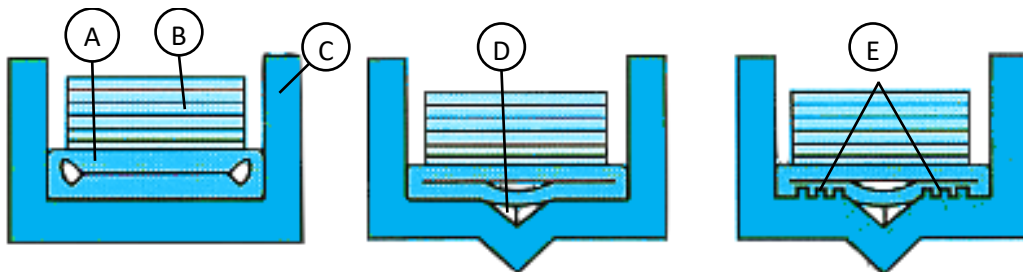


Figure 25 – Section view of: a conventional roller clamp (left); the Adelberg clamp v1 (middle); and the Adelberg clamp v2 (right). The components are: A tubing; B wheel; C housing; D tapered groove; E ridges. Adapted from [97].

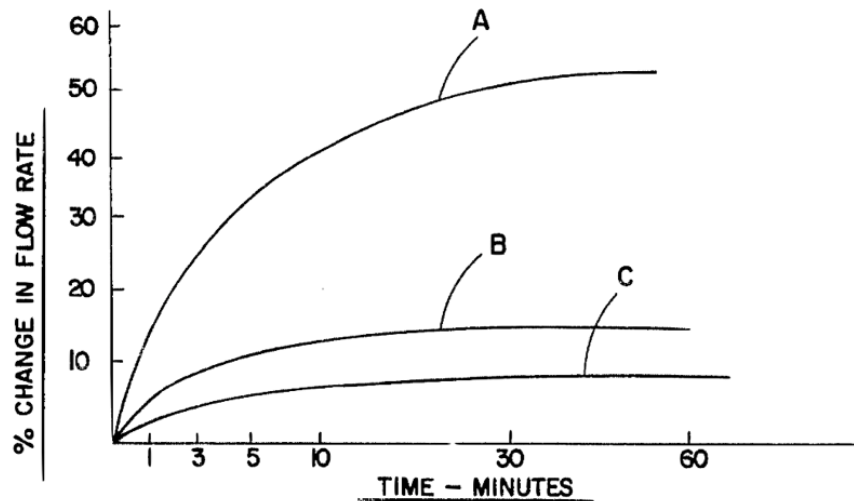


Figure 26 – Flow rate change over time tested by Adelberg. The lines indicate the: A conventional roller clamp; B Adelberg clamp v1; C Adelberg clamp v2. Adopted from [77].

4.2.2 Evaluation of partial solutions

Only the most relevant results of the experiments are shown below (additional graphs are provided in Appendix E).

Material of critical components

The flow rate over time and the mean flow rate accuracy errors of the material experiment are presented in Figure 27 and 28. As expected, the steel pincher indeed had a lower mean flow rate accuracy error than the plastic version. Since steel was considered creep-resistant and the mean accuracy error was still around 45% after 50 minutes, the rest of the accuracy error was related to the PVC tubing.

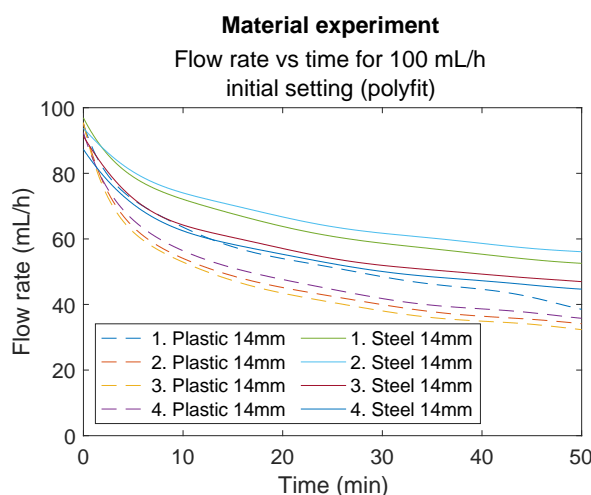


Figure 27 - Material experiment: Flow rate [mL/h] versus time [min] at an initial setting of 100 mL/h using a 14mm wide plastic pincher and a 14mm wide steel pincher.

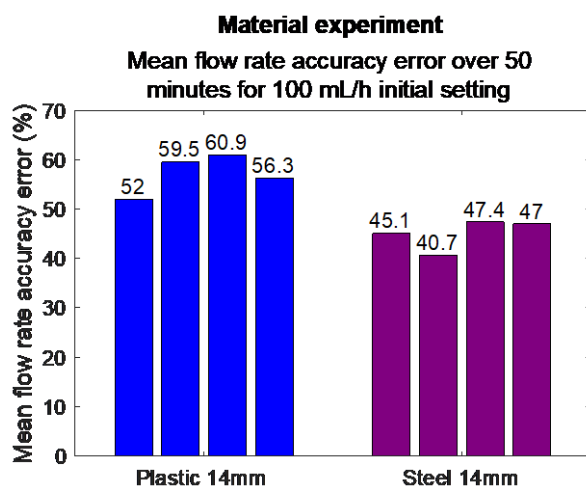


Figure 28 – Material experiment: the mean flow rate accuracy error over 50 minutes for a 100 mL/h initial flow using a 14mm wide plastic pincher and a 14mm wide steel pincher.

Shape of pincher

In Figure 30 and 29, the results of the first shape experiment are shown. Again, only the most essential range of 0-200 mL/h is used in the figures. The relations correspond to the earlier findings from the simulations; the wider pincher (Figure 30 middle) provides more gradual regulation control. There was some scatter of results of the tests with the double pinchers (Figure 30 bottom), but the regulation control was clearly improved. However, as shown in Figure 29, the pinchers with an improved regulation control need a higher pinching force.

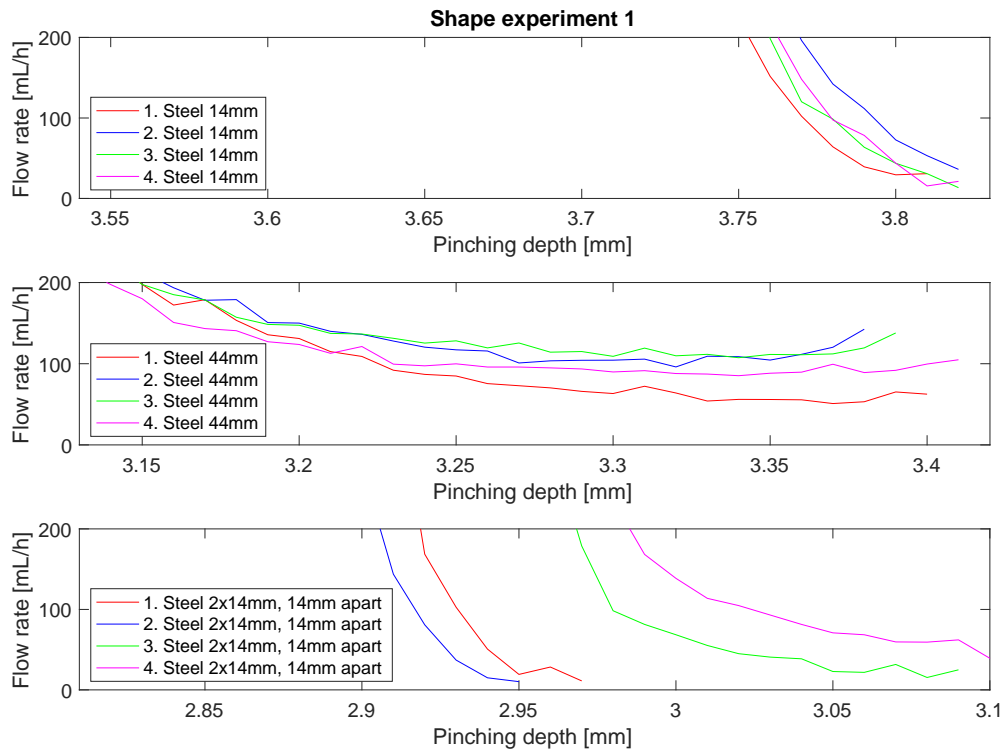


Figure 30 – Shape experiment 1: Flow rate [mL/h] (up to 200 mL/h) versus pinching depth [mm] using a 14mm wide steel pincher (top), a 44mm wide steel pincher (middle) and a double 14mm wide steel pincher with a distance of 14mm in between (bottom).

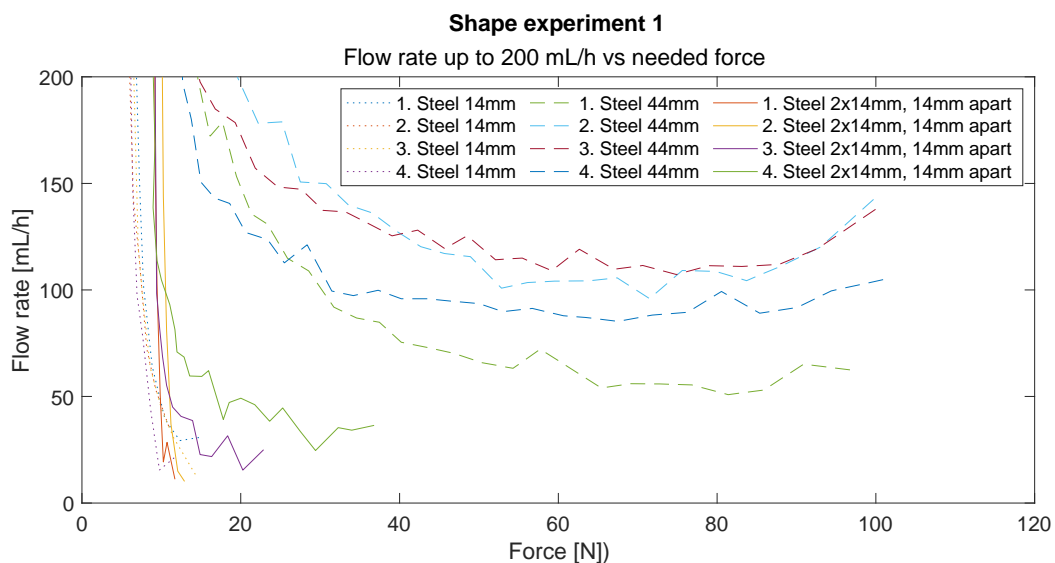


Figure 29 – Shape experiment 1: Flow rate [mL/h] (up to 200 mL/h) versus needed pinching force [N] using a 14mm wide steel pincher, a 44mm wide steel pincher and a double 14mm wide steel pincher with a distance of 14mm in between.

Figure 31 shows the results of the additional shape experiment. The mean accuracy error for the wider 44mm pincher was still around 45% after 50 minutes. So, the width of the pincher had no evident influence on the flow rate accuracy.

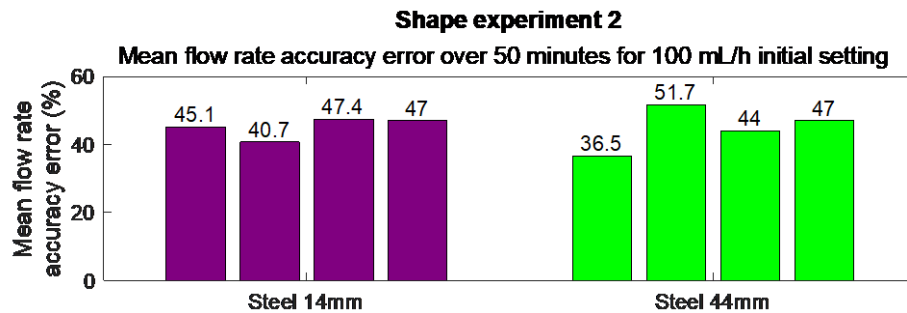


Figure 31 – Shape experiment 2: the mean flow rate accuracy error over 50 minutes for a 100 mL/h initial flow rate setting, using a 14mm wide steel pincher and a 44mm wide steel pincher. The data of the 14mm wide pincher comes from the material experiment.

Contact area of pincher

The flow rate accuracy errors of this experiment are presented in Figure 32. The tested roller clamp with its housing provides an improved flow rate accuracy over time. The mean accuracy error for the plastic wheel was 57% after 50 minutes, while the roller clamp provides an error of 35%. Since the plastic wheel used in this roller clamp was equal to the one used in the material experiment, the only difference was the housing. Hence, the tapered groove of the housing causes the improvements.

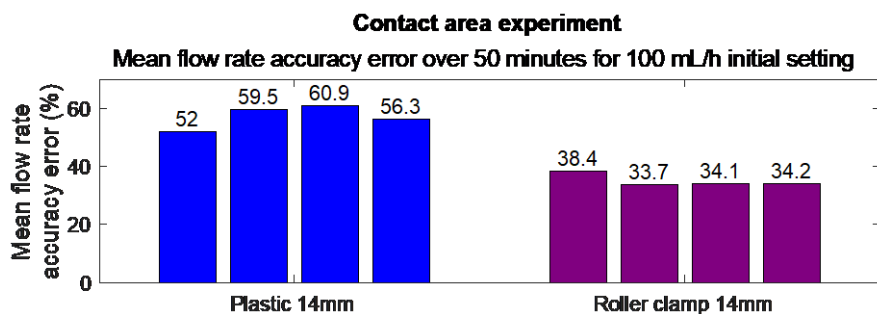


Figure 32 – Contact area experiment: the mean flow rate accuracy error over 50 minutes for a 100 mL/h initial flow rate setting, using a 14mm wide plastic pincher and a roller clamp with the same pincher. The data of the plastic pincher comes from the material experiment.

4.2.3 Selection of partial solutions

Regulation mechanism for non-uniform pinching

The partial solutions using a screw-type mechanism are not preferred because of the slow operation speed; quick opening or closing is difficult. Furthermore, the lever mechanism needs a relatively large lever to achieve the desired fine regulation step size.

On the other hand, the drop cam has the desirable property of the possibility of a fine regulation step size while simultaneously keeping the mechanism compact. This property is contrary to the conventional roller clamp, which needs much more (rolling) space when the wheel is enlarged. The same holds for the non-uniform ramp when used for fine flow rate regulation, but it can be used for fast coarse settings. The separated coarse and fine adjustments mechanism also has its benefits. Using this mechanism, it is easier to deal with different tubing diameters, and also quick opening or closing is possible through the coarse setting. However, as mentioned, screw-type operations are undesirable.

For the above reasons, a combination of this mechanism and the non-uniform ramp and drop cam was chosen: a hybrid solution. The non-uniform ramp takes care of the coarse flow rates adjustments (open, close, flow) and the drop cam mechanism provides the fine flow rate regulation.

Attach flow regulator to infusion set

Clamping the flow regulator to the infusion set, like the roller clamp, is challenging because of its weight and its centre of gravity which is not in line with the tubing. Connecting it to the IV pole counters the possible swinging of the infusion set during patient transportation. This way, a more stable flow rate is realised. For this reason, connecting the flow regulator to the IV pole was chosen over attaching it to the drop counter. In addition, the flow regulator is also more versatile as it does not depend on a specific type of drop counter.

Fix tube in place

Locking up of the tube was rejected as it results in additional components and therefore costs. Let the flow regulator slide over the line is the same principle as the roller clamp uses. However, the Luer-lock (Figure 4) should also fit through, and therefore the dimensions would have to increase. Furthermore, attaching and detaching the flow regulator is less convenient. Since both the form-fitting pincher and the push-through component are placed at separated locations, both were used to ensure the tube is fixed.

Number of pinchers

As using multiple pinchers was shown not to provide substantial regulation advantages but would add cost due to added complexity, a single pincher was used.

Shape of pincher

Since no puncture or damage to the tubing is allowed (Section 3.1.1), a round shape is preferred over the pointy-shaped pincher. Furthermore, based on the results of the evaluation of the partial solutions, a wider pincher or multiple pinchers were preferred as they allow for more gradual control of the fluid flow. The performance of the 44mm wide pincher and multiple pinchers cannot be directly compared, also because of their difference in total width. However, to keep the improved flow regulator as compact as possible, one pincher was used. An increase in width of the pincher also increases needed pinching force, which adversely affects the user-friendliness. Thus, for the exact dimensions of the pincher, a balance has been sought (Section 4.2.4).

Contact area of pincher

Based on the accuracy performance of the conducted experiments, a groove was made into the pincher's contact area. Adding ribbons into the pincher's contact area was claimed only to provide slight improvement. Besides, the fine ribbons provide added complexity in terms of manufacturability. For these reasons, ribbons were not yet implemented into the contact area of the pincher.

Material of critical components

The partial solution generation section (4.2.1) shows that a creep-resistant material can be found for each material class. However, polymer injection moulding is preferred as the manufacturing method because of its low cost at high production rates. Besides, injection

moulding provides excellent quality and accuracy, and a wide variety of plastic materials with various properties can be used [98]. Given the above and its lowest cost price (Appendix F), the widely used injection moulding material, polyethene terephthalate (PET) was used. This material choice holds for all the components subjected to the applied flow rate setting forces.

In Table 3, the selected partial solutions for each category are indicated by a green rectangle.

4.2.4 Prototyping and final design

The rapid prototyping process resulted in a final design (Figure 33), hereinafter referred to as the DropAdjust. In Appendix G, the design and prototype steps can be found, including the explanations of complications and improvements. Also, additional renders of each separate component are provided. Appendix H provides the exact dimensions of each component in technical drawings, except for the leaf spring.

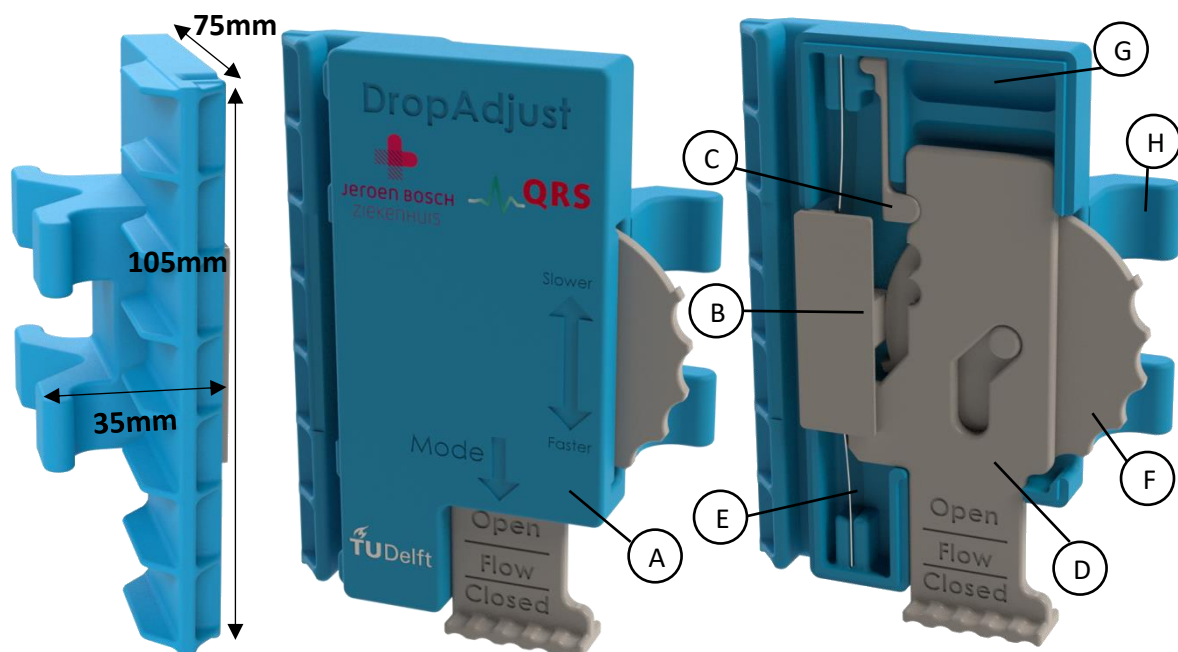


Figure 33 – Renders of the DropAdjust in its open mode. Left: side view, middle: frontal view, right: frontal view of the inside without the housing cap. Table 4 shows the meaning of the assigned labels. Created with SolidWorks Visualize [89].

Figure 34 shows an exploded view of all components, and the assigned labels are described in Table 4. The non-uniform ramp (D) is used to set the DropAdjust to one of the three different flow rate modes: open, flow, or closed. A compliant safety pin (C) ensures this desired mode is maintained, also during patient transportation. The flow mode is reached by moving the ramp upwards from its open mode (Figure 33). At this position, the pincher (B) already pinches the tubing to bring the flow rate back to roughly 200-500 mL/h (coarse adjustment). The tubing of the infusion set is positioned in the rectangular groove in the housing base (G), left of the pincher. When the DropAdjust is in its flow mode, rotating the drop cam (F) is used to set the desired flow rate (fine adjustment). The pincher (B) moves closer or further away from the tubing by rotating this drop cam. A leaf spring (E) makes sure this pincher is always linked to the drop cam. The pole bracket (H) is placed on the back of the housing base to connect the DropAdjust to an IV pole using rubber bands. A housing cap (A) closes the DropAdjust and minimises the number of accessible moving parts for safety reasons.

At the closed mode of the DropAdjust, the protruding part left on the non-uniform ramp pushes the pincher even further onto the tubing to shut off the flow. This way, when an infusion bag needs to be swapped, the DropAdjust can temporarily stop the fluid flow. After the regulator is put in its flow mode again, the former flow rate will be restored.

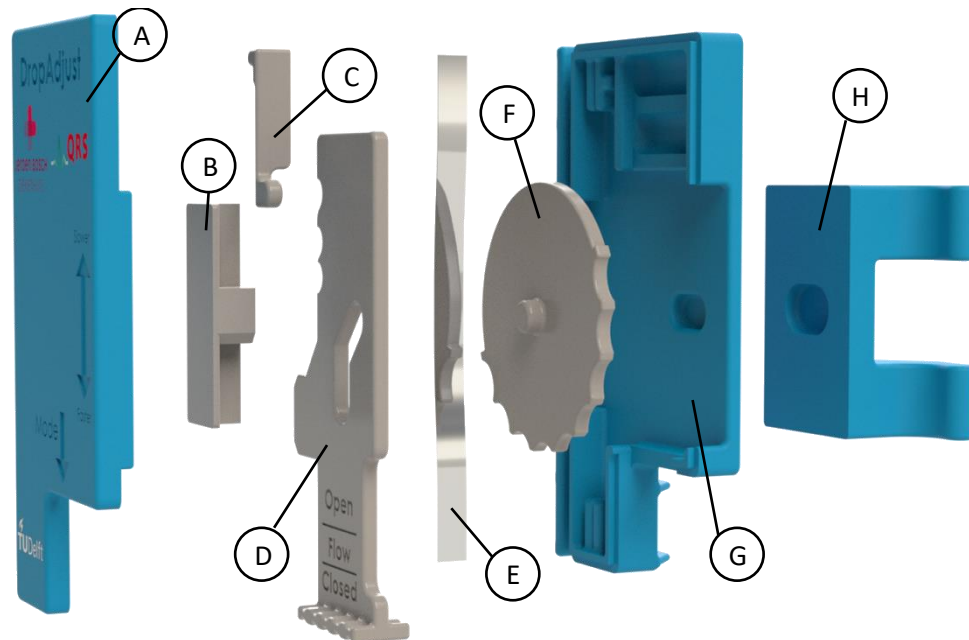


Figure 34 – Exploded view of the DropAdjust. The assigned labels are explained in Table 4. Created with SolidWorks Visualize [89].

Table 4 – Component names, materials, outer dimensions and cost price of DropAdjust assembly shown in Figure 34. The function of each component is explained in the text. Cost price with the asterisk is excluding machining. PET part prices depend on the type of mould used, and the mould costs are excluded (Appendix I).

Label	Component	Material	Outer dimensions [mm]	Cost price (€/part)
A	Housing cap	PET	101.0x50.8x6.8 mm	€0.47-€1.59
B	Pincher	PET	39.9x14.4x8.0 mm	€0.36-€1.36
C	Compliant safety pin	PET	28.1x10.72x6.6 mm	€0.34-€1.33
D	Non-uniform ramp	PET	87.0x38.1x10.8 mm	€0.41-€1.47
E	Leaf spring	Spring steel	95.0x0.2x6 mm	€0.06* [99]
F	Drop cam	PET	50.4x9.4 mm	€0.39-€1.43
G	Housing base	PET	101.0x62.9x16.1 mm	€0.61-€1.87
H	Pole bracket	PET	46.7x51.46x21.8 mm	€0.45-€1.55
Total				€3.09-€10.66

As mentioned earlier, all the components will be manufactured through plastic injection moulding, except for the steel leaf spring. Table 4 also provide the estimated cost prices per part, mainly based on the quote of Protolabs [95] (see Appendix I for the full quote). The steel leaf spring is a commercial off-the-shelf product [99], and only needs to be machined to the desired dimensions. When all the parts are assembled, the housing cap and pole bracket are joined to the housing base through ultrasonic welding. This is one of the most popular methods for merging injection moulded parts [100] for several reasons: it is fast (<1s), the required tools are relatively inexpensive, and automation is straightforward [100, 101].

Pictures of the latest demo prototype built using an FDM printer can be seen in Figure 35. Two screws were used to join the housing base and cap in order to keep the prototype modular. Superglue was used to fasten the IV pole bracket to the housing base.



Figure 35 – Demo prototype of the DropAdjust. Left: frontal view, right: frontal view of the inside without housing cap.

5 Design evaluation

5.1 Methods

5.1.1 FEM Analysis

Multiple FEM static analyses (FEA's) were conducted for the possible critical components to check if the proposed design can withstand the applied forces during usage. The housing, pincher and non-uniform ramp were expected to be the essential parts because they are subjected to the highest pinching forces at the closure of the tubing (closed mode). The material properties of PET were obtained from Granta Edupack [74]. These properties were imported into SolidWorks for conducting the FEA's. Based on the maximum pinching force of 61.3N (Appendix J), and to keep an additional safety factor of ≈ 1.5 , the total applied force on the critical components was set at 90N. The simulations were divided into three parts: housing (cap and base); pincher; and non-uniform ramp. By using fixed supports, a simplification of the usage in practice was mimicked (Figure 36).

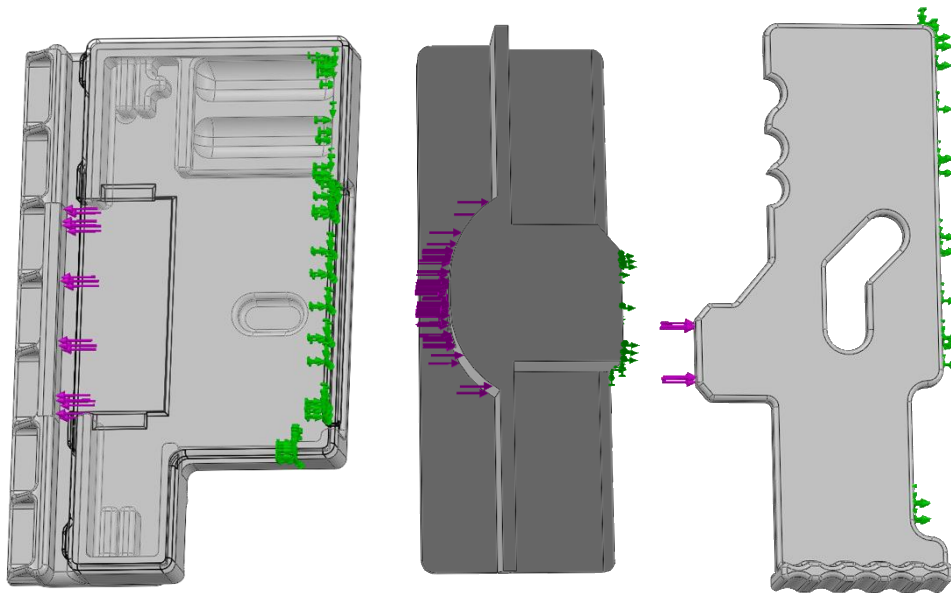


Figure 36 – Simulation models. Left: housing base and cap (transparent), middle: bottom of pincher, right: non-uniform ramp. The green arrows are the fixed supports, and the purple arrows are the 90 N of applied force.

The maximum Von Mises stress should stay under the yield strength of PET of 52.44 MPa [74] to prevent plastic deformation and failure. Though, to ensure a long life-cycle, the maximum Von Mises stress is preferred to also remain under the fatigue strength of 28.72 MPa [74]. Furthermore, to maintain high regulation precision, only minor material deformations of 0.1mm were allowed.

5.1.2 Validation experiments

As plastic injection moulding is expensive for small batches, the tested prototype was built using additive manufacturing. The material properties of the PLA demo prototype did not comply. Thus, to ensure that the quality and strength of the prototype is high enough to perform the experiments, the Photopolymer Resin of Formlabs (Appendix K) combined with a SLA printer was used (Figure 37). The housing cap was made of a transparent material to display the mechanism inside when the cap is attached.

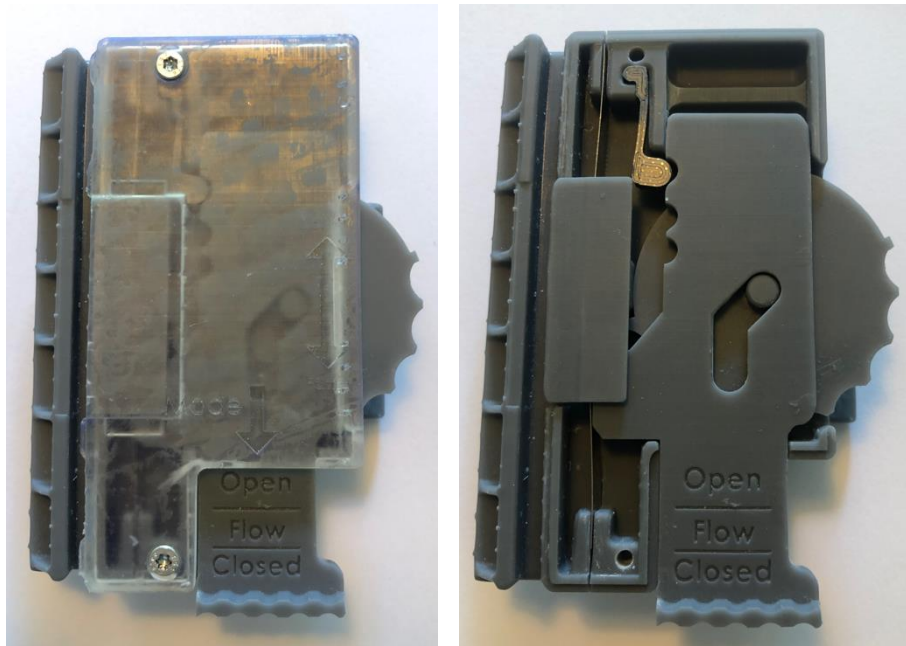


Figure 37 – Experiment prototype of the DropAdjust. Left: frontal view, right: frontal view of the inside without housing cap.

The Heat Deflection Temperature [102] of the resin is comparable to that of PET (resin: 73.1°C, PET: 75.0°C [103], at 0.46MPa). For this reason, also a similar creep behaviour was expected.

Two DropAdjust experiments were set up to evaluate the DropAdjust's flow rate accuracy over time: short-term and long-term. The short-term DropAdjust accuracy experiment was the same (method, setup, protocol) as the contact area experiment (Section 4.1.2), but now the DropAdjust was attached to the IV tubing (Figure 38). Thus, the flow rate was initially set at 100 mL/h with the help of the Monidrop and then recorded for 60 minutes. A mean flow rate accuracy error was computed using MATLAB [75]. This experiment was repeated four times. These results were compared to the results of the roller clamp from the contact area experiment.

The long-term DropAdjust accuracy experiment was a pilot experiment of two different runs. This pilot corresponded to the A.2 flow regulator test of ISO 8536-14 [33]. As with the short-term experiment, the DropAdjust was attached to the IV tubing of the experiment setup (Figure 15). The flow rate was initially set at 21 mL/h, a commonly used flow rate [96]. After fifteen minutes, the decreased flow rate was again set at 21 mL/h and recorded for six hours. Most of the creep should occur in these first fifteen minutes [45]. The mean flow rate accuracy error was measured at every hour and processed using MATLAB. The pilot experiment was repeated using the roller clamp instead of the DropAdjust to compare the accuracy performance.

The complete experiment plans are provided in Appendix L.

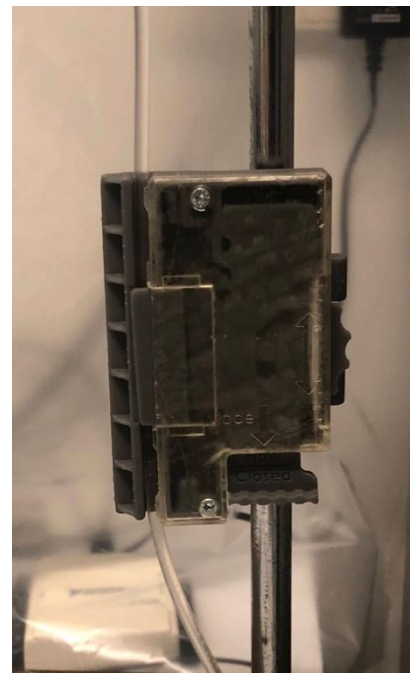


Figure 38 – The DropAdjust, connected to the IV tubing of the experiment setup of Figure 15. The DropAdjust replaces the pinching setup (F).

5.1.3 Prototype evaluation

This section evaluates the DropAdjust prototype on the set design requirements based on the above experiments and the expected performance. The evaluation is summarised in an overview.

5.2 Results

5.2.1 FEM Analysis

Figure 39, 40 and 41 present the results of the FEA's.

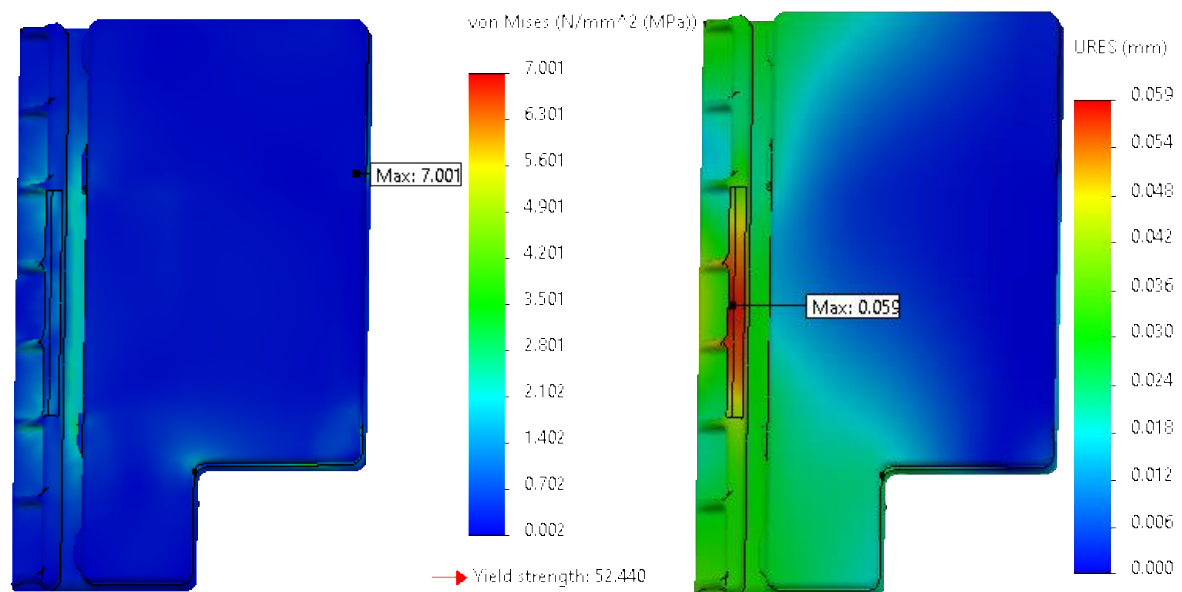


Figure 39 – FEA results of the housing base and cap. Left: von Mises stresses [MPa], right: resultant displacements (URES) [mm].

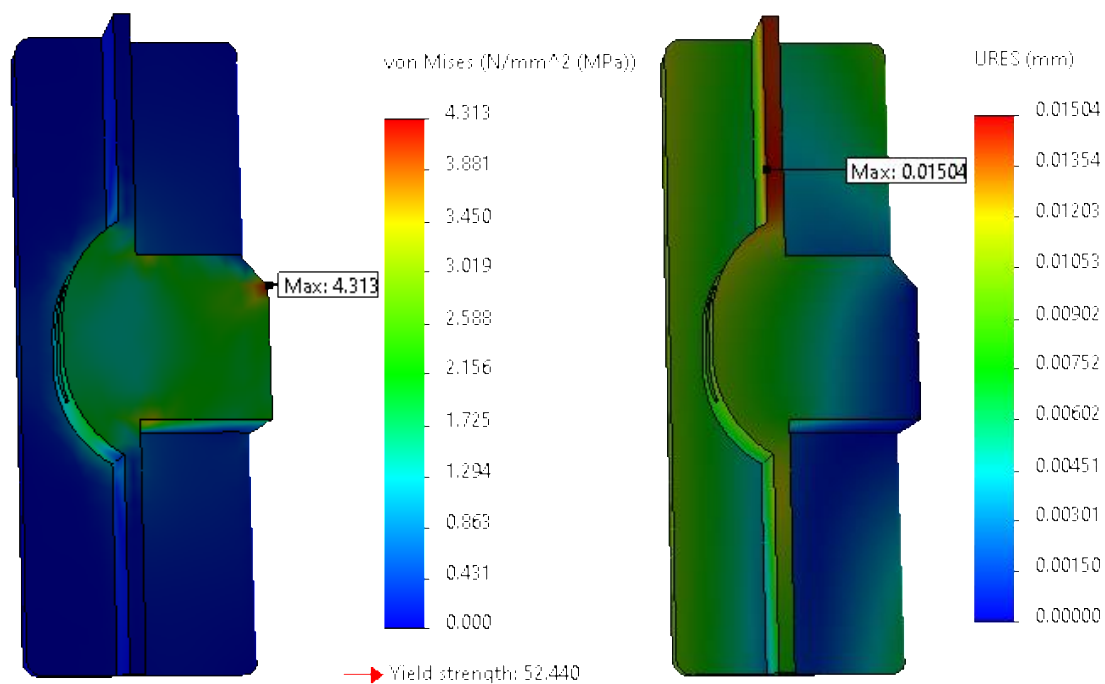


Figure 40 - FEA results of the pincher. Left: von Mises stresses [MPa], right: resultant displacements (URES) [mm].

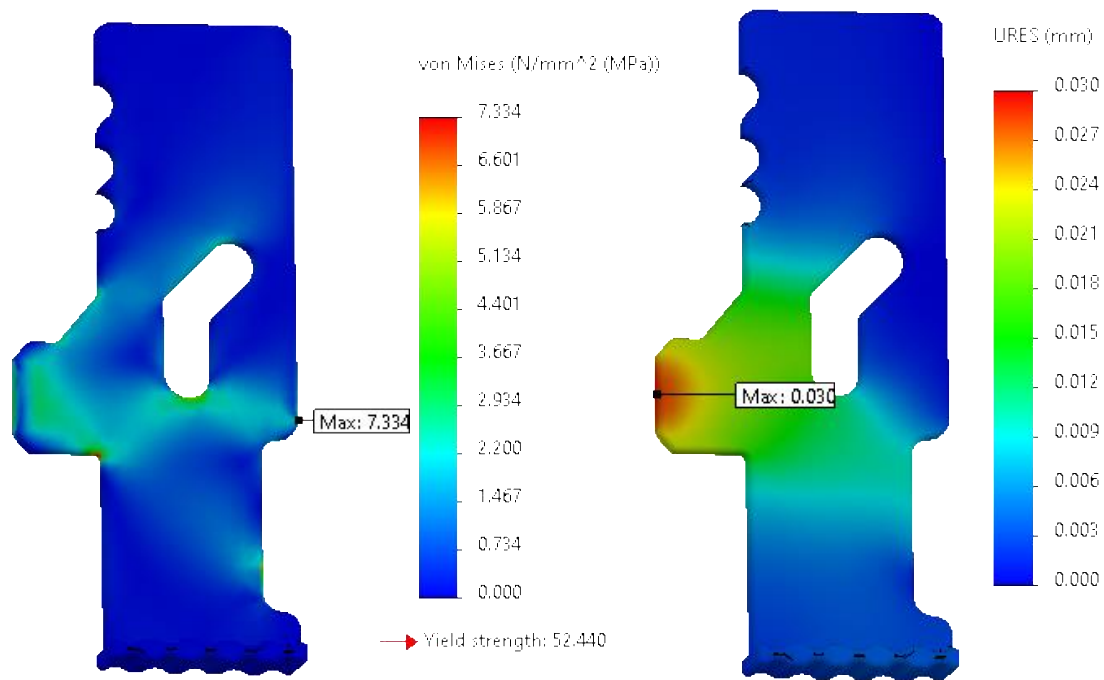


Figure 41 - FEA results of the non-uniform ramp. Left: von Mises stresses [MPa], right: resultant displacements (URES) [mm].

As illustrated in the figures, the stresses in all components stayed well under the fatigue strength of 28.72 MPa. The expected material deformations were microscopic and also well within the prescribed range.

5.2.2 Validation experiments

The mean flow rate accuracy error for both the roller clamp and DropAdjust of the short-term experiment are shown in Figure 42. The data of the roller clamp were obtained from the earlier contact area experiment. As expected based on the earlier experiments, the DropAdjust performs better than the roller clamp in terms of mean flow rate accuracy. The accuracy error of the roller clamp was around 23.5%, while the DropAdjust's error was around 4.5%.

The results of the long-term accuracy experiment of the roller clamp and DropAdjust are shown in Figure 44 and 43. Once again, the DropAdjust outperformed the roller clamp in terms of mean accuracy. In the first hour, the mean flow rate accuracy error of the DropAdjust was 10.9%, but this mean error decreased over time. Over six hours, the mean accuracy error was 5.8%. The accuracy error of the roller clamp increases every hour, and the mean flow rate accuracy error over six hours was 23.2%.

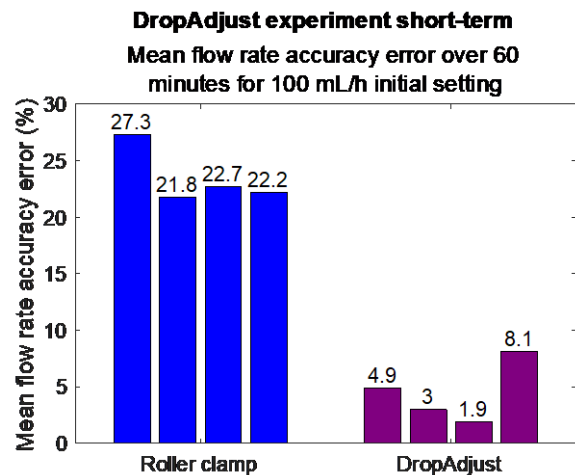


Figure 42 – DropAdjust experiment short-term: the mean flow rate accuracy error over 60 minutes for a 100 mL/h initial flow rate setting, using a roller clamp and the DropAdjust. The data of the roller clamp is coming from the contact area experiment.

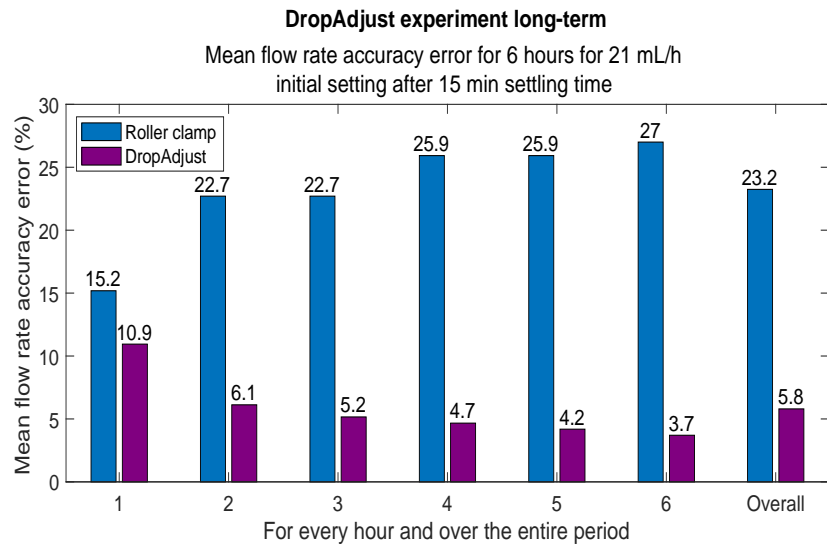


Figure 44 – DropAdjust experiment long-term: the mean flow rate accuracy error over 60 minutes for a 21 mL/h initial flow rate setting after 15 min settling time. A roller clamp and the DropAdjust were used.

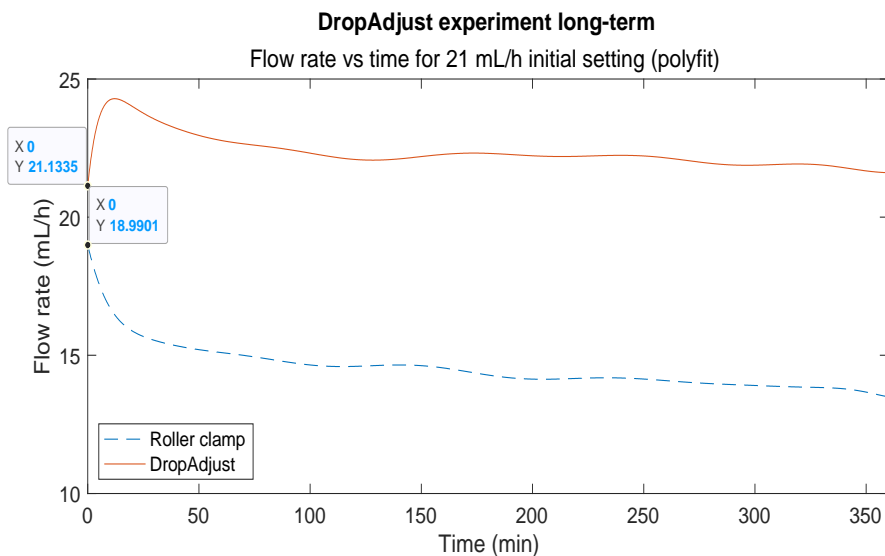


Figure 43 – DropAdjust experiment long-term: Flow rate [mL/h] versus time [min] at an initial setting of 21 mL/h after 15 min settling time. A roller clamp and the DropAdjust were used. The initial flow rate is labelled, where the top one is the DropAdjust.

Figure 43 also provides some indication of whether a fine regulation step size was possible. The initial flow rate of the roller clamp was within 9.6% of the desired 21 mL/h, while the DropAdjust was within 0.6%.

5.2.3 Prototype evaluation

In Table 5, the overview of the evaluation is presented. Almost all criteria were satisfied. The only criteria that still needs some attention is user-friendliness.

Table 5 – Evaluation of the DropAdjust based on the earlier set design requirements. Green indicates that the criterion is satisfied, light green indicates a promising result of a pilot experiment, and yellow is still to be tested.

Criterion	Value	Satisfied?
Mean flow rate accuracy error over one hour without prior settling	$\leq 23.7\%$	4.5%
Flow rate deviation over 6 hours after 15 min settling time	$< 10\%$	Overall: 5.8%, 1 st hour: <u>10.9%</u> (only one run)
Fine regulation step size possible	$\leq 1\%$ of desired flow rate	0.6% (only one run)
Cost price	$\leq \text{€}50,-$	€3.09-€10.66 (excluding assembly costs)
Compatibility range of external tubing diameters	3.0-4.5 mm	Yes
Safe in use and no puncture or damage to the flexible tubing	-	Yes
Number of needed movements of subcomponents to disconnect the flow regulator	≤ 2	1
Number of movements of subcomponents in a single plane to lock the flow regulator's position	≤ 1	1
User-friendly	-	-
Modular prototypes, but end product impossible to disassemble by customers	-	Yes
Compatible with the Monidrop [73]	-	Yes
Open-close time	$\leq 2 \text{ s}$	$\pm 1 \text{ s}$ (self-tested)
Maximum dimensions	$\leq 15 \times 10 \times 5 \text{ cm}$	10.5x7.5x3.5 cm
No line modifications are necessary	-	Yes

6 Discussion

Through various (FEA) analyses and experiments, an improved manually controlled over-line flow regulator for gravity-driven infusion was developed: the DropAdjust.

The material experiment demonstrated the influence of the pincher's material on the flow rate accuracy. As expected, the steel pincher performed better (45.1%) than the plastic pincher (57.2%) in terms of mean flow rate accuracy over 50 minutes. The existence of an accuracy error for the creep-resistant steel pincher must be related to the PVC tubing, which makes sense because flexible PVC is most prone to creep of all the involved materials. Interestingly, the discovery of the impact of the pincher's material is in contrast to earlier findings of Flack & Whyte [44]. Given the lack of detailed experiment setup and experimental data of their research, it is hard to explain the discrepancy in results. Furthermore, as seen in Figure 26, ribbons were claimed to provide a decrease in creep. The tested plastic wheel of the material experiment had some small ribbons that could positively have influenced the flow rate accuracy. If so, this the material's influence on the flow rate accuracy could even be more prominent. Anyhow, as the material experiments were only executed four times, more research is needed to make it possible to quantify the degree of influence.

The fluid mechanic calculations, FEM-model, and shape experiments demonstrated a clear correlation between the width of the pincher and the flow rate. The use of a wider or multiple pincher(s) allowed for more gradual flow rate regulation. There is however one downside to these pinchers with an improved regulation control: a higher pinching force is needed. This increased pinching force did not result in the expected increasement of the mean flow rate accuracy error. Thus, for the shape of the pincher, there is only a balance between user-friendliness (needed pinching force) and regulation control.

The results of the contact area experiment were in accordance with the claims made by Adelberg [77, 78]: a tapered groove in the housing indeed improves the flow rate accuracy.

In terms of mean accuracy error, the short-term DropAdjust experiment demonstrated a significant improvement of the DropAdjust (4.5% over one hour) compared to the conventional roller clamp (23.5% over one hour). This improvement was expected as several design enhancements were applied based on the earlier experiment results.

Also, the long-term accuracy of the DropAdjust seemed promising during the pilot experiment. Nevertheless, the DropAdjust showed some unexpected behaviour at the first hour, as the mean flow rate increased by 10.9%. After this temporarily increase, the gradient over time was again as expected. No explanation was found, but additional long-term research could maybe shed some light on this behaviour. Furthermore, it was also interesting to see that a settling time of 15 minutes was not enough for the roller clamp, as it was still decreasing drastically for 25 minutes. Thus, contrary to the 15 minutes suggested by Simon et al. [45], a minimum settling time of 40 minutes is advised for the conventional roller clamp.

This pilot experiment also indicated whether a fine regulation step size was possible using the DropAdjust. With an initial flow rate within 0.6% of the desired flow rate, the DropAdjust outperformed the conventional roller clamp (9.6%). Nevertheless, this was only one run during a pilot experiment.

There were several limitations to the performed experiments. The initial water level in the reservoir was not always exactly the same, as the desired level was marked with a thick line ($\approx 5\text{mm}$). However, as the height was 1.87m , this results in a hydrostatic pressure deviation of 0.27% .

Furthermore, it was hard to start all the experiment runs with an equal initial flow rate. As the creep-effect is more prominent for lower flow rates, this deviating initial flow rate could also be of influence. This creep-effect possibly occurred at the lowest flow rates of the first shape experiment. During the needed measuring interval, the flow rate decreased faster than the flow rate increased through reducing the pinching depth. However, as most experiments were initially set at a high flow rate setting, the creep-effect should be minimal.

Another limitation was that the U-profile of the pinching setup (Figure 14) was broader than the pinchers designed to slide into it. This made it challenging to precisely align the tubing and pincher. Consequently, the tubing could have squeezed in between the side of the pincher and the U-profile, making it harder to shut off the tubing completely. Although, if noticed the pincher was reoriented, it may have been overlooked. This phenomenon explains the higher needed pinching depth for two runs of the double 14mm wide steel pincher (Figure 30).

At last, all the flow rate accuracy experiments were performed at one initial flow rate setting (100 mL/h) and using the same bag-cannula height. For this reason, additional experiments for a wider range of flow rates at various heights are recommended to evaluate the performance of the DropAdjust more thoroughly. Furthermore, since the flow rate accuracy over time in practice is dependent on various parameters (Table 1), in vivo experiments are suggested to evaluate DropAdjust's sensitivity to these parameters.

The focus of this thesis was to deliver a practice-ready prototype. Unfortunately, not all components were optimally developed because of the size of this process, the number of components, and the time constraint. For instance, the chosen pincher width was based on only a couple of prototype iterations. Supplementary research and more diverse experiments could be conducted to find the ideal balance between the needed pinching force and regulation range.

Another component that was not developed thoroughly is the compliant safety pin (Figure 34). The development of the compliant safety pin is delicate. The dimensions of this pin are a balance between safety (rigid) and ease of use (flexible). As the user-friendliness of the DropAdjust was not yet researched in this thesis, such research in collaboration with healthcare providers is recommended. The safety pin considerations could then be included in that research. One more element to investigate during this research is the location and shape of the control knob attached to the non-uniform ramp. The developed mechanism lends itself to various location and shape possibilities.

Another possible follow-up research could examine the possibility of implementing the earlier mentioned Adelberg ribs (Figure 25 and 26). The inventor's claims and the limited experiments looked promising, although the Adelberg groove was of more influence.

Lastly, given the sustainability benefits, one could also look into possibilities to keep the design modular but at the same time inaccessible for customers. For instance, by implementing a snap-fit in the housing base that can only be altered or accessed using a tool.

Apart from the mentioned (dimensional) optimisations, a practice-ready prototype was delivered that is already close to an end product.

To be able to go from this practice-ready prototype to an end product, some essential steps have to be made. For instance, endurance tests need to be performed. Although the FEA's of Section 5.2.1 were promising, actual practice tests are still necessary.

Additionally, as preparing a design for injection moulding is a profession on its own, it is still advised to acquire advice from a well-regarded company or experienced specialist. A thing to consider is the margins for the moving parts of the DropAdjust, which are currently optimised for 3D printing. They can possibly also advise on the needed draft angles for the walls in the DropAdjust as this differs per mould type and product.

Furthermore, although the results from the DropAdjust accuracy experiments looked hopeful, additional tests are probably necessary to verify its safety and functionality to qualify for a CE marking.

At last, a patent application for the DropAdjust could be considered. Based on the patents of the priorly conducted literature study [60], the DropAdjust provides an unknown ingenious combination of components to achieve unprecedented performance. With a mean flow rate accuracy error of 4.5%, it can even compete with the flow rate accuracy of the infusion pumps (0.5-6%). The cost price of the DropAdjust is €3.09-€10.66 (excluding assembly), and a drop counter costs €290-€495. As infusion pumps cost €1800+, high-profit margins are possible for the DropAdjust. Thus, the return on investment of a patent application seems promising. An intellectual property business case study is suggested to explore the future possibilities.

7 Conclusion

This study aimed to design and develop a precise and accurate manually controlled over-line flow regulator for gravity-driven infusion. With such a flow regulator, drop counters can be used to their full potential. These combined pose an interesting alternative to the expensive, relatively immobile, and sometimes scarce infusion pumps.

Supported by FEA analyses and validation experiments, the developed DropAdjust is such precise and accurate flow regulator. The mean flow rate accuracy error over one hour without prior settling was 4.5%, in contrast to the 23.5% of the conventional manual flow regulator (roller clamp). The results of a six-hour pilot run were also promising as the DropAdjust was four times more accurate than the roller clamp. Furthermore, this pilot's data suggested that the DropAdjust was better in accurately setting the desired flow rate, and therefore an improved flow rate precision is expected.

The pilot experiment was part of the ISO 8536-14 standard requirements set for flow regulators without fluid contact [33]. Despite the promising mean flow accuracy of the pilot run (5.8% error), the DropAdjust did not yet satisfy the criterion for the ISO standard. In the first hour, the mean flow rate deviated 0.9% above the allowed range. As this was a pilot experiment, additional experiments are necessary for a more definitive verdict. The DropAdjust does however meet all the other ISO 8536-14 requirements.

The DropAdjust satisfies all tested design criteria and outperformed the roller clamp in terms of accuracy and precision. Moreover, it even shows a mean flow rate accuracy error comparable to the electronic infusion pumps (0.5-6% [22, 23]). The cost price of the DropAdjust is €3.09-€10.66 (excluding assembly and profit margin), and the drop counter is priced at €290-€495 [6, 24, 51]. Hence, the combination of the DropAdjust and a drop counter is also considerably cheaper than infusion pumps (€1800+ [25, 26]).

The DropAdjust also has an additional practical feature: it can temporarily close the infusion line without losing the last-used flow rate setting. When an infusion bag needs to be swapped, the DropAdjust is put in its closed mode. After the regulator is put in the flow mode again, the former flow rate will be restored.

Given the above, and apart from some possible (dimensional) optimisations, a practice-ready prototype with high potential was delivered. Possible next steps are conducting endurance tests and acquiring injection moulding advice at a well-regarded company or experienced specialist. Furthermore, as suggested, more long-term flow rate accuracy ISO 8536-14 tests are recommended to verify the safety and functionality of the DropAdjust. This verification is needed to comply with the EU MDR requirements and receive the obligatory CE marking.

This DropAdjust combined with a drop counter has the potential to improve the accessibility as well as the affordability of accurate infusion in the future, and therefore contribute to better healthcare.

Bibliography

1. Baranowski, L., *Presidential address: take ownership*. J Intraven Nurs, 1995. **18**(4): p. 162-4.
2. Beecham, G.B. and G. Tackling, *Peripheral Line Placement*, in StatPearls. 2020, StatPearls Publishing: Treasure Island (FL).
3. Zingg, W. and D. Pittet, *Peripheral venous catheters: an under-evaluated problem*. International Journal of Antimicrobial Agents, 2009. **34**: p. S38-S42.
4. Hobbs, J., et al., *Flow rate accuracy of ambulatory elastomeric and electronic infusion pumps when exposed to height and back pressures experienced during home infusion therapy*. Expert Review of Medical Devices, 2019. **16**.
5. Choi, G., et al., *Accuracy of an Automatic Infusion Controller (AutoClamp) for Intravenous Fluid Administration*. The Open Anesthesiology Journal, 2015. **9**: p. 23-28.
6. Couperus, K., K. Kmiecik, and C. Kang, *IV DripAssist: An innovative way to monitor intravenous infusions away from an outlet?* Military Medicine, 2019. **184**: p. 322-325.
7. Van Der Eijk, A.C., et al., *A literature review on flow-rate variability in neonatal IV therapy*. Paediatric Anaesthesia, 2013. **23**(1): p. 9-21.
8. Rothschild, J.M., et al., *A controlled trial of smart infusion pumps to improve medication safety in critically ill patients*. Critical Care Medicine, 2005. **33**(3): p. 533-540.
9. Steenhoek, A., *Geneesmiddelen via een infuus - II. Regeling van de toedieningssnelheid*. Pharmaceutisch Weekblad Scientific Edition, 1981. **3**(1): p. 909-916.
10. Fraser, N., et al., *Intravenous fluid therapy: A randomized controlled trial to investigate the effectiveness of the IV2TM flow medical device*. Journal of Clinical Nursing, 2007. **16**(9): p. 1593-1601.
11. Bissett, I.P., Brandt, T.P., Windsor, J.A., *Survey of intravenous fluid therapies and accuracy of gravity-fed infusions in a teaching hospital*. Samoa Medical Journal, 2010. **2**(2): p. 25-28.
12. Carleton, B.C., et al., *Method for evaluating drip-rate accuracy of intravenous flow-regulating devices*. American Journal of Hospital Pharmacy, 1991. **48**(11): p. 2422-2426.
13. Cooper, D.M., T. Rassam, and A. Mellor, *Non-flushing of IV administration sets: An under-recognised under-dosing risk*. British Journal of Nursing, 2018. **27**(14): p. S4-S12.
14. Cousins, D.H., et al., *Medication errors in intravenous drug preparation and administration: A multicentre audit in the UK, Germany and France*. Quality and Safety in Health Care, 2005. **14**(3): p. 190-195.
15. Crass, R.E. and J.R. Vance, *In vivo accuracy of gravity-flow i.v. infusion systems*. American Journal of Hospital Pharmacy, 1985. **42**(2): p. 328-331.
16. Kaushal, R., et al., *Medication errors and adverse drug events in pediatric inpatients*. Journal of the American Medical Association, 2001. **285**(16): p. 2114-2120.
17. Feleke, S.A., M.A. Mulatu, and Y.S. Yesmaw, *Medication administration error: magnitude and associated factors among nurses in Ethiopia*. BMC Nurs, 2015. **14**: p. 53.
18. Cwladis, *Lecture 6: Introduction to IVs*, <http://www.cwladis.com/math104/lecture6.php>, Editor. 2021.

19. BD, *Alaris™ GP Plus Volumetric Pump with Guardrails™*, <https://www.bd.com/en-uk/products/infusion/infusion-devices/alaris-plus-platform-with-guardrails-safety-software/alaris-gp-plus-volumetric-pump-with-guardrails>, Editor. 2021.
20. Infinita, *Syringe pump HK-400*, <https://infinita-medical.eu/en/vet-equipment/250-syringe-pump-hk-400.html>, Editor. 2021.
21. Kim, U.R., R.A. Peterfreund, and M.A. Lovich, *Drug infusion systems: Technologies, performance, and pitfalls*. Anesthesia and Analgesia, 2017. **124**(5): p. 1493-1505.
22. Fiedorova, K., M. Augustynek, and M. Penhaker, *Influence of the use of gravity sets in a pressure volumetric infusion pump with an impact on the accuracy of infusion solution flows*. Lekar a Technika, 2020. **50**(1): p. 23-31.
23. Stull, J.C., et al., *Decreased flow accuracy from volumetric infusion pumps*. Crit Care Med, 1989. **17**(9): p. 926-8.
24. Buonora, J.E., *Management of gravity intravenous infusions in an austere environment using the DripAssist infusion rate monitor*. AANA Journal, 2019. **87**(1): p. 65-70.
25. Kemper, B., M. Koopmans, and R. Does, *Quality Quandaries*: The Availability of Infusion Pumps in a Hospital*. Quality Engineering, 2009. **21**: p. 471-477.
26. B.V., K. *Infuuspomp voor thuiszorg, anesthesie en medicatie*. 2021 [cited 2021 30/01/2021]; Available from: <https://www.klinimed.nl/medische-apparatuur/infuuspomp.html?dir=asc&order=price>.
27. Mediq. *B. braun infuussysteem intrafix safeset basic luer*. 2021 [cited 2021 30/01/2021]; Available from: <https://pluspunt.mediqmedeco.nl/bbraun-infuussysteem-intrafix-safeset-basic-luer-180-cm-4063000-steriel.html>.
28. Shah, K., et al., *Maji: a new tool to prevent overhydration of children receiving intravenous fluid therapy in low-resource settings*. Am J Trop Med Hyg, 2015. **92**(5): p. 1053-8.
29. Crotti, N., *Next COVID-19 device shortage? 'Smart' infusion pumps*. 2020, Medical Design & Outsourcing.
30. Slabodkin, G., *The latest coronavirus shortage: hospital infusion pumps*. 2020, MedTech Dive.
31. Buckley, B. and D. Wild, *Strategies for Managing Smart Pumps During COVID-19*. 2020.
32. Judy Smetzer, B., RN, FISMP, et al., *Planning for anticipated shortage of smart infusion pumps and dedicated administration sets*. ISMP Medication Safety Alert! Acute Care, 2020. **25**(7).
33. ISO, *8536-14 Part 14: Clamps and flow regulators for transfusion and infusion equipment without fluid contact*, in *Infusion equipment for medical use*. 2016, ISO.
34. Maiguy-Foinard, A., et al., *Criteria for choosing an intravenous infusion line intended for multidrug infusion in anaesthesia and intensive care units*. Anaesthesia Critical Care and Pain Medicine, 2017. **36**(1): p. 53-63.
35. Peterfreund, R.A. and J.H. Philip, *Critical parameters in drug delivery by intravenous infusion*. Expert Opinion on Drug Delivery, 2013. **10**(8): p. 1095-1108.
36. Loner, C., et al., *Accuracy of Intravenous Infusion Flow Regulators in the Prehospital Environment*. Prehospital Emergency Care, 2018. **22**(5): p. 645-649.
37. Fonkalsrud, E.W., K. Carpenter, and M. Adelberg, *A new even-flow intravenous infusion clamp*. Archives of surgery (Chicago, Ill. : 1960), 1971. **102**(5): p. 530-531.
38. Calabrese, A.D., et al., *Medication administration errors in adult patients in the ICU*. Intensive Care Med, 2001. **27**(10): p. 1592-8.
39. Lee, P., *Risk-score system for mathematical calculations in intravenous therapy*. Nurs Stand, 2008. **22**(33): p. 35-42.

40. Steenhoek, A., *Geneesmiddelen via een infuus - III. Diameterregelaars: beschrijving en in vitro onderzoek; kostenaspect*. Pharmaceutisch Weekblad, 1982. **117**: p. 57-67.
41. Caruba, T., et al., *Evaluation of flow rate regulators for intravenous infusion*. Annales Francaises d'Anesthesie et de Reanimation, 2009. **28**(11): p. 936-942.
42. Chaput de Saintonge, D.M., J. Dixon, and M.S. Newman, *Letter: Variation in intravenous infusion rates*. Br Med J, 1974. **4**(5943): p. 532-3.
43. Clarke, E.W., J.P. Jamison, and J.B. Quartey-Papafio, *Impairment of flow in routine gravity-fed intravenous infusions to surgical patients*. Clinical Science, 1979. **57**(6): p. 515-520.
44. Flack, F.C. and T.D. Whyte, *Behaviour of Standard Gravity-Fed Administration Sets used for Intravenous Infusion*. British Medical Journal, 1974. **3**(5928): p. 439-443.
45. Simon, N., et al., *Mathematical and physical model of gravity-fed infusion outflow: Application to soft-bag-packed solutions*. European Journal of Drug Metabolism and Pharmacokinetics, 2011. **36**(4): p. 197-203.
46. Ziser, M., M. Feezor, and M.W. Skolaut, *Regulating intravenous fluid flow: controller versus clamps*. American Journal of Hospital Pharmacy, 1979. **36**(8): p. 1090-1094.
47. Rooker, J.C. and D.A. Gorard, *Errors of intravenous fluid infusion rates in medical inpatients*. Clinical Medicine, Journal of the Royal College of Physicians of London, 2007. **7**(5): p. 482-485.
48. Gundersen, J., *Pitfalls in Drip-Infusion Technique: A New Device for Automatic Control of Infusion Rate*. Acta Anaesthesiologica Scandinavica, 1972. **16**(2): p. 117-122.
49. Laufer, N., et al., *A New Infusion Flow Stabilizer*. Archives of Surgery, 1977. **112**(1): p. 53-54.
50. Park, K., et al., *Infusion volume control and calculation using metronome and drop counter based intravenous infusion therapy helper*. International Journal of Nursing Practice, 2013. **19**(3): p. 257-264.
51. Lie L., S.L., Wyatt L., Eijssen M., *Het juiste infuussysteem voor de juiste situatie*. 2020: p. 89.
52. Alexander, M.R., *IV infusion devices: Are they always justified?* Drug Intelligence and Clinical Pharmacy, 1987. **21**(3): p. 255-257.
53. Bivins, B.A., et al., *Electronic Flow Control and Roller Clamp Control in Intravenous Therapy: A Clinical Comparison*. Archives of Surgery, 1980. **115**(1): p. 70-72.
54. Monidor, *Monidrop w2*, <https://monidor.com/assets/images/monidrop-w2.png>, Editor. 2021.
55. Vetland, *DripAssist Fluid Administrator*, https://vetlandmedical.com/vet_products/drip-assist/, Editor. 2021.
56. Munro, S., *Safer, Low Cost, Intravenous Fluid Delivery: The Monidrop Infusion System*. Journal of Perioperative Practice, 2019. **07**(06).
57. Labs, S., *DripAssist 4 Page Promo Booklet*, in ShiftLabs. Seattle, United States.
58. Fabrycky, W., *Systems Analysis: Its Proper Utilization in Systems Engineering Education and Practice*. 2015.
59. AnthroTronix, *Engineering Process Model*, <https://www.anthrotronix.com/rd-capabilities/overview/>, Editor., AnthroTronix.
60. Donders, W.E.C., *Flow regulators for gravity-driven infusion*. 2021.
61. ISO, *8536-4 Part 4: Infusion sets for single use, gravity feed*, in *Infusion equipment for medical use*. 2019, ISO.

62. Al Salloum, H., et al., *Characterization of the surface physico-chemistry of plasticized PVC used in blood bag and infusion tubing*. Materials Science and Engineering C, 2017. **75**: p. 317-334.
63. Bernard, L., et al., *Effects of flow rate on the migration of different plasticizers from PVC infusion medical devices*. PLoS ONE, 2018. **13**(2).
64. Petrachi, T., et al., *Microscopic and chemical characterization of PVC tube used for dialysis lines: A new approach*. International Journal of Artificial Organs, 2021. **44**(2): p. 75-84.
65. Braun, B., *Roller Clamp for IV administration sets*, <https://www.bbraun.nl/content/dam/catalog/bbraun/bbraunProductCatalog/S/AEM2015/nl-nl/b1/brochure-rollerclampforivadministrationsetseng.pdf>, Editor.
66. Systèmes, D., *SolidWorks*. 2020, Vélizy-Villacoublay, France.
67. Systèmes, D. *Hyperelastic Blatz-Ko Model*. 2020 [18/06/2021]; Available from: https://help.solidworks.com/2020/english/SolidWorks/cworks/c_Hyperelastic_Blatz-Ko_Model.htm.
68. White, F.M., *Fluid mechanics*. 2017.
69. Ashby, M.F., H. Shercliff, and D. Cebon, *Materials : engineering, science, processing and design*. 2019.
70. Ashby, M.F., H. Shercliff, and D. Cebon, *Materials : engineering, science, processing and design*. 2014.
71. Haydock, M.D., et al., *Interaction between objective performance measures and subjective user perceptions in the evaluation of medical devices: A case study*. International Journal of Technology Assessment in Health Care, 2016. **31**(5): p. 297-303.
72. Council, E., *Regulation (EU) 2017/745 on medical devices*. 2017, Official Journal of the European Union.
73. (Ltd), M.O. *Monidrop W Infusion monitor*. 2021; Available from: <https://monidor.com/monidrop/>.
74. Granta, *EduPack*. 2020, Ansys, Canonsburg, Pennsylvania, U.S.
75. MathWorks, *MATLAB*. 2021, MathWorks, Natick, Massachusetts, USA.
76. ADERUBAAGU, M., *INTERRUPTING MECHANISM OF CLAMPING DEVICE FOR ADJUSTING FLOW OF FLUID IN PLASTIC TUBING*, JPH0718489B2, Editor. 17/11/1988.
77. MARVIN, A. and A. M., *PINCH VALVE*, AU1943676A, Editor. 18/05/1978.
78. ADERUBAAGU, M., *CLAMP FOR CONTROLLING FLUID FLOW IN PLASTIC TUBE*, JPS53103685A, Editor. 09/09/1978.
79. -, *SAMENSTEL VAN SLANG EN KLEM.*, NL165936B, Editor. 10/03/1971.
80. Thorlabs. *PT1/M - 25.0 mm Translation Stage with Standard Micrometer, M6 Taps* Newton, New Jersey, United States 2021; Available from: <https://www.thorlabs.de/thorproduct.cfm?partnumber=PT1/M#ad-image-0>.
81. Futek. *Miniature S-Beam Jr. Load Cell 2.0*. Irvine, CA 92618 USA 2021; Available from: <https://www.futek.com/store/load-cells/s-beam-load-cells/miniature-s-beam-jr-LSB205/FSH04097>.
82. Futek. *Miniature S-Beam Jr. Load Cell*. Irvine, CA 92618 USA 2021; Available from: <https://www.futek.com/store/load-cells/s-beam-load-cells/miniature-s-beam-LSB200/QSH02188>.
83. Scaime, *Strain gage conditioner CPJ*, https://scaime.com/media/thumbs/cpj-2s-web_465x330.jpg, Editor. 2021.
84. Instruments, N., *NI USB-6008*, <https://www.ni.com/nl-nl/support/model.usb-6008.html>, Editor. 2021, Austin, Texas, U.S.

85. Instruments, N., *LabVIEW*. 2018, Austin, Texas, U.S.
 86. Dell. *Latitude 5570*. Round Rock, Texas, USA.
 87. Monidor, *Monidrop W Infusion monitor*, in <https://monidor.com/materiaalit/monidrop-manual-en.pdf>. 2021.
 88. MARVIN, A. *Clamp for adjusting the flow opening in a plastic hose.*; Available from: <https://patents.google.com/patent/NL178810C/en>.
 89. Systèmes, D., *SolidWorks Visualize*. 2020, Vélizy-Villacoublay, France.
 90. Company, R. *Part Design Guidelines for Injection Molded Thermoplastics*. 2017; Available from: <https://www.rtpcompany.com/wp-content/uploads/RTP-Part-Design-Guidelines-for-Injection-Molded-Thermoplastics.pdf>.
 91. cthornsberry, *Injection Molding: Rib Design*, in *3space*. 2019.
 92. HUBS. *The manufacturing & design guide Injection molding*. 2021; Available from: <https://www.hubs.com/guides/injection-molding/#design-for-injection-molding>.
 93. Systems, D. *Basics of Injection Molding Design*. 2021; Available from: <https://www.3dsystems.com/quickparts/learning-center/injection-molding-basics>.
 94. Xometry. *Design Guide: Injection Molding*. 2021; Available from: https://cdn2.hubspot.net/hubfs/340051/Design_Guides/Xometry_DesignGuide_InjectionMolding.pdf.
 95. Lukis, L., *Protolabs*. www.protolabs.com, Maple Plain, Minnesota, United States.
 96. Jeroen Bosch Ziekenhuis (JBZ). Available from: jeroenboschziekenhuis.nl.
 97. Laboratories, A., *Clamp compare*, <https://www.adelberglaboratories.com/images/clamp-compare.jpg>, Editor. 2002.
 98. Chen, Y.-M. and J.-J. Liu, *Cost-effective design for injection molding*. Robotics and Computer-Integrated Manufacturing, 1999. **15**(1): p. 1-21.
 99. ERIKS. *RECORD Metaalfolie Staal roestvrij 150x2500x0,200mm*. 2021; Available from: <https://shop.eriks.nl/nl/bevestigingsmaterialen-precisie-folie-en-vulplaten/metaalfolie-staal-roestvrij-150x2500x0-200mm-23422520/>.
 100. Benatar, A., *12 - Ultrasonic welding of plastics and polymeric composites*, in *Power Ultrasonics*, J.A. Gallego-Juárez and K.F. Graff, Editors. 2015, Woodhead Publishing: Oxford. p. 295-312.
 101. Grewell, D. and A. Benatar, *Welding of Plastics: Fundamentals and New Developments*. International Polymer Processing, 2007. **22**(1): p. 43-60.
 102. International, A., *ASTM D648-18, Standard Test Method for Deflection Temperature of Plastics Under Flexural Load in the Edgewise Position*. 2018, www.astm.org: West Conshohocken, PA.
 103. Omnexus. *HDT @0.46 Mpa (67 psi)*. 2021; Available from: <https://omnexus.specialchem.com/polymer-properties/properties/hdt-0-46-mpa-67-psi>.
 104. Paar, A. *Viscosity of Water*. 2008 [cited 2021 22/04/2021]; Available from: <https://wiki.anton-paar.com/en/water/>.
 105. White, F.M., *Fluid Mechanics*. 7th in SI Units ed. 2011, New York: McGraw-Hill.
 106. Lide, D.R., *CRC Handbook of Chemistry and Physics, 86th Edition*. 2005: Taylor & Francis.
 107. Tonog, P. and A.D. Lakhkar, *Normal Saline*, in *StatPearls*. 2021, StatPearls Publishing
- Copyright © 2021, StatPearls Publishing LLC.: Treasure Island (FL).
108. Futek, *LSB200 Miniature S-Beam Jr. Load Cell*, <https://media.futek.com/images/store/LSB200-MINIATURE-S-BEAM-2.JPG>, Editor. 2021.

109. Dell, *Latitude 15 5000 Series*, <https://www.dell.com/you/business/p/latitude-e5570-laptop/pd>, Editor. 2021.
110. Thorlabs. *PT101/M - Base Plate for PT Series Translation Stages, M6 Mounting Holes*. Newton, New Jersey, United States 2021; Available from: <https://www.thorlabs.com/thorproduct.cfm?partnumber=PT101/M>.
111. Qosina. *Medical Roller Clamps*. 2021 [cited 2021 07/06/2021]; Available from: <https://www.qosina.com/roller-clamps-2>.
112. Braun, B. *Roller Clamps*. 2021 [cited 2021 07/06/2021]; Available from: <https://us.bbraunoem.com/en/products/b/oem-us-roller-clamps.html>.
113. Promepla. *Roller clamp*. 2021 [cited 2021 07/06/2021]; Available from: <https://catalog.promepla.com/subcategory/roller-clamps?field=genericmaterial&dir=asc>.
114. Medical, E. *Roller Clamps*. 2021 [cited 2021 07/06/2021]; Available from: <https://catalog.elcam-medical.com/catalogue/group/82/nameblock/Roller-Clamps>.
115. Gruntfest, I.J., E.M. Young Jr, and W. Kooch, *Mechanical behavior of plastics*. Journal of Applied Physics, 1957. **28**(10): p. 1106-1111.

Appendix A – Fluid Mechanics

Model

Friction is increasing when pinching the tubing. Thus, narrowing its diameter causes an increase in flow velocities and therefore an increase in friction losses (squared). In Figure 45, the pinching configuration is displayed. The flow was assumed to be at steady state (fully developed) and laminar. Furthermore, the pinching was assumed to create an orifice at the centre of a round pipe of inner diameter D_i . The same setup as described in Appendix E is used.

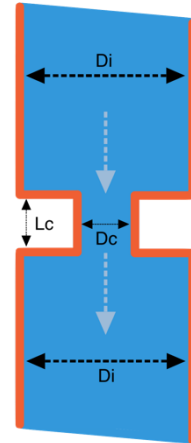


Figure 45 - Simplification of the pinching configuration with inner diameter D_i , contraction diameter D_c and contraction width L_c .

Parameters

Table 6 provides the used parameters, corresponding values and the source it comes from.

Table 6 – Parameters, values and sources of the model shown in Figure 45.

Parameter and symbol	Value	Source
Inner diameter, D_i	3 mm	Appendix B
Length tube, L	1.5 m	Appendix E
Density water, ρ	998.02 kg/m ³	At 21°C [104]
Dynamic viscosity water, μ	0.0009775 Pa*s	At 21°C [104]
Maximum volume flow rate, Q_{\max}	19,000 mL/h	Appendix C
Bag-cannula height, z	1.87 m	Appendix E
Loss coefficient inlet K_{inlet}	0.5	[105]
Loss coefficient exit K_{exit}	1	[105]
Gravitational acceleration g	9.81 m/s ²	-

Equations

The equations used for this model are given below.

$$\text{Reynolds number [105]} \quad Re = \frac{v * D_i * \rho}{\mu} \quad \text{Equation 4}$$

$$\text{Flow velocity [105]} \quad v = \frac{Q}{A} \quad \text{Equation 5}$$

$$\text{Surface tube} \quad A = \pi * \left(\frac{D_i}{2}\right)^2 \quad \text{Equation 6}$$

$$\text{Pressure drop tube due to friction [105]} \quad \Delta p_f = \frac{1}{2} * \rho * v^2 * f * \frac{L}{D_i} \quad \text{Equation 7}$$

Friction factor laminar pipe flow [105]

$$f = \frac{64}{Re} \quad \text{Equation 8}$$

Pressure drop due to minor losses [105]

$$\Delta p_m = \frac{1}{2} * \rho * v^2 * \Sigma K \quad \text{Equation 9}$$

Conservation of mass, where 2 denotes the area after pinching and c the area of pinching [105].

$$v_c * A_c = v_2 * A_2 \quad \text{Equation 10}$$

Where Q is the volume flow rate [m^3/s], and ΣK is the sum of all the minor loss coefficients [-].

Calculations

First, it was checked whether the pipe flow was indeed laminar in free flow configuration ($D_c = D_i$). Using the parameters of Table 6 and Equation 4, 5, and 6, a Reynolds number of 229 was found. Because this value is far below the laminar boundary value of 2300 [105], it can indeed be considered laminar.

Then, the influence of minor losses was examined. The pressure drop due to minor losses was compared to the pressure drop due to friction. Parameters of Table 6 and Equation 7, 8 and 9 give:

$$\frac{\Delta p_{f,tube}}{\Delta p_m} = \frac{\Sigma K * 64 * L}{Re * D_i} = 93.2$$

Thus, the pressure drop due to friction is 93.2 as high than due to minor losses, and therefore the minor losses were regarded as negligible.

Using these findings a steady flow energy was set up [105]:

$$p_1 + \frac{\alpha}{2} * \rho * v_1^2 + \rho * g * z_1 = p_2 + \frac{\alpha}{2} * \rho * v_2^2 + \rho * g * z_2 + \Delta p_{f,tube} + \Delta p_{f,contraction} + \Delta p_{other}$$

Where Δp_{other} is the pressure drop [Pa] of the components labelled A-D from Figure 15. $\Delta p_{f,tube}$ is the pressure drop due to friction over the tubing, excluding the contraction part (Figure 45). The friction and corresponding pressure drop of the contraction part are labelled as $\Delta p_{f,contraction}$. The subscript one denotes the situation at the reservoir and two at the end of the tubing. α is the kinetic energy correction factor [-], set at 2.0 for fully developed laminar flow [105]. p_1 and p_2 are both the atmospheric pressure [Pa] and therefore are cancelled out. The velocity at the surface of the large reservoir can be regarded as negligible ($V_1 \approx 0 \frac{\text{m}}{\text{s}}$). Furthermore, the tubing's end is set at height zero ($z_2 = 0 \text{ m}$). Given the above and the earlier mentioned parameters, the pressure drop Δp_{other} for free flow ($\Delta p_{f,contraction} = 0 \text{ Pa}$) was computed:

$$\Delta p_{other} = 13,859 \text{ Pa}$$

This pressure drop was assumed to be fixed when the tube is compressed as described. The pressure drops due to friction is (Equation 7):

$$\Delta p_{f,tube} = \frac{1}{2} * \rho * v_2 * \frac{64 * \mu}{D_i * \rho} * \frac{L - L_c}{D_i}$$

$$\Delta p_{f,contraction} = \frac{1}{2} * \rho * v_c * \frac{64 * \mu}{D_c * \rho} * \frac{L_c}{D_c}$$

Combined with Equation 10, the following steady flow energy balance is formed:

$$\rho * g * z_1 = \frac{\alpha}{2} * \rho * v_2^2 + v_2 * \frac{32 * \mu * (L - L_c)}{D_i^2} + v_2 * \frac{A_2 * 32 * \mu * L_c}{A_c * D_c^2} + \Delta p_{other}$$

Where v_2 is the flow rate [m³/s], depending on the chosen L_c [mm] and D_i [mm].

Matlab results

The above found steady flow energy balance was visualised with the use of MATLAB [75]. The graph representing the volume flow rate [mL/h] versus pinching depth [mm] for several pinching widths [mm] is shown in Figure 46. For each L_c and D_i -combination it was checked if the flow is still laminar, otherwise the model does not hold.

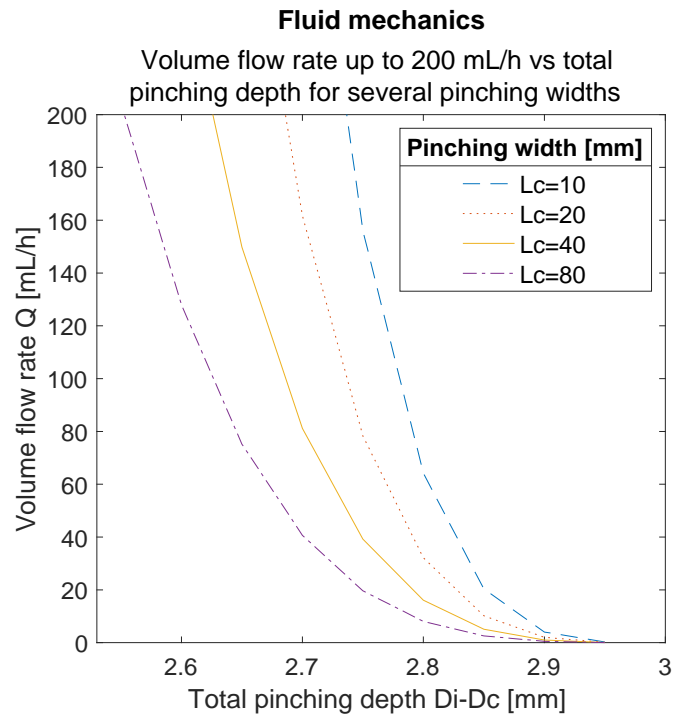



Figure 46 – Fluid mechanics: volume flow rate [mL/h] up to 200 mL/h versus total pinching depth [mm] for several pinching widths.

Appendix B – Technical Data Sheet of Volumed infusion set

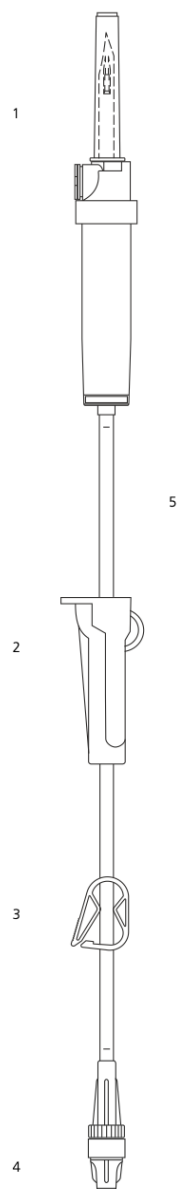


TECHNICAL DATA SHEET

Product Name	Volumed ® Set
Product Description	Volumed Set, DEHP-Free PVC, 235cm, Robson Clamp and Male Luer Lock
Features	Sterile, apyrogenic. Product to be sold individually
Product Class	Disposable medical device – IIa Class
Intended Use	Medical device used for physiological (saline) infusion and pharmaceutical solutions
CND Code	A03010101
CE Certificate	Certificate Nr. MED 27039 issued by Notified Body nr.0476
D.M. List Registration	13549/R
Manufacturing Process	The product is totally manufactured in clean room Class 100000 – ISO 8
Single Packaging	Blister (printed medical paper + transparent film PP/PE)
Multiple Packaging	Nr 100 in 1 cardboard box (cm. 24x39x39)
Product Duration	5 Years
Storage Method	
Disposal Method	After use, dispose of the product as hospital waste
Method of Sterilization	Ethylene Oxide – Residual ETO ≤ 10ppm (ref. “Farmacopea Europea Ufficiale”)
Test	Physical test according to ISO 594-1, ISO 594-2, ISO 8536/4 Chemical and Biological test according to “Farmacopea Italiana Ufficiale” and “Farmacopea Europea Ufficiale”, ISO 11737-1
Manufacturer Informations	Phoenix s.r.l.; Via Leonardo da Vinci -41038 San Felice sul Panaro (MO); Tel+Fax 0039 0535 20085; eMail phoenixbiomed@hotmail.it – info@phoenixbiomed.it; CF+P.IVA 02501570366

arcomed Code	Description	Priming Volume	Box Quantity
APPPK0J	Volumed Set, DEHP-Free PVC, 235cm, Robson Clamp and Male Luer Lock	16 ml	100

TECHNICAL DRAWING



Warning
 Do not use with blood or plasma.
 Use only with PVC compatible solutions.
 Use with Volumed® µVP 5005/7000 PVC Pumps

Components list: APPPKOJ	
1	Protective Hood + Vented Spike + Air Inlet+ Drip tube + DEHP Free PVC Drip Chamber + 15µm Filter
2	Roller Clamp (orange)
3	Robson Clamp
4	Male Luer Lock + Protection Cap
5	Ø 3x4.1 Tubing DEHP Free PVC - 2200 mm

Appendix C – Free flow rate experiment

Volumed infusion set

Purpose

Identify the free flow rate for the Volumed infusion set (Appendix B).

Method and setup

The same method and setup as described in Appendix E was used.

Measurement protocol

Plastic wheel

1. Execute the measurement preparations step 1-6 of Appendix E.
2. Set the loop time to 50 ms.
3. Fill the reservoir with 7 litres of (recycled) purified water; up to the marking on the reservoir.
4. Empty the measuring cup and set the offset of the scale load cell in LabVIEW.
5. Make sure the end of the tubing is exactly above the middle of the scale load cell.
6. Open the ball valve.
7. Start saving the LabVIEW data.
8. Let the experiment run until the measuring cup is almost full.
9. Stop the LabVIEW script.
10. Close the ball valve.
11. Repeat the process for each new infusion set.

Results

Figure 47 shows the volume over time for six different infusion sets. The slope is constant, and a first-order polynomial was fitted to extract the corresponding flow rate for each infusion set.

*Flow rate infusion set 1: 19,186 mL/h,
Flow rate infusion set 2: 19,198 mL/h,
Flow rate infusion set 3: 19,345 mL/h,
Flow rate infusion set 4: 18,883 mL/h,
Flow rate infusion set 5: 18,975 mL/h,
Flow rate infusion set 6: 18,771 mL/h.*

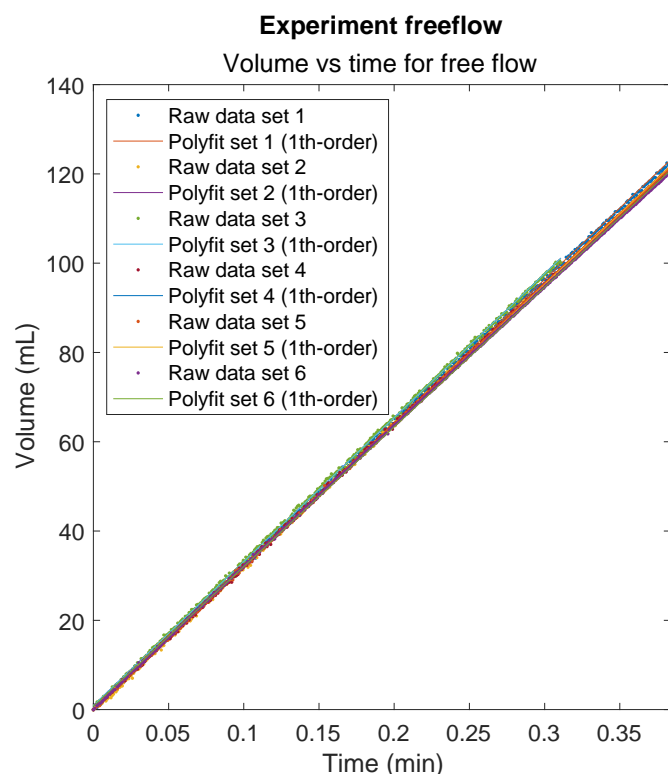


Figure 47 – Free flow rate experiment: volume (mL) over time (min) for the six Volumed infusion sets. A first-order polynomial was fitted through the RAW data.

Appendix D - SolidWorks flow simulations results

SolidWorks visuals

Figure 48 and 49 illustrate the two models containing two and three pinching areas for the SolidWorks flow simulations. Figure 50 and 51 show one stage of the SolidWorks flow simulations for each model.

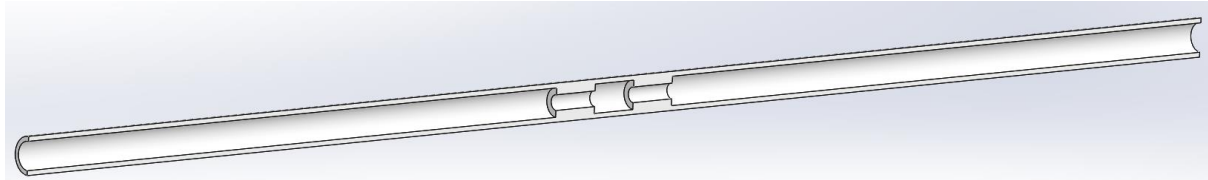


Figure 48 – Section view of the 150mm long 3x4.1 mm PVC tubing model with two pinching areas. Created with SolidWorks [66].

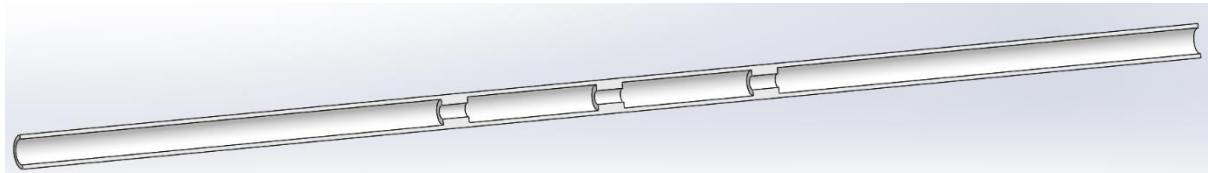


Figure 49 - Section view of the 150mm long 3x4.1 mm PVC tubing model with three pinching areas. Created with SolidWorks [66].

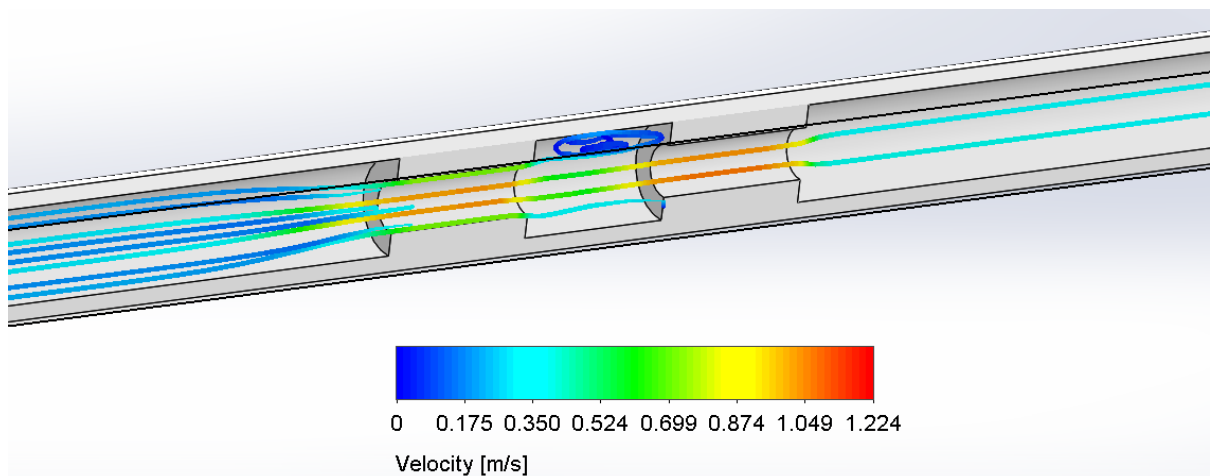


Figure 50 - Close-up section view of flow simulation for the model in Figure 48 for pinching diameter $D_i=1.6\text{mm}$. The colours indicate the fluid velocity [m/s], and the legend is shown below the model. Created with SolidWorks [66].

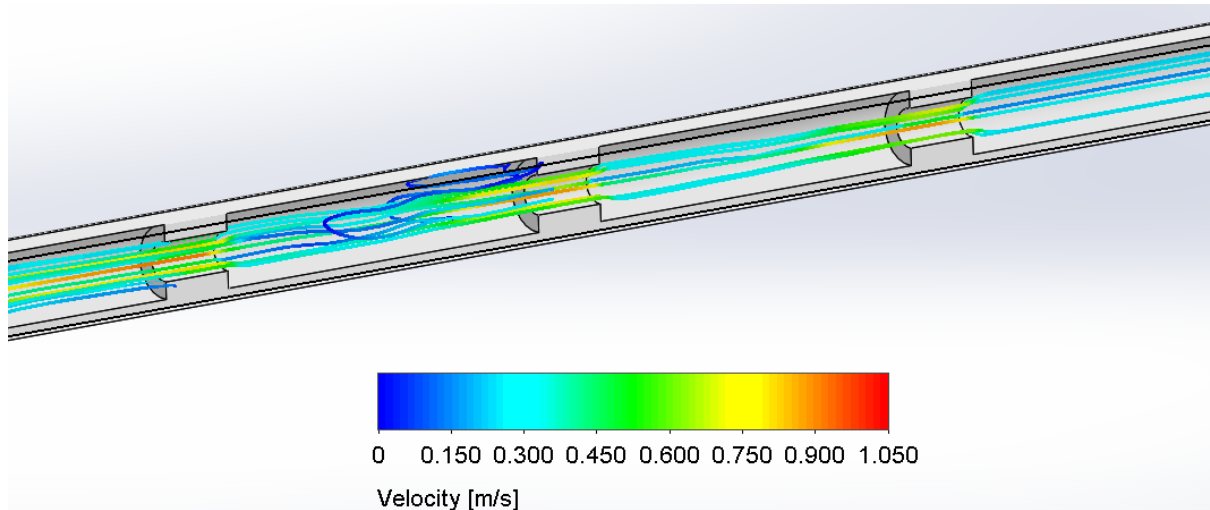


Figure 51 - Close-up section view of flow simulation for the model of Figure 49 for pinching diameter $D_i=1.6\text{mm}$. The colours indicate the fluid velocity [m/s], and the legend is shown below the model. Created with SolidWorks [66].

Matlab results

MATLAB [75] was used for creating visualisations of the data extracted from SolidWorks. Figure 52, 53 and 54 show the results for flow rates up to 200 mL/h.

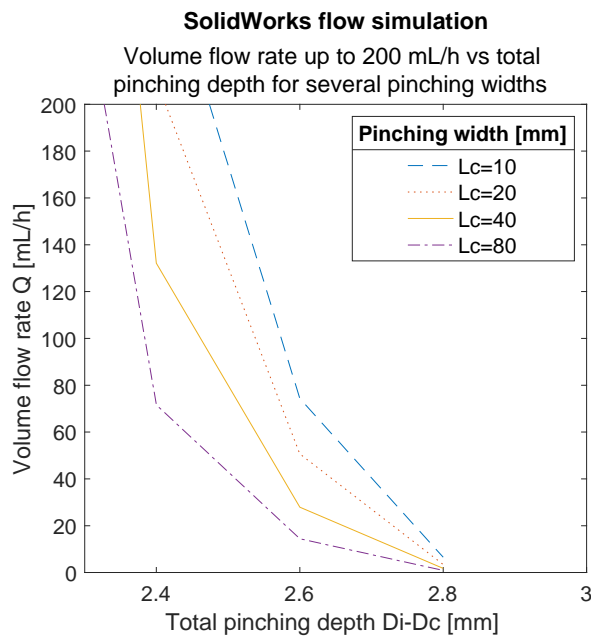


Figure 52 – SolidWorks flow simulation: volume flow rate [mL/h] up to 200 mL/h versus total pinching depth [mm] for several pinching widths.

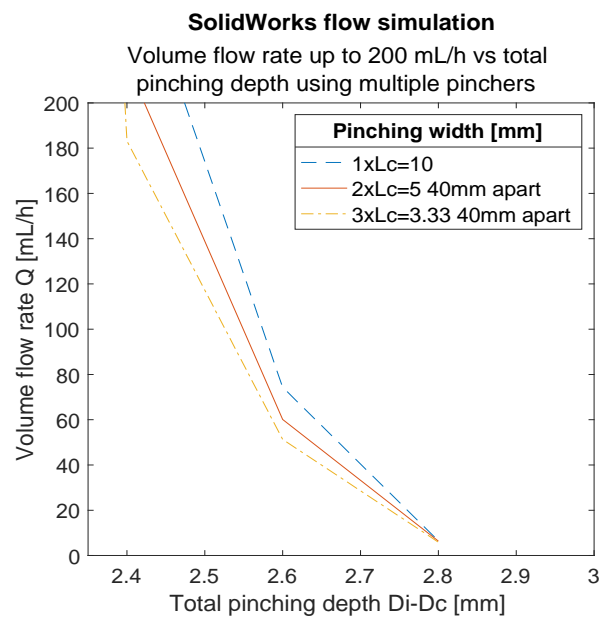


Figure 53 – SolidWorks flow simulation: volume flow rate [mL/h] up to 200 mL/h versus total pinching depth [mm] for a 10mm wide pincher, two 5mm wide pinchers with 40mm in between and three 3.33mm wide pinchers with 40mm in between.

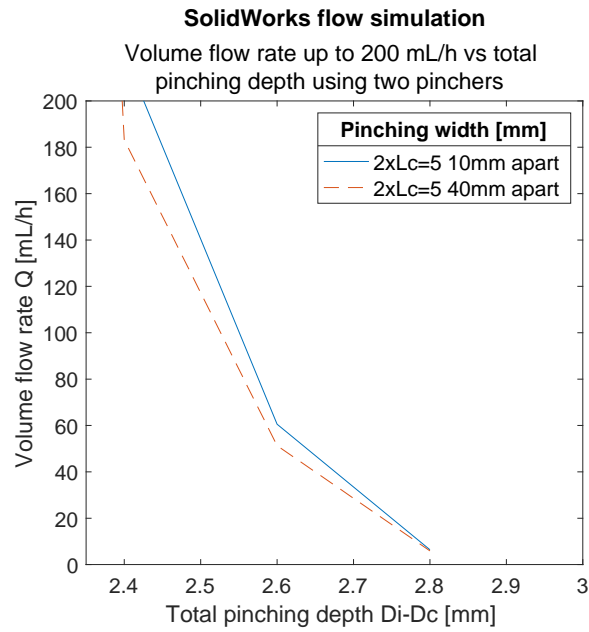


Figure 54 - SolidWorks flow simulation: volume flow rate [mL/h] up to 200 mL/h versus total pinching depth [mm] for two 5mm wide pinchers with 10mm and 40mm in between.

Appendix E - Experiments for evaluation of partial solutions

Purpose

Four lab experiments were conducted, which were subdivided into three different categories and corresponding purposes:

Material experiment

Research the influence of the material choice on the flow rate deviation [ml/h] over time [s].

Shape experiments

- Research the influence of the pincher's shape on the regulation range: flow rate [ml/h] versus pinching depth [mm].
- Research the influence of the pincher's shape on the flow rate deviation [ml/h] over time [s].

Contact area experiment

Research the influence of the pincher's contact area on the deviation of the flow rate [ml/h] over time [s].

Method

During the experiments purified water was used as infusion fluid because the dynamic viscosity and density is comparable to 0.9% NaCl; $\mu_{water,20^{\circ}C} = 1.00 \text{ mPa}\cdot\text{s}$, $\rho_{water,20^{\circ}C} = 1.00 \text{ g/cm}^3$ [104] and $\mu_{0.9\% \text{ NaCl},20^{\circ}C} = 1.02 \text{ mPa}\cdot\text{s}$, $\rho_{0.9\% \text{ NaCl},20^{\circ}C} = 1.00 \text{ g/cm}^3$ [106]. This fluid 0.9% NaCl is commonly used for intravenous infusion [107]. Furthermore, the use of water during testing is conform ISO 8536-4 [61]. The influence of water evaporation was already researched before in a similar setup and can be neglected [51]. Because of the clogging of the filter in the drip chamber in this earlier research, purified water was used.

Figure 55 shows the experiment setup. The setup composes of aluminium extrusion profiles and was considered rigid. A wide water reservoir (A) was chosen to keep the bag-cannula height difference as constant as possible. Besides, the reservoir was placed as high as possible within the limits of the available lab space. This way, the bag-cannula height difference due to bag deflation relative to the overall hydrostatic pressure was reduced. The decrease of the hydrostatic pressure

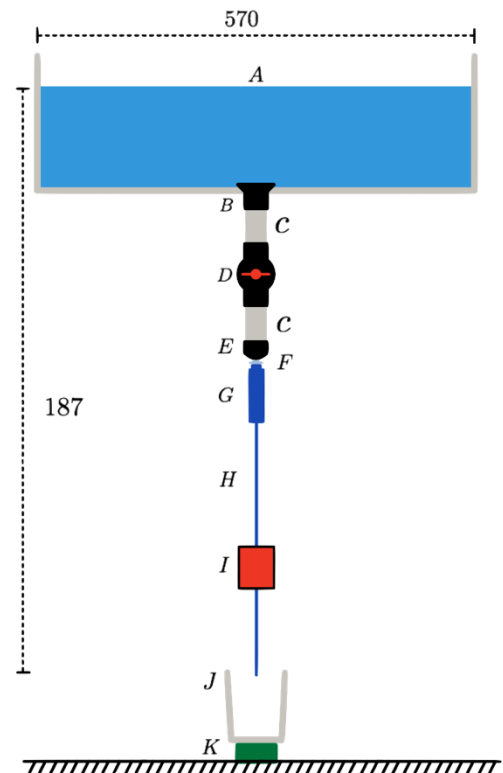


Figure 55 – Experiment setup. A: water reservoir, B: PVC flange feedthrough, C: PVC pipe, D: PVC ball valve, E: PVC end cap, F: infusion-bag insert, G: drip chamber and Monidrop, H: tubing, I: pinching setup (Figure 56), J: measuring cup, K: load cell.

can be simply calculated using the specifications provided in Table 7 and Figure 55:

Maximum volume change $V_{max} = 250 \text{ mL} = 0.0025 \text{ m}^3$, Bag-cannula height $z = 1.87 \text{ m}$, width reservoir $w_r = 0.39 \text{ m}$, length reservoir $L_r = 0.57 \text{ m}$. Thus, the maximum height difference of the reservoir $\Delta h_r = 0.011 \text{ m}$ and the relative decrease in pressure $\frac{\Delta h_{reservoir}}{z} \times 100 = 0.6 \%$.

Before each test, the reservoir was filled with the same amount of purified water (7L), so the hydrostatic pressure at each test was identical.

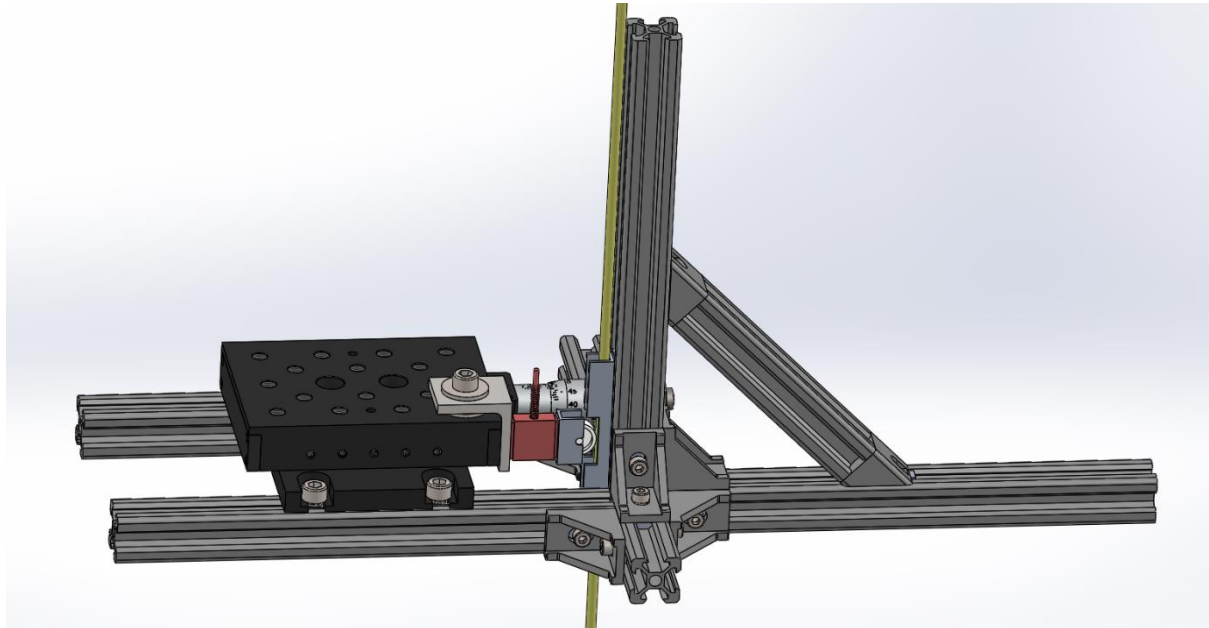


Figure 56 – SolidWorks overview of the pinching setup. The setup existed of a Thorlabs linear stage (black) mounted on a configuration of aluminium extrusion profiles combined with connection elements (grey). The infusion line (yellow) is clamped in between the vertical profile and the pincher (white) with a load cell (red). This load cell is mounted on the linear stage.

The water will flow from the reservoir through the ball valve (D) into the infusion set with the Monidrop attached (G, H). A linear stage, with a calibrated load cell attached, will variably pinch the tube and therefore control the flow rate (label I of Figure 55 and 56). The pincher used to clamp the infusion line differed per experiment. The fluid flows from the infusion set in the measuring cup, placed on another calibrated load cell. That load cell acted as a scale to measure the fluid volume. A measurement chain (Figure 57) read out the load cells and processed the data. By converting the voltage from the load cell to a force, the flow volume

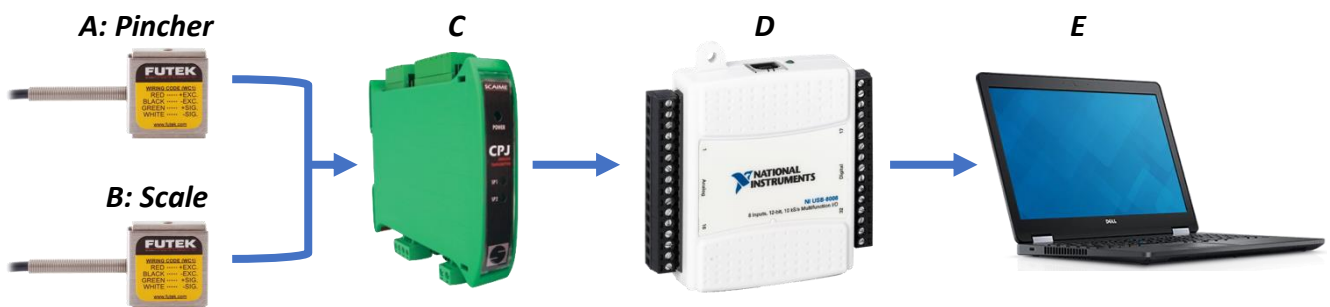


Figure 57 - Measurement chain. A: Futek LSB200 S-Beam jr. 4.5N load cell, adopted from [108]. B: Futek LSB200 S-Beam jr. 111N load cell. C: Scaime CPI Rail amplifier, adopted from [83]. D: National Instruments NI USB-6008 converter, adopted from [84]. E: Dell Latitude 5570 with LabVIEW 2018 [85], adopted from [109].

was computed. Using the elapsed time also the flow rate [mL/h] was found. The Monidrop was used for initial flow rate setting and as an extra check if the values from the load cell K were reasonable.

Because all the experiments were conducted under similar conditions and with the same protocol, predominantly random errors and no systematic errors were expected. Influences of the environment, like humidity and temperature, were assumed to be constant over all experiments. Also, possible vibrations of people passing by were considered negligible. Furthermore, minimal scatter between the samples was expected, and therefore the sample size was set at N=4.

According to the manufacturer, the measurement accuracy of the Monidrop is $\pm 1.8\%$ [87]. The Monidrop's display resolution is variable: the higher the flow rate, the lower the display resolution. The display resolution for a flow rate of 100 mL/h is 5 mL/h, so the total Monidrop uncertainty (including the measurement accuracy) is ± 4.3 mL/h. For flow rates below 50 mL/h, the display resolution is 1 mL/h, so the Monidrop uncertainty is ± 0.5 mL/h.

The load cells also have an uncertainty, which can be again based on its resolution, which is 1/1000 of the set maximum force. Thus, the load cell acting as scale provides an uncertainty of 0.0045N ($=0.46$ mL/h). The uncertainty of the load cell attached to the pincher is 0.111 N.

At last, the linear stage has engraved graduations every 0.01mm. The space between those graduations can be roughly distributed in ten parts, resulting in an uncertainty of 0.001mm.

General List of Materials (LoM)

The necessary materials for the experiment setup of Figure 55 are summarised in Table 7.

Table 7 - List of Materials (LoM) for the experiment setup.

Part	Amount	Specifications
Water reservoir	1	57x39x17cm (38 litres)
PVC glue	1	Bison PVC Adhesive
PVC pipe	1	32mm (outer diameter), length: 1.5m
PVC ball valve	1	32mm
PVC flange feedthrough	1	32mm
PVC end cap	1	32mm
Infusion bag	1	500mL
Infusion set	3	Volumed Set (Appendix B)
Measuring cup	1	Volume: 250mL
Load cell	1	Futek LSB200 S-Beam jr. 4.5N [82]
Amplifier	1	Scaime CPJ Rail [83]
Converter	1	National Instruments NI USB-6008 [84]
Monidrop	1	E001152 [73]
Pinching setup	1	-

In Table 8 the materials for the pinching setup of Figure 56 are shown.

Table 8 - List of Materials (LoM) for the pinching setup.

Part	Amount	Specifications
Linear stage	1	Thorlabs PT1/M [80]
Stage mount	1	Thorlabs PT101/M [110]

L-profile	1	3x3x2.5cm
U-profile	1	8.9x10x1.5mm, 9cm
Tubing	1	4mm (outer diameter), 1.5m
Load cell	1	Futek LSB200 S-Beam jr. 2.0 111N [81]
Aluminium extrusion profile	2	20x20mm, 300mm
Aluminium extrusion profile	3	20x20mm, 200mm
Aluminium extrusion profile	1	20x20mm, 100mm
Corner brackets profile incl. mounting material	5	20x20mm
45-degree connection incl. mounting material	2	20x20mm
Countersunk screw	4	M3 4mm
Washer	3	M6
Socket head screw	8	M6 20mm
Nut	2	M6
T-slot	2	M3
T-slot	4	M4

Data processing

LabVIEW 2018 [85] provided the forces applied on the calibrated load cells using its voltage. These data was saved in a .txt file with a force [N] for each set loop time period [ms].

For the load cell acting as scale, the force was converted to actual volume [mL] using Equation 11, assuming a constant water temperature of 21°C.

$$Volume [ml] = \frac{force [N]}{9.81 \left[\frac{m}{s^2} \right]} * 1.00 \left[\frac{g}{cm^3} \right] \quad \text{Equation 11}$$

Because the flow was dripping into the measuring cup, the scale's data consisted of repeatedly high peaks that settled afterwards. However, there was a clear overall trendline in the increase of the volume. A tenth-order polynomial was fitted to obtain this trendline. Because data fitting is a delicate and sensitive procedure, each run's data and possible trendline was analysed and checked thoroughly. Through this polynomial's derivative, the needed flow rate [mL/h] over time was derived.

The load cell's output attached to the pincher was processed immediately because no significant peaks as with the scale were expected.

Measurement preparations

- 1) Set the experiment up, as shown in Figure 55. If starting a new experiment, attach a non-used infusion set and carry out the free flow rate experiment of Appendix C. Furthermore, cut off a part of the tube, so the total height of the tubing setup is 1.87m (see Figure 55).
- 2) Visually check the infusion line for dents or kinks and replace if needed.
- 3) Put some water in the reservoir, open the PVC ball valve and fill the drip chamber up until one-third.
- 4) Close the PVC ball valve.
- 5) Connect the amplifiers and converter to the wall outlet. Attach the USB of the converter to the laptop.
- 6) Open up LabVIEW 2018:

- a) Check the name of the new file.
 - b) Check if the file type is set to .txt.
 - c) Check if the load cells are visible.
 - d) Check if the data will be saved.
- 7) Turn on the Monidrop and check the battery.

Material experiment

Pinching setup

Figure 58 shows a schematic of the pinching setup of this experiment. The flow rate was set to 100 mL/h by turning the linear stage and wheel away from its closed position. This position was maintained for 60 minutes, and the volume over time was measured. This volume was converted to a flow rate through data processing. This experiment was repeated four times ($N=4$) using a plastic wheel (Figure 59: left) and four times using a steel wheel (Figure 59: right). ABS, PE, Acetal, and PS are commonly used materials for the plastic roller clamp wheel [111-114]. Unfortunately, it was unknown which specific material was used in the wheel of the infusion set to be tested. The laser-cut steel wheel had the exact dimensions of the plastic wheel but was made of S235JR steel.

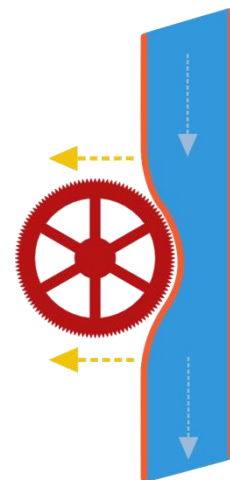


Figure 58 – Schematic illustration of the material experiment setup. The roller clamp (red) moves from its closed position.

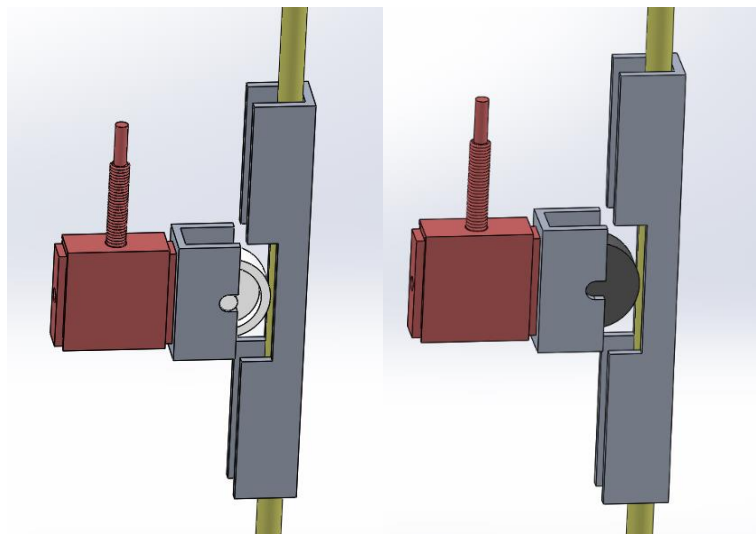


Figure 59 – SolidWorks model of pincher (white/dark grey) attached to the load cell (red). The infusion line (yellow) is guided by a housing (grey). Left: plastic wheel (white), right: steel wheel (dark grey)

Hypothesis

As the influence of bag deflation on the flow rate [45, 49] was minimised by using a wide water reservoir, the creep of the tubing [37, 43-45, 49] should be the main factor influencing the flow rate over time. Thus, the flow rate was expected to decrease over time. This decrease would be the highest in the first fifteen minutes as most creep occurs in that period [45]. However, during this experiment, the influence of the material choice of the pincher (roller clamp wheel) was researched.

Creep occurs when the melting point or glass temperature (amorphous materials) is approached [70]. It strongly relies on the applied load and temperature. The higher the load and/or temperature, the larger the creep strain.

Table 9 shows the melting and glass temperatures for the used materials. For metals, creep is often only of relevance when exceeding the temperature $T > 0.35 \cdot T_m$ [70], where T_m is the melting temperature. Using the above, creep was not expected to occur in the steel wheel or the setup's aluminium profiles.

Table 9 – Melting and glass temperatures of main materials used in the pincher setup. *: could be one of those materials.

Component	Material	Melting/glass temperature
Steel wheel	S235JR Steel	T_m : 1480-1530°C [74]
Setup	Aluminium	T_m : 524-650°C [74]
Plastic wheel*	Acetal	T_m : 160-175°C [74]
Plastic wheel*	PE	T_m : 125-132°C [74]
Plastic wheel*	ABS	T_g : 102-115°C [74]
Plastic wheel*	PS	T_g : 89.9-99.9°C [74]
Tubing	PVC	T_g : 79.9-87.9°C [74]

According to Ashby et al. [70], crystalline polymers with melting temperatures of 150-200°C as well as glassy polymers with melting temperatures of 50-150°C tend to slowly creep at room temperature when loaded. As the creep rate and significance depend on the melting and glass temperature, the PVC tubing was expected to show the most considerable creep effects. The occurrence of creep in PVC is a long known and researched phenomenon; in 1957, the first research on this topic appeared already [115]. However, depending on the specific used material, the pincher can also be of influence.

Measurement protocol

Plastic wheel

1. Execute the earlier mentioned list of 'measurement preparations'.
2. Attach the plastic wheel pincher (Figure 59: left).
3. Set the offset of the pinching load cell in LabVIEW.
4. Set the loop time to 1000ms.
5. Open the ball valve.
6. Turn the linear stage towards the tube until no fluid is entering the drip chamber.
7. Fill the reservoir with 7 litres of (recycled) purified water; up to the marking on the reservoir.
8. Empty the measuring cup and set the offset of the scale load cell in LabVIEW.
9. Make sure the tube is exactly above the middle of the scale load cell.
10. Start saving the LabVIEW data.
11. Turn the linear stage away from the tube until the Monidrop displays a value of 100 mL/h for 10 seconds.
12. Let the experiment run for 60 minutes without additional actions.
13. Note the Monidrop flow rate and stop the LabVIEW script.
14. Close the ball valve.
15. Turn the linear stage away from the tube until there is no contact anymore.
16. Mark the used part of the tube, let it recover for 10 minutes and shift it so a new run (N) on a new tubing part can be started.
17. Repeat steps 5-16 for four times (N=4).

Steel wheel

18. Attach the steel wheel pincher (Figure 59: right).
19. Repeat steps 5-17.

Shape experiment 1

Pinching setup

Again, the linear stage and its pincher are turned away from its closed position, but now incrementally by 0.01 millimetre. This process was repeated until the measuring cup was full. There was a pause of thirty seconds at each pinching depth. For each set pinching depth, the volume over time was measured. Through the data processing, this was converted to a flow rate. This experiment was repeated four times (N=4) using the same steel wheel pincher used in the material experiment (Figure 59: right, Figure 60: left). Then the process was repeated using a 44mm wide pincher (Figure 60: middle, Figure 61:left). Finally, a double 14mm wide pincher with the roller clamp wheel dimensions was used (Figure 60: right, Figure 61: right).

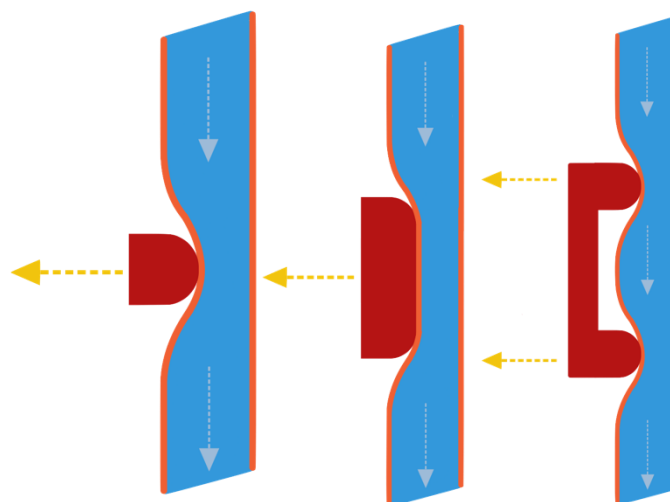


Figure 60 - Schematic illustration of shape experiment 1 setup. The steel pincher (red) moves from its closed position. Left: 14mm wide steel pincher, middle: 44mm wide steel pincher, right: two 14mm wide pinchers with a distance of 14mm in between.

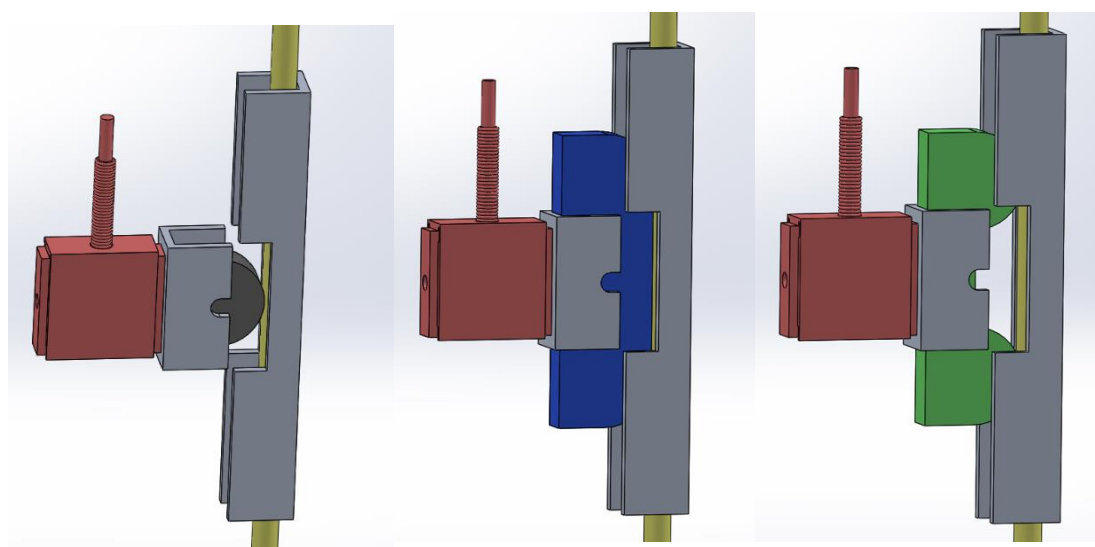


Figure 61 - SolidWorks model of pincher (blue/green) attached to the load cell (red). The infusion line (yellow) is guided by a housing (grey). Left: 14mm wide steel pincher (dark grey), middle: 44mm wide steel pincher (blue), right: two 14mm wide pinchers with a distance of 14mm in between (green).

Before each experiment with a new pincher was started, and therefore the linear stage was potentially moved, the setup was tested without tubing. This test was done to obtain a position reference for the linear stage to be able to compare the used pinchers afterwards.

As the influence of creep on the flow rate is relatively more prominent for lower flow rates, the measurements at each position was done as fast as possible. A balance was found for the time interval at each step, to obtain a representative flow rate. Based on the results of the material experiment, a time interval of 30 seconds was chosen.

Hypothesis

As shown in Section 4.2.1, a non-linear relationship was expected between the pinching depth and the flow rate. Furthermore, the wider pincher will probably provide more gradual control of the fluid flow. The same holds for the combined pincher.

Measurement protocol

14mm steel pincher

1. Execute the earlier mentioned list of 'measurement preparations'.
2. Attach the 14mm wide steel pincher (Figure 59: right).
3. Set the offset of the pinching load cell in LabVIEW.
4. Set the loop time to 100ms.
5. Temporarily take the tubing out of the U-profile and turn the linear stage towards the tube until the pincher contacts the U-profile. Note this reference location of the linear stage.
6. Empty the measuring cup and set the offset of the scale load cell in LabVIEW.
7. Make sure the tube is exactly above the middle of the scale load cell.
8. Fill the reservoir with 7 litres of (recycled) purified water; up to the marking on the reservoir.
9. Open the ball valve.
10. Turn the linear stage towards the tube until no fluid enters the drip chamber or until the force on load cell 2 exceeds the maximum of 100N.
11. Turn the linear stage away from the tube until the Monidrop displays a value and note the location of the linear stage. This step can be skipped when at step 10 the maximum force was reached.
12. Start saving the LabVIEW data.
13. Wait 30 seconds and stop the LabVIEW script.
14. Turn the linear stage another 0.01mm away from the tube.
15. Repeat steps 11-13 until the measuring cup is almost full.
16. Note the total displacement of the linear stage at that moment.
17. Close the ball valve.
18. Turn the linear stage away from the tube until there is no contact anymore.
19. Mark the used part of the tube, let it recover for 10 minutes and shift it so a new run (N) on a new tubing part can be started.
20. Repeat steps 3-17 for four times (N=4).

44mm steel pincher

21. Attach the 30mm wide steel pincher (Figure 61: left).
22. Repeat steps 5-18.

Two 14mm wide pinchers with a distance of 14mm in between

23. Attach the double 14mm wide steel pincher, which is 14mm apart (Figure 61: right)
24. Repeat steps 5-18.

Shape experiment 2

Pinching setup

The same setup was the same as during the material experiment, only now the 44mm wide steel pincher (Figure 62) was used.

Hypothesis

Shape experiment 1 showed that, compared to the 14mm wide steel pincher, the 44mm wide steel pincher needed a significantly higher force for setting the 100mL/h flow rate. As the creep is depending on the applied load, also a larger deviation over time was expected.

Measurement protocol

The same measurement protocol holds as during the material experiment.

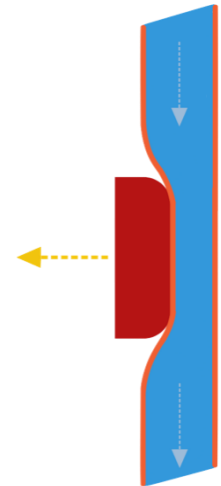


Figure 62 - Schematic illustration of the shape experiment 2 setup. The 44mm wide steel pincher (red) moves from its closed position.

Contact area experiment

Pinching setup

Again, almost the same setup and process as used in the material experiment was used for this experiment. The difference was that now the roller clamp of Figure 63 was tested. The pinching setup had become redundant for these tests.

Hypothesis

The tapered groove (Figure 64) is claimed to reduce the creep in the fluid flow region (Section 4.2.1). Because of this, the deviation of the flow rate over time was expected to be less than found using the plastic wheel in the material experiment.

Measurement protocol

1. Execute the earlier mentioned list of 'measurement preparations'.
2. Attach the plastic roller clamp (Figure 63).
3. Set the offset of the pinching load cell in LabVIEW.
4. Set the loop time to 1000ms.
5. Open the ball valve.
6. Turn the roller clamp wheel towards the tube until no fluid is entering the drip chamber.
7. Fill the reservoir with 7 litres of (recycled) purified water; up to the marking on the reservoir.
8. Empty the measuring cup and set the offset of the scale load cell in LabVIEW.
9. Make sure the tube is exactly above the middle of the scale load cell.
10. Turn the roller clamp wheel away from the tube until the Monidrop displays a value of 100 mL/h for 10 seconds.
11. Start saving the LabVIEW data.
12. Let the experiment run for a minimum of 60 minutes without additional actions.



Figure 63 – Plastic roller clamp for the contact area experiment.

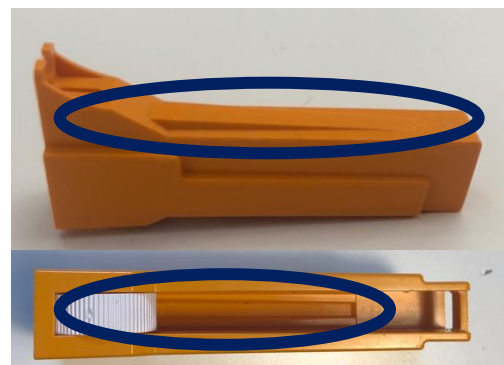


Figure 64 – Plastic roller clamp. The blue ellipse indicates the tapered groove.

13. Stop the LabVIEW script.
14. Close the ball valve.
15. Turn the roller clamp wheel away from the tube until there is no contact anymore.
16. Mark the used part of the tube, let it recover for 10 minutes and shift it so a new run (N) on a new tubing part can be started.
17. Repeat steps 5-16 for four times (N=4).

Additional Matlab results

Figure 65 and 66 show additional graphs to support the results presented in Section 4.2.2.

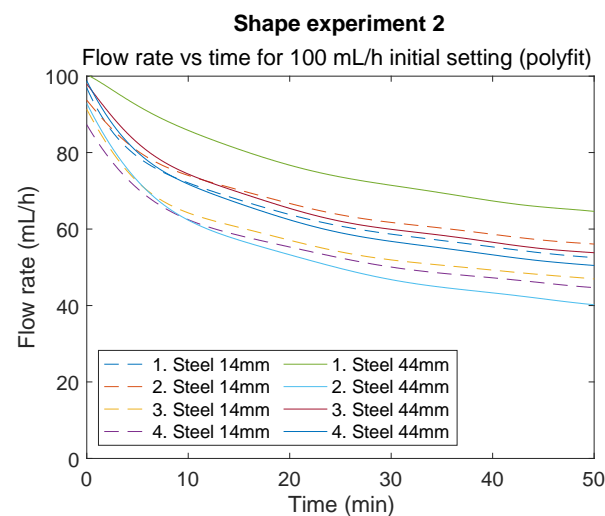


Figure 65 – Shape experiment 2: Flow rate [mL/h] versus time [min] at an initial setting of 100 mL/h using a 14mm wide steel pincher and a 44mm wide steel pincher. The data of the 14mm wide pincher is coming from the material experiment.

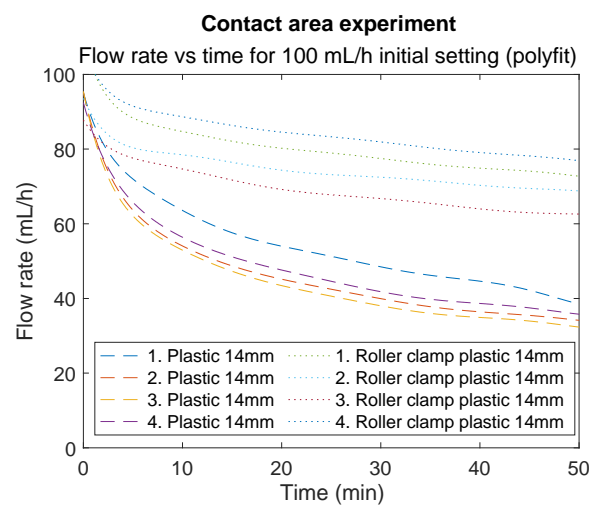


Figure 66 – Contact area experiment: Flow rate [mL/h] versus time [min] at an initial setting of 100 mL/h initial flow rate setting, using a 14mm wide plastic pincher and a roller clamp with the same pincher. The data of the plastic pincher is coming from the material experiment.

Appendix F - Granta Edupack 2020 material analysis

As described in Section 2.3, some materials with a specific glass or melting point creep at room temperature ($\approx 21^\circ\text{C}$). Using Granta Edupack [74], materials that will likely not suffer from this were extracted. Besides avoiding creep, properties such as price, stiffness, and density were also considered to ensure the material's feasibility.

The lower melting point and glass transition points are different for each type of material and are provided in Table 10.

Table 10 – The minimum required melting or glass temperature for each type of material to prevent creep at $\approx 21^\circ\text{C}$. T_m is the melting temperature and T_g is the glass transition temperature.

Type of material	Minimum required melting/glass temperature
(Semi)-Crystalline polymers	$T_m \geq 200^\circ\text{C}$ [74]
Amorphous polymers	$T_g \geq 150^\circ\text{C}$ [74]
Metals	$T_m \geq 60^\circ\text{C}$ [74]
Ceramics	$T_m \geq 47^\circ\text{C}$ [74]

The resulting charts of materials that satisfy the above conditions are shown in Figure 67, 68, 69, 70, 71, 72, 73 and 74. All materials of the 'Level 2' category of Edupack were included. The lower limits from Table 10 were plotted as a minimum horizontal line in the applicable charts. Materials with potential regarding their properties were labelled.

(Semi)-crystalline polymers

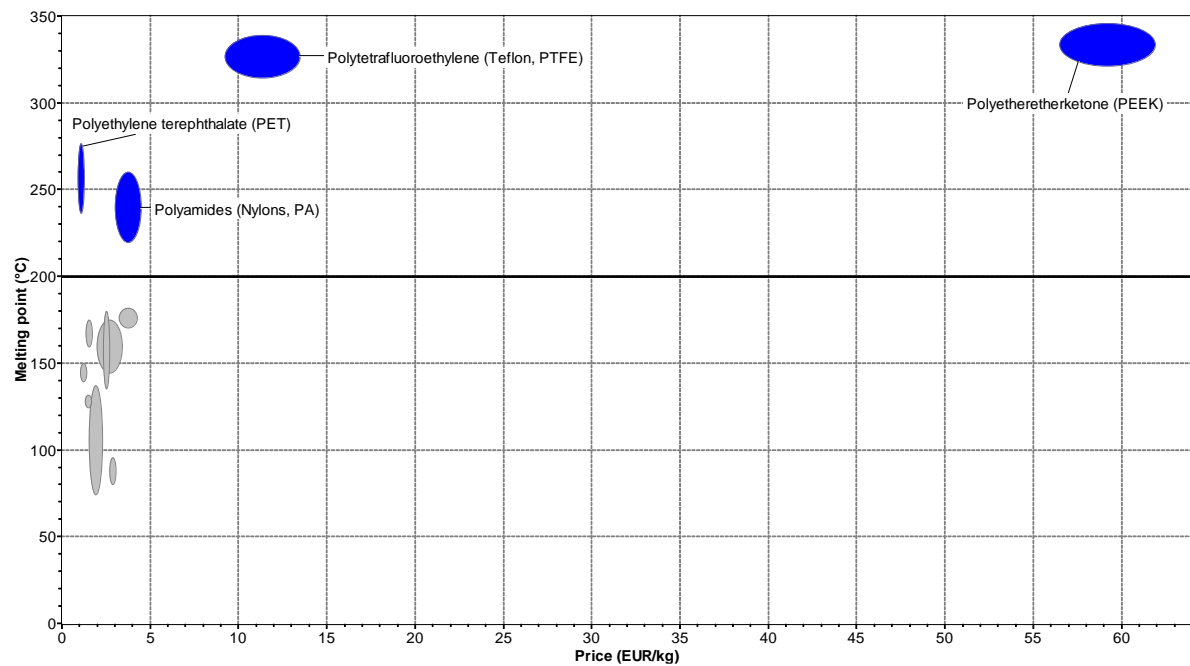


Figure 67 – (Semi)-crystalline polymers: melting point [°C] versus price [€/kg]. The black horizontal line at 200°C is set as a minimum. The chart is created using Granta Edupack 2020 [74].

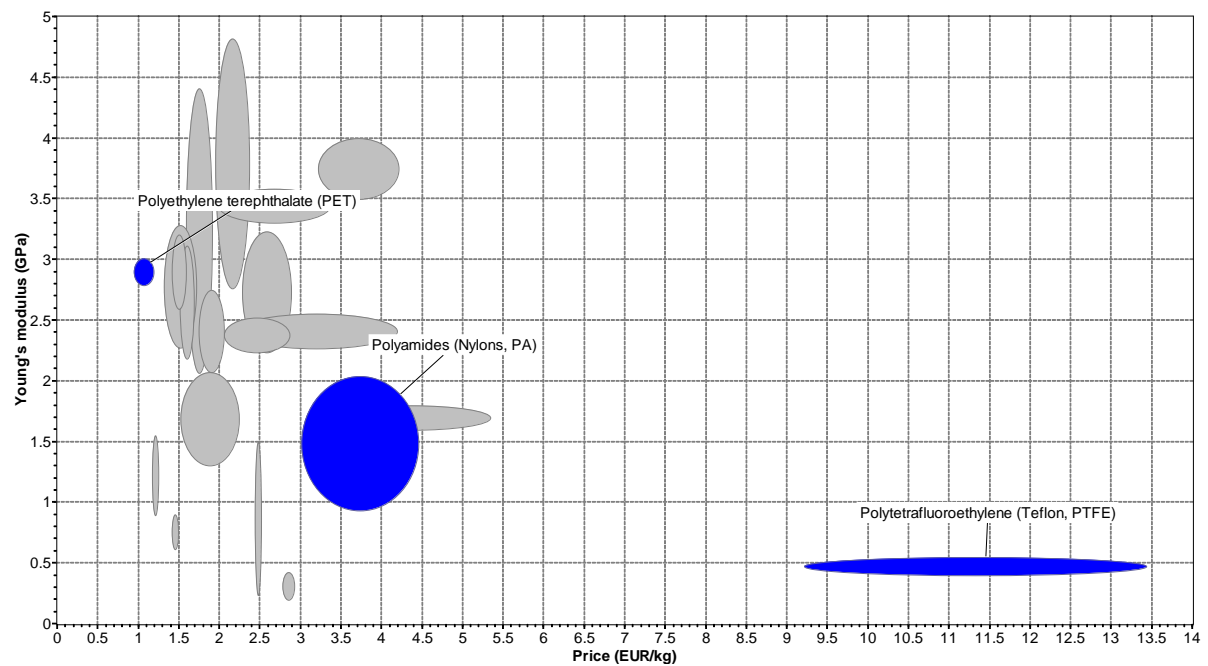


Figure 68 - (Semi)-crystalline polymers: young's modulus [GPa] versus price [€/kg]. The chart is created using Granta Edupack 2020 [74].

Amorphous polymers

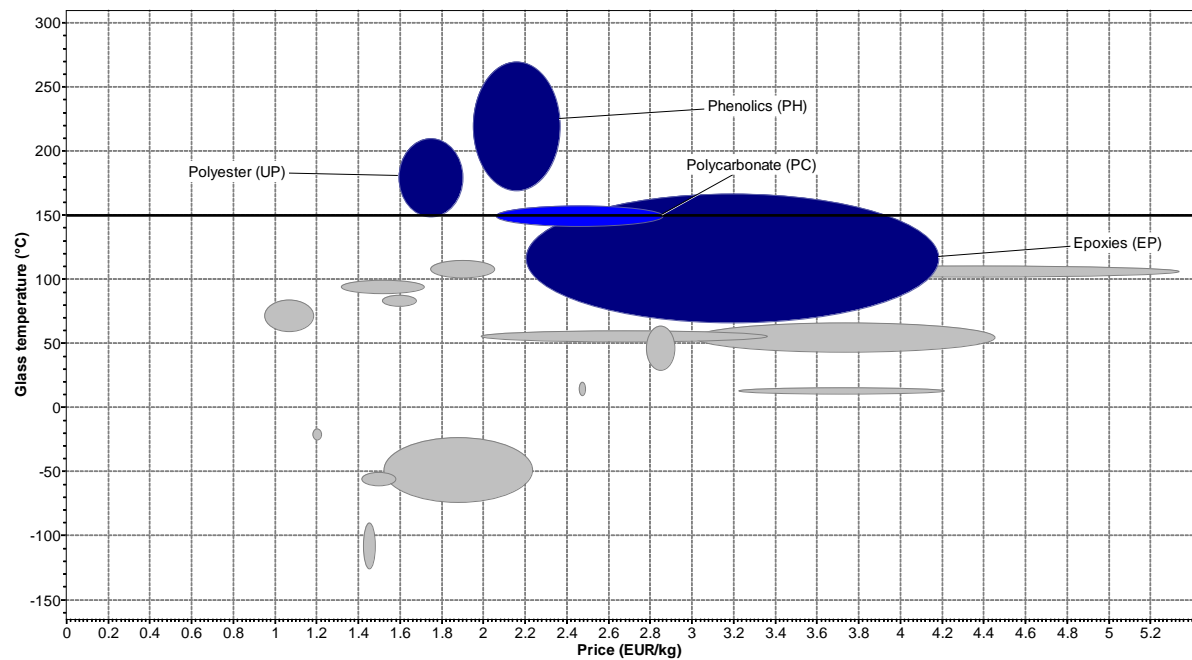


Figure 69 - Amorphous polymers: glass temperature [°C] versus price [€/kg]. The black horizontal line at 150°C is set as a minimum. The chart is created using Granta Edupack 2020 [74].

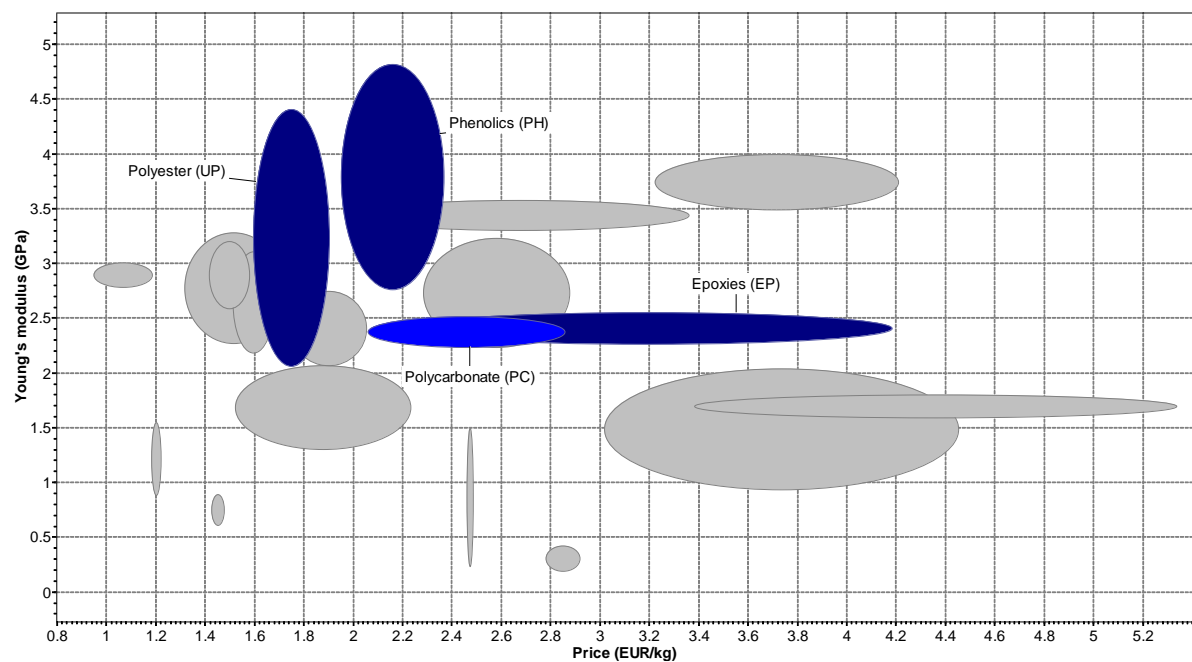


Figure 70 - Amorphous polymers: young's modulus [GPa] versus price [€/kg]. The chart is created using Granta Edupack 2020 [74].

Metals

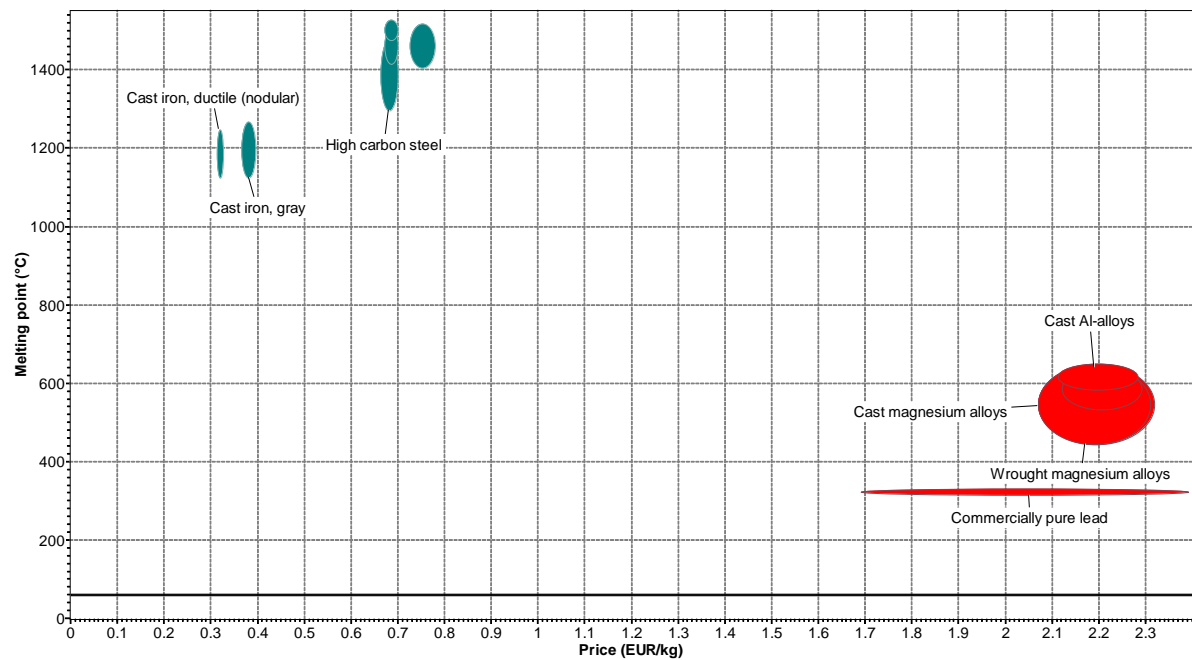


Figure 71 - Metals: melting point [°C] versus price [€/kg]. The black horizontal line at 60°C is set as a minimum. The chart is created using Granta Edupack 2020 [74].

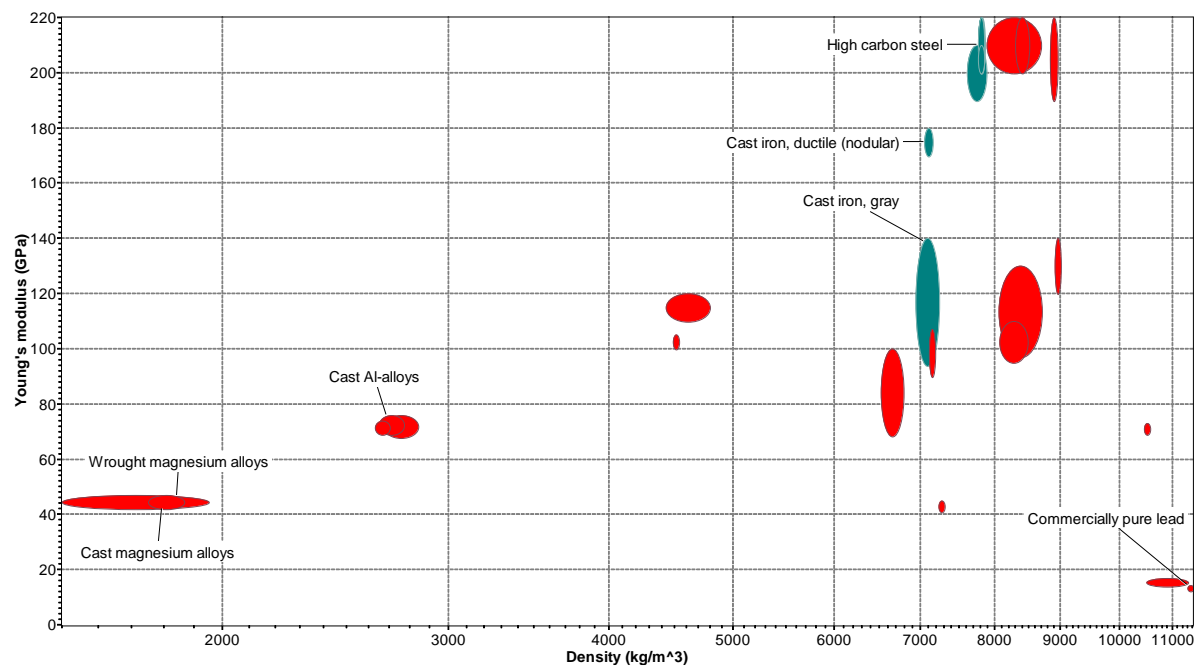


Figure 72 - Metals: young's modulus [GPa] versus density [kg/m³]. The chart is created using Granta Edupack 2020 [74].

Ceramics

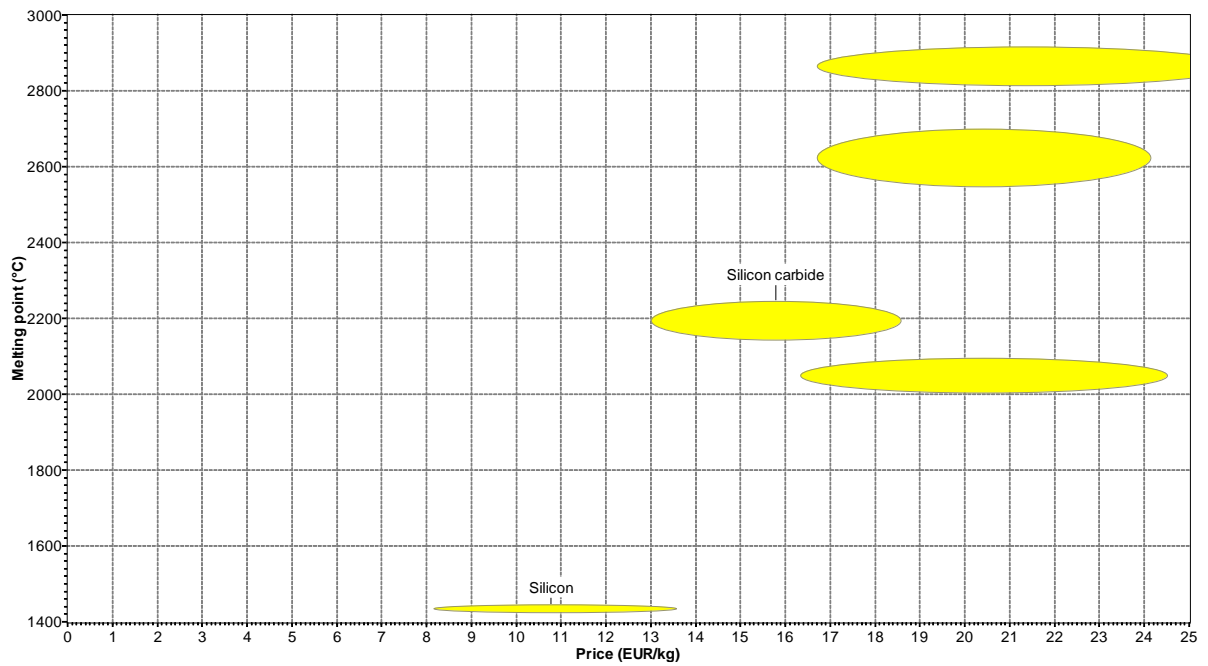


Figure 73 - Ceramics: melting point [°C] versus price [€/kg]. The chart is created using Granta Edupack 2020 [74].

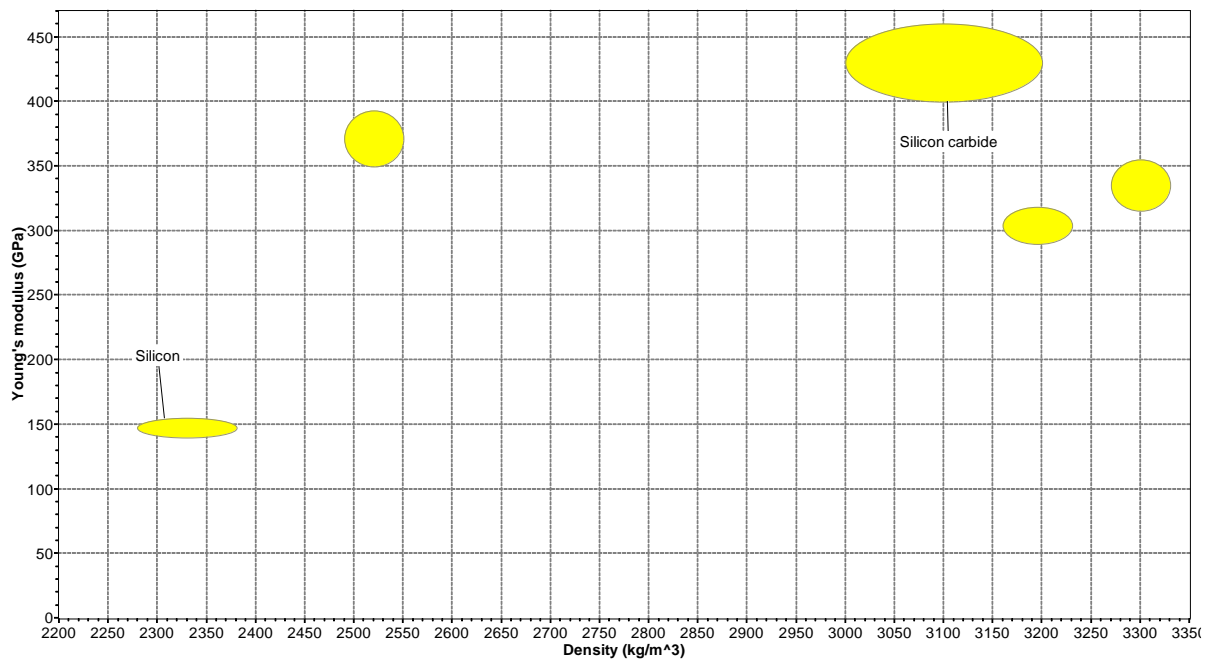


Figure 74 - Ceramics: young's modulus [GPa] versus density [kg/m³]. The chart is created using Granta Edupack 2020 [74].

Appendix G - Prototyping iterations and final design

Prototyping iterations

Figure 75 shows one of the first rough sketches of the design. This sketch was the inspiration for the first CAD models, preparatory to the rapid prototyping process.

In Figure 76, the first CAD model version and the corresponding prototype are shown. The top pincher was for the coarse flow rate setting, and the bottom pincher was for the fine setting. The leaf spring appeared to be too short to achieve the needed displacement of the pincher and therefore needed to be enlarged. The prototype already contained this improvement (Figure 76, right).



Figure 75 – First sketch of the design.

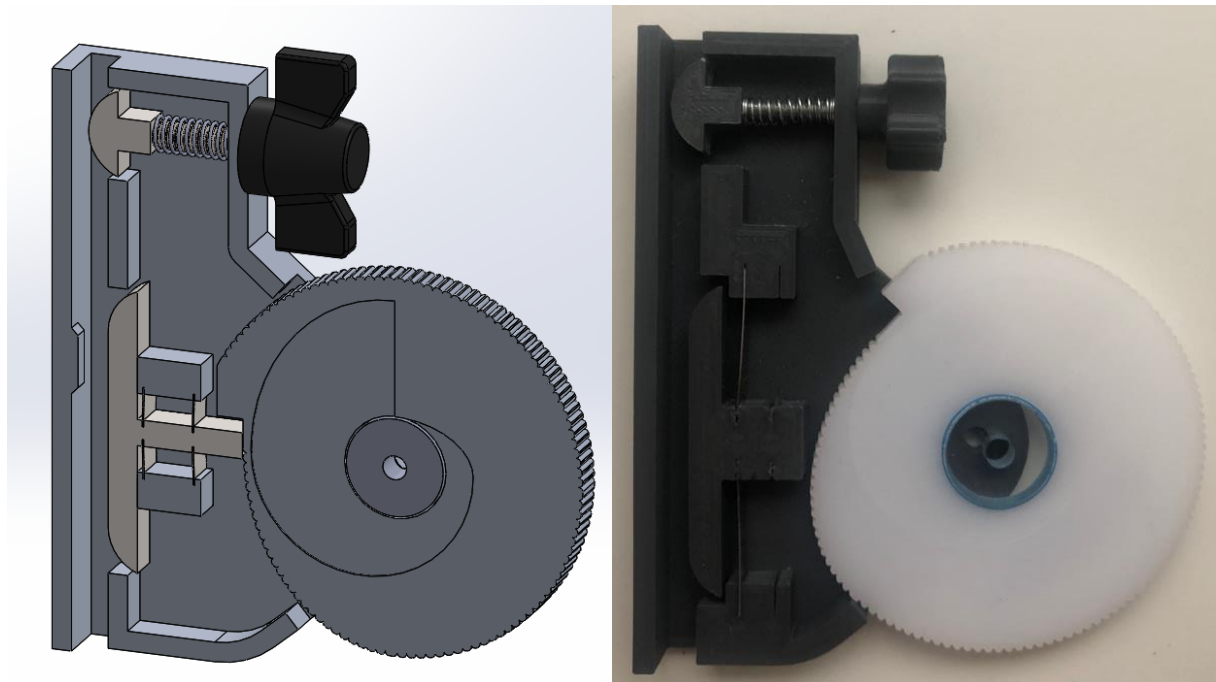


Figure 76 – Frontal view of the design v1 CAD model (left) and prototype (right). Shown without housing cap.

The successor of design version one is presented in Figure 77. A new mechanism was developed for the coarse flow rate setting, so screwing would not be necessary anymore.

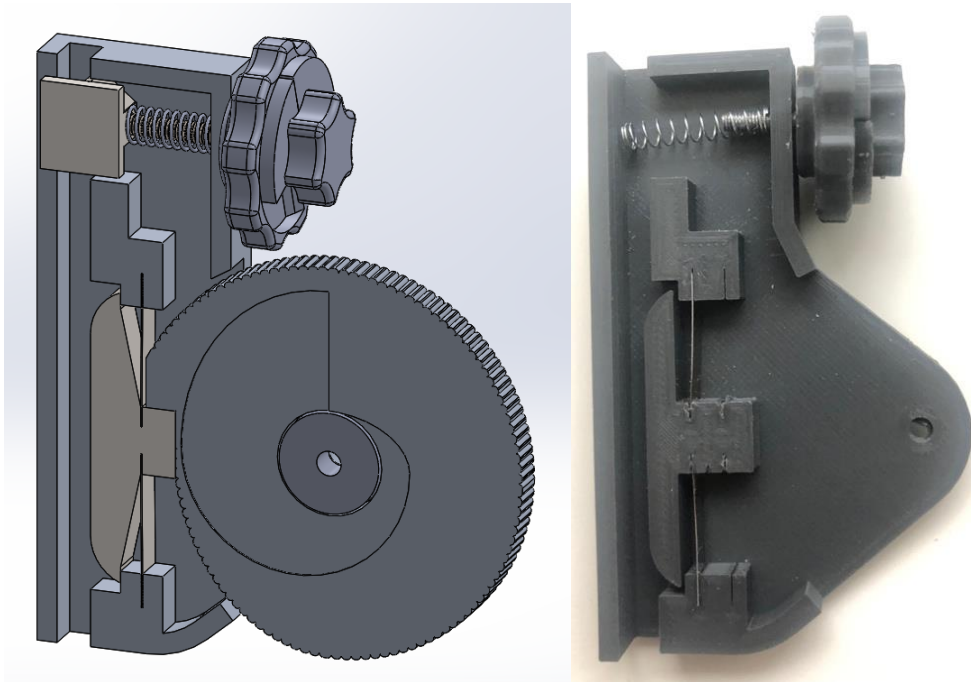


Figure 77 - Frontal view of the design v2 CAD model (left) and a part of the prototype (right). Shown without housing cap.

The third version contained an entirely new mechanism, where both the coarse and fine flow rate settings were combined (Figure 78). Three different modes were introduced: 1 open, 2 flow, 3 closed. Furthermore, the pincher was adjusted to enclose the tube when pinching. Also, the leaf spring consisted out of one part instead of two.

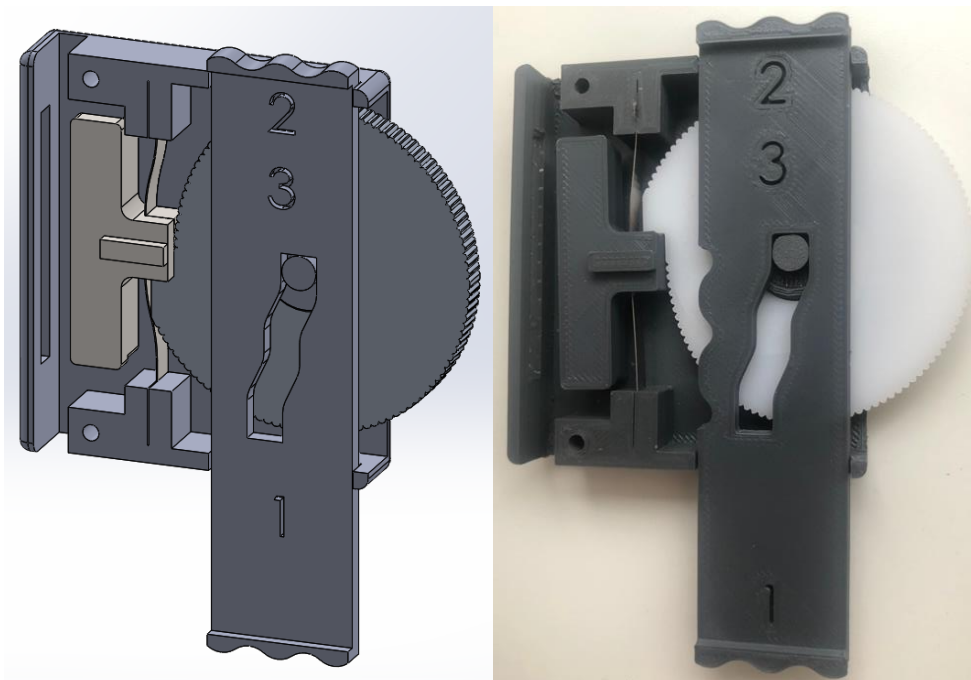


Figure 78 - Frontal view of the DropAdjust v3 CAD model (left) and prototype (right). Shown without housing cap.

Figure 79 shows the fourth prototype version of the DropAdjust. Again, the leaf spring was enlarged, and the housing was closed at the top to prevent possible fluid entry. Furthermore, the undercut at the left was removed to simplify the moulding process. Moreover, the different mode numbers were replaced by text. A compliant safety pin needs to make sure the modes are maintained during use. At last, the drop cam was adjusted to minimise the friction at the pincher's side and provide more grip for control on the other side (not shown in Figure 79, left).

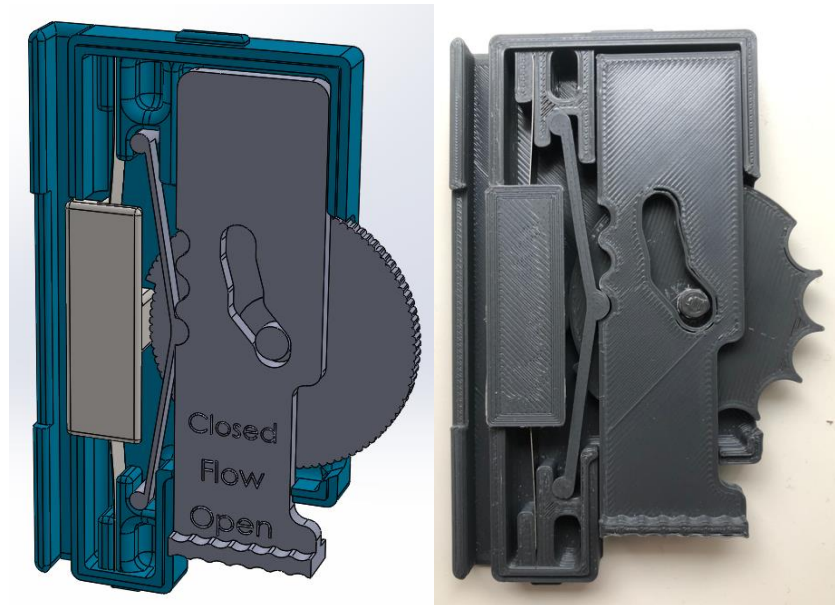


Figure 79 - Frontal view of the DropAdjust v4 CAD model (left) and prototype (right). Shown without housing cap.

The latest prototype is shown in Section 4.2.4 and contained ribs and gussets to strengthen the housing. Also, the bulge of version one returned to keep the tubing in place. A Pole bracket was mounted on the backside of the housing base to attach the DropAdjust to an IV pole. Another addition was the bag-replacement feature. At the closed mode of the DropAdjust, the protruding part left on the non-uniform ramp pushes the pincher even further onto the tubing to shut off the flow. This way, when an infusion bag needs to be swapped, the DropAdjust can temporarily stop the fluid flow. After the regulator is put in its flow mode again, the former flow rate will be restored. The compliant safety pin was also redesigned to make space for this feature.

Renders of this latest prototype are shown below.

Renders final design

Figure 80 shows the housing and Figure 81 the pinching mechanism of the latest DropAdjust prototype.

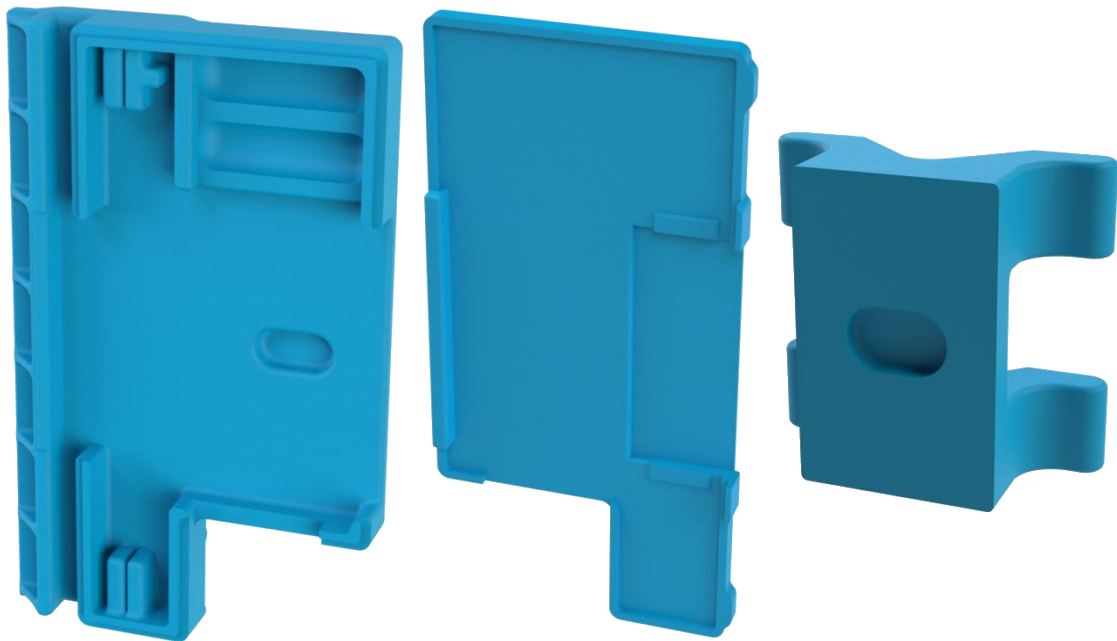


Figure 80 - The housing base (left), housing cap (middle), and pole bracket (bracket) of the DropAdjust.

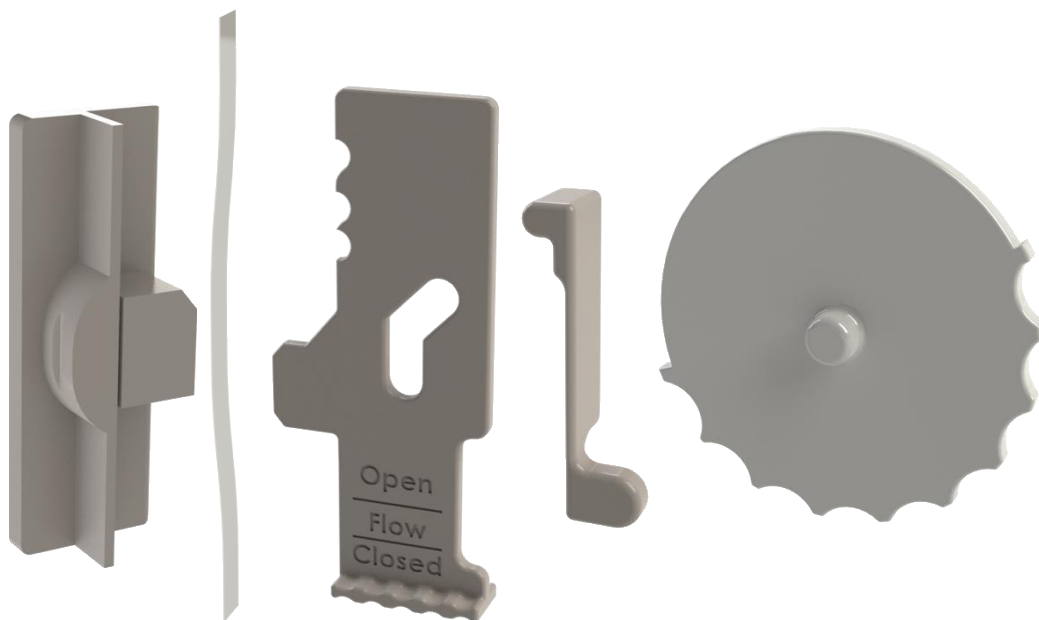
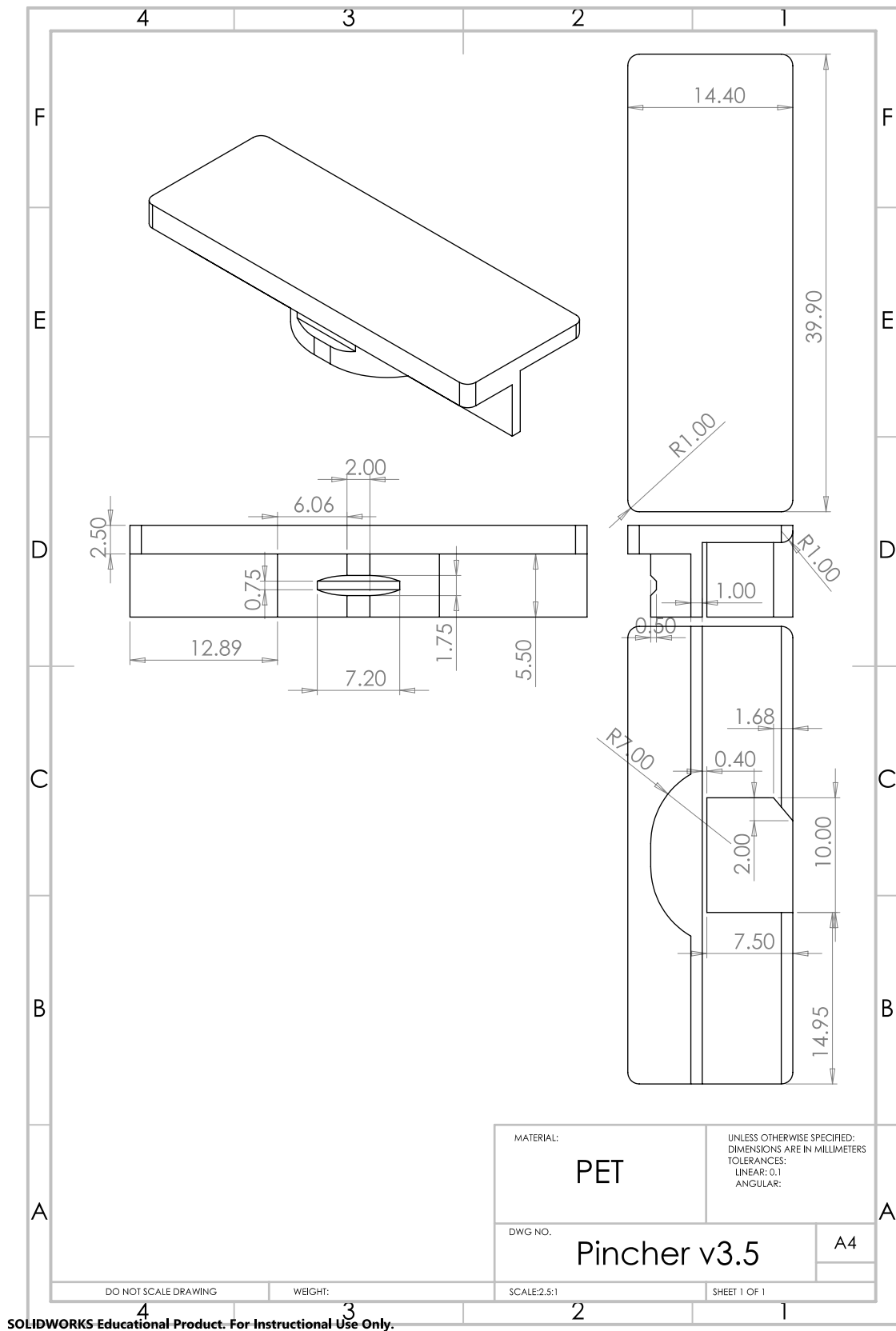
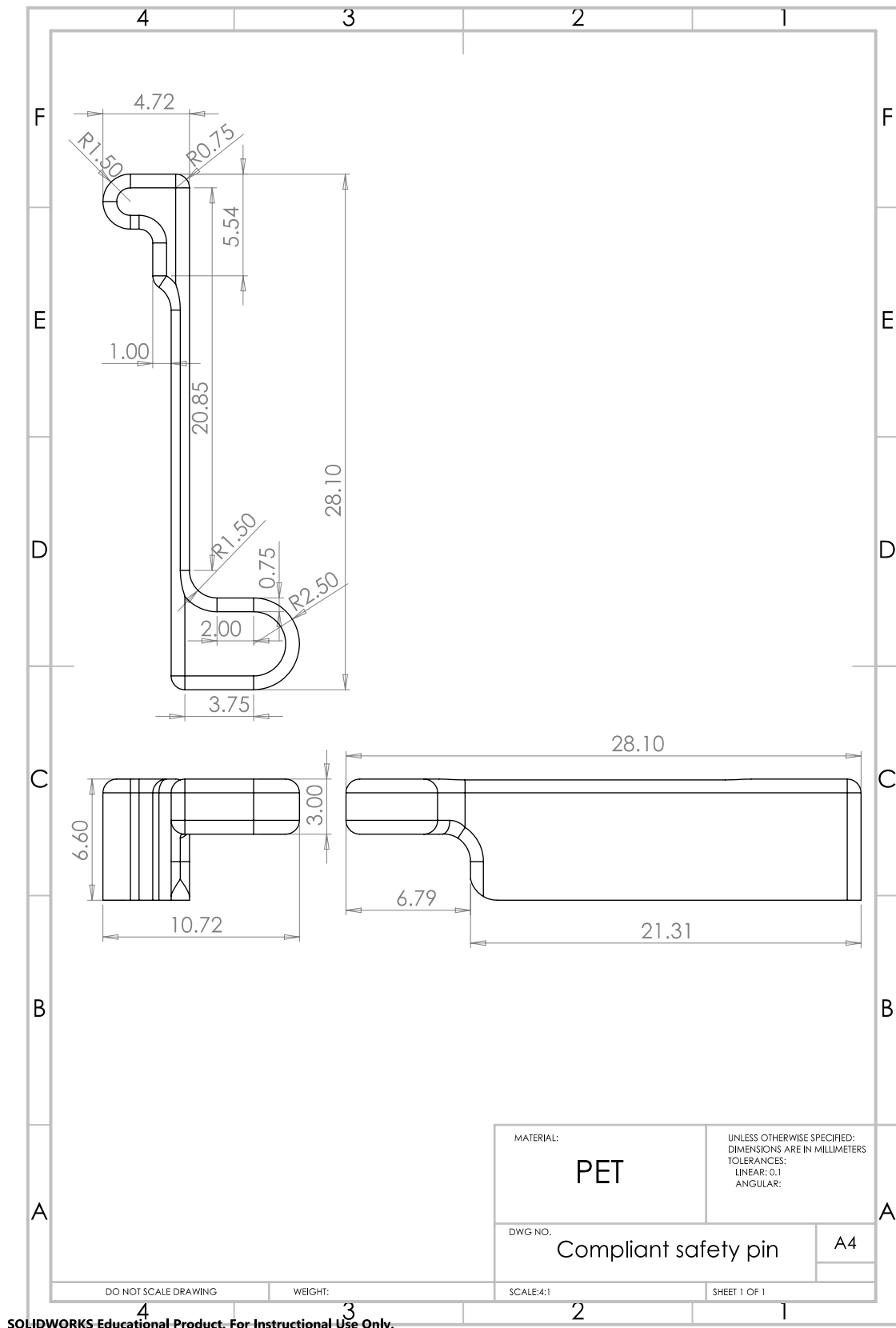


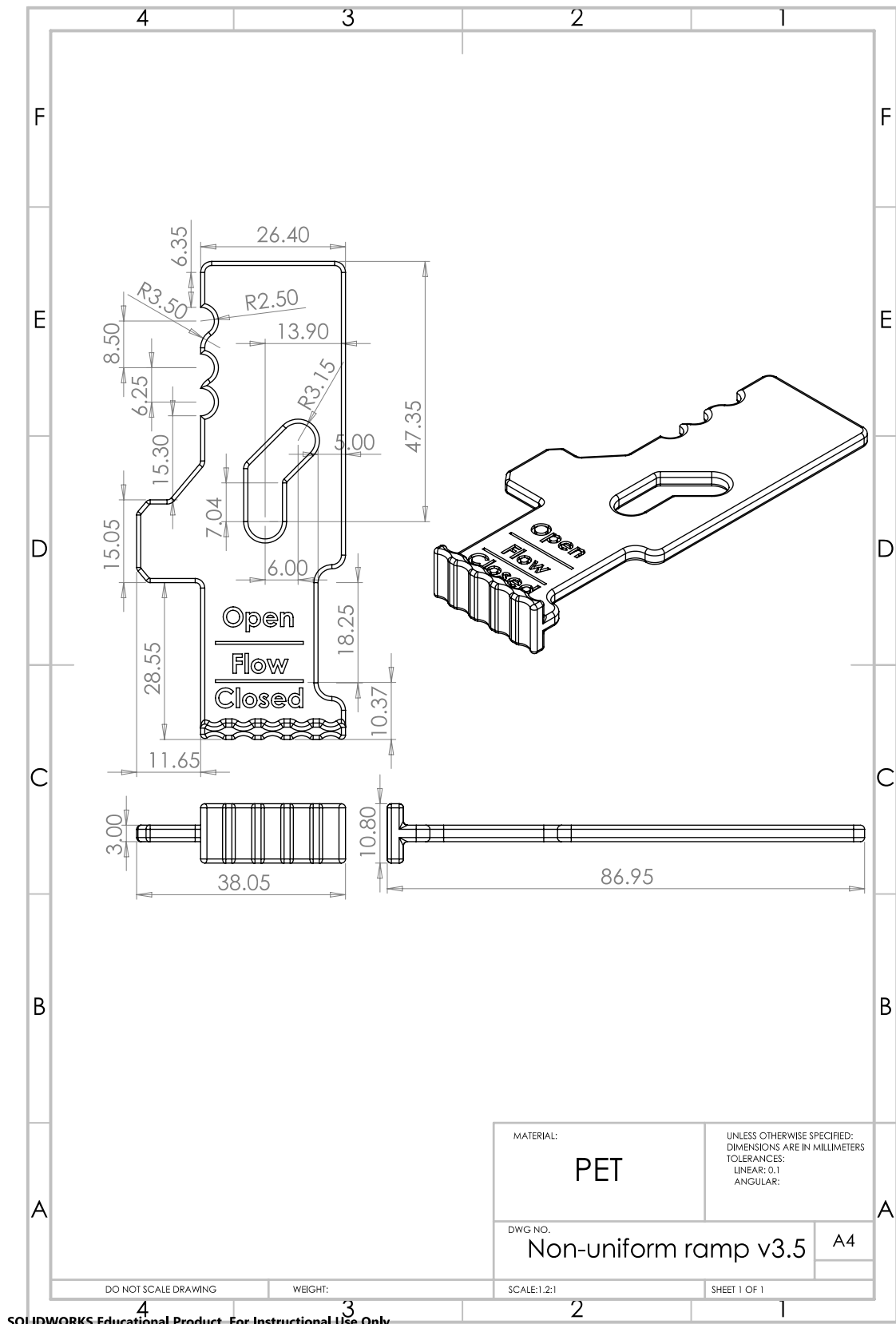
Figure 81 – The inside components of the DropAdjust. LTR: pincher, leaf spring, non-uniform ramp, compliant safety pin, and drop-cam. The scale of the renders is not the same.

Appendix H – Technical drawings

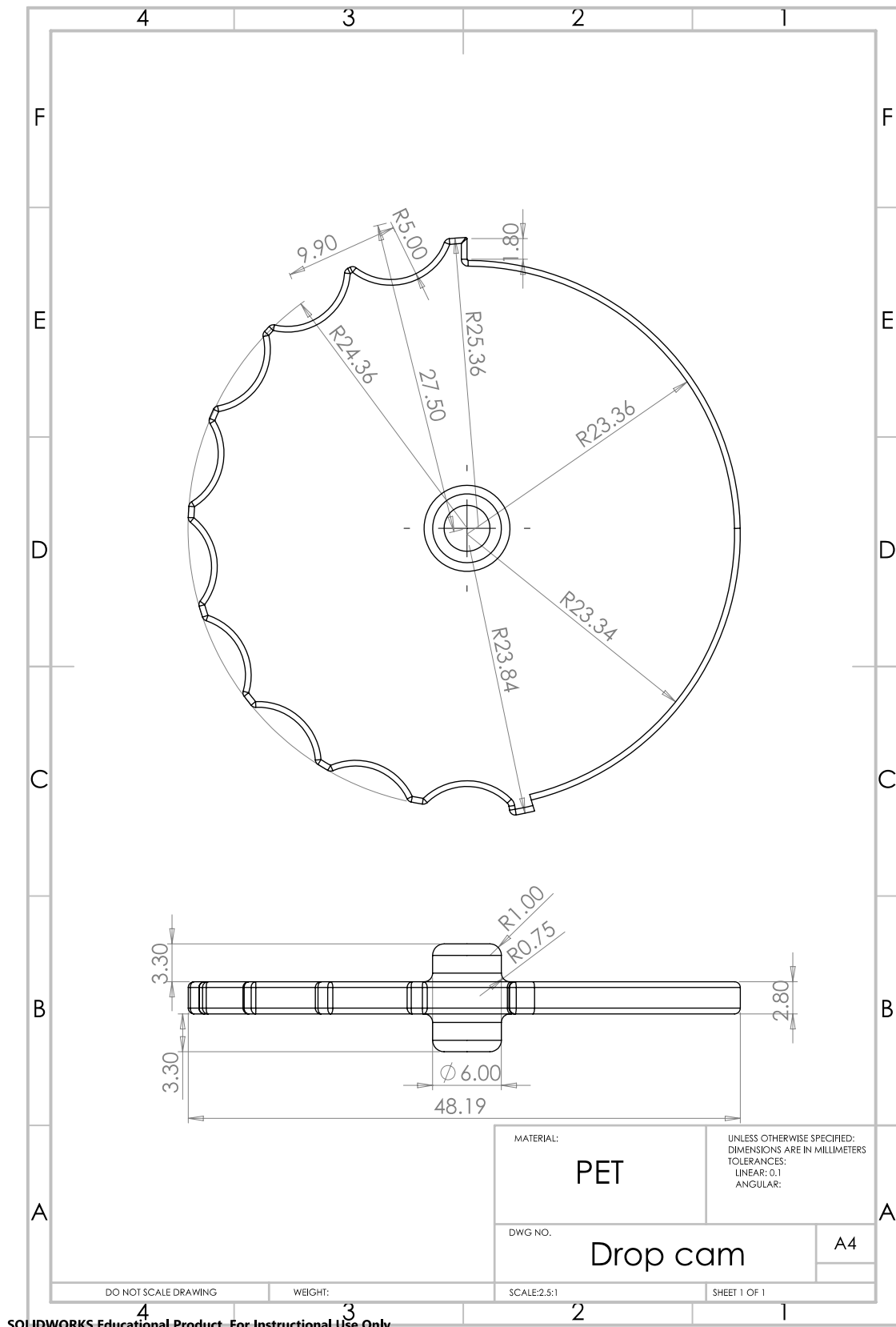




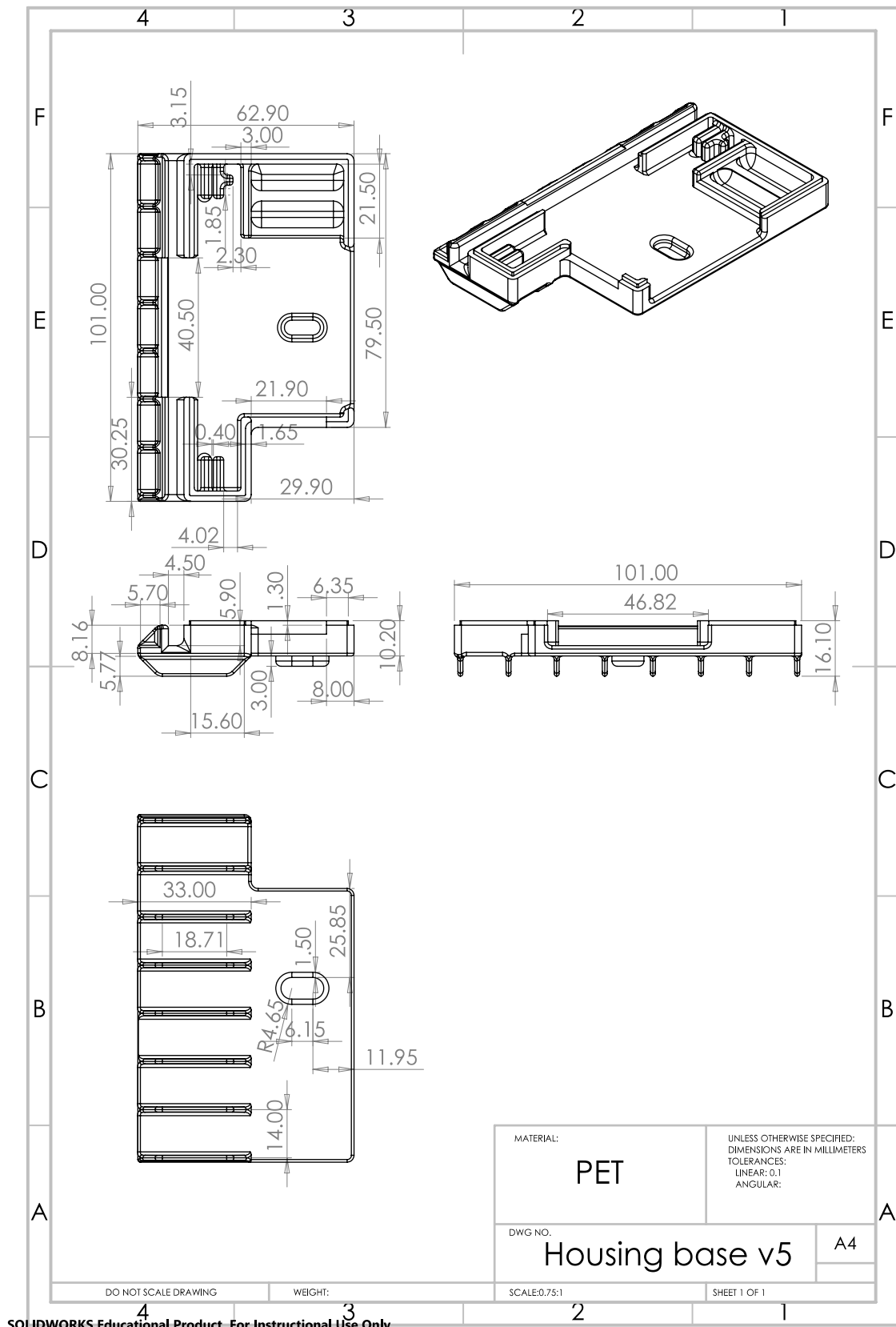
SOLIDWORKS Educational Product. For Instructional Use Only.



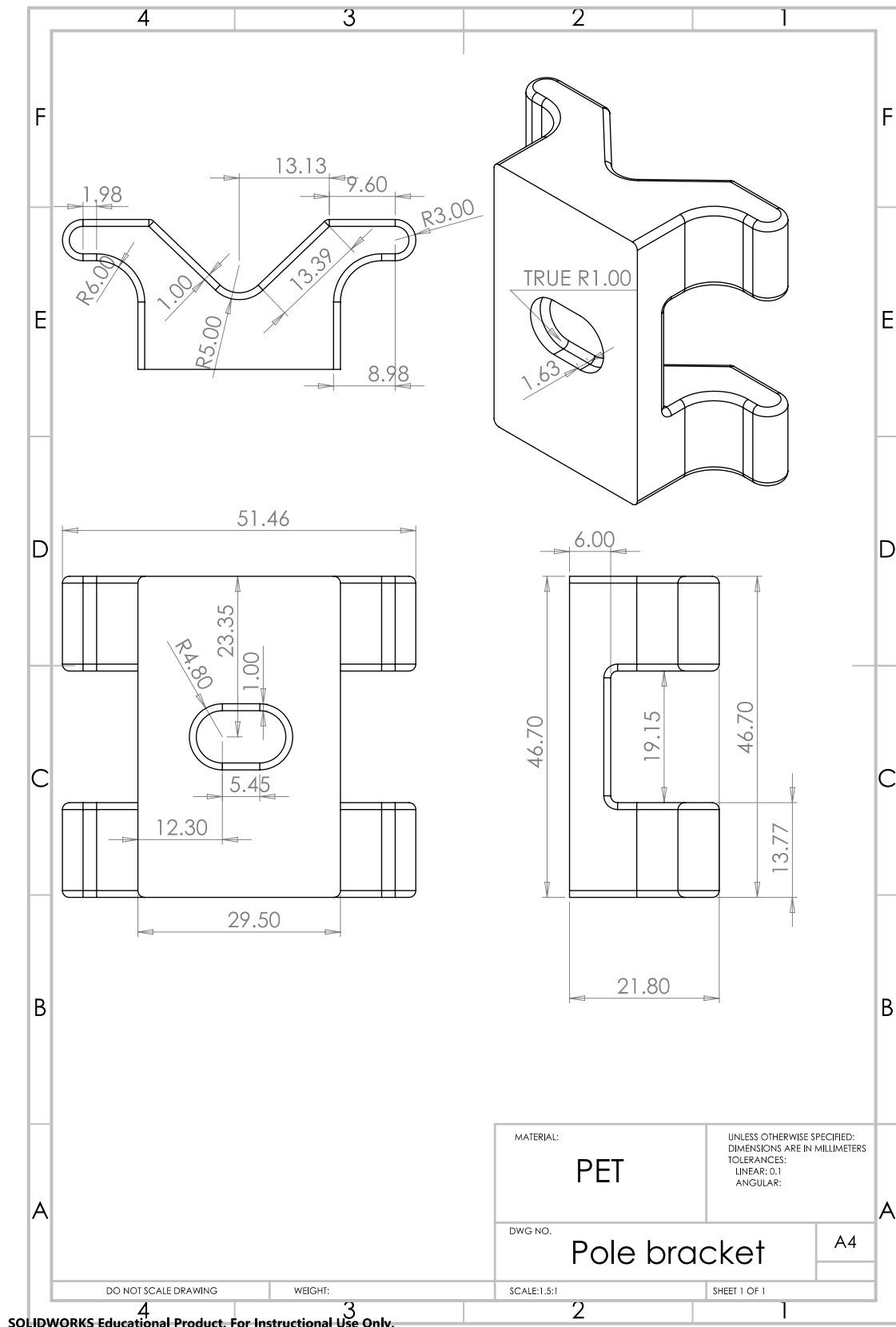
SOLIDWORKS Educational Product. For Instructional Use Only.



SOLIDWORKS Educational Product. For Instructional Use Only.



SOLIDWORKS Educational Product. For Instructional Use Only.



SOLIDWORKS Educational Product. For Instructional Use Only.

Appendix I – Protolabs inquiry



Quote Date: 24 August 2021

Quote 9142-375

Prepared for Delft University of Technology

Injection Moulding (7 Parts)



Part 1

1809-9587-001
Current Revision: 1
Mould Life: Limited
1 Cavity
ABS : Polylac PA-717 C (Black)
Black (Original Material Colour)
Cosmetic: PM-F0
Non-Cosmetic: PM-F0
X: 38.04mm Y: 10.80mm Z: 87.00mm
Machining Tolerance: +/- 0.003 in. (0.0...
Material Tolerance: +/- 0.002 in./in. (0....

Sample Quantity
500

[See volume pricing as low as €0.40](#)

500 Parts @ €2.13	€1,065.00
Mould	€2,065.00
Total	€3,130.00

⚠ This part needs your attention ⓘ

Due to shipping uncertainties from Brexit, your order could be delayed up to 2 days.

Order by: Today 17:00
Receive by:

Mon, 30 Aug	Fri, 3 Sep	Mon, 6 Sep	Fri, 10 Sep	Mon, 13 Sep	Fri, 17 Sep
+ €2,065.00	+ €1,032.00	+ €867.00	+ €86.00	+ €351.00	



Part 2

1711-6305-001
Current Revision: 1
Mould Life: Limited
1 Cavity
ABS : Polylac PA-717 C (Black)
Black (Original Material Colour)
Cosmetic: PM-F0
Non-Cosmetic: PM-F0
X: 10.72mm Y: 6.60mm Z: 28.10mm
Machining Tolerance: +/- 0.003 in. (0.0...
Material Tolerance: +/- 0.002 in./in. (0....

Sample Quantity
500

[See volume pricing as low as €0.33](#)


500 Parts @ €2.01	€1,005.00
Mould	€1,295.00
Total	€2,300.00

⚠ View analysis details & approve ⓘ

Due to shipping uncertainties from Brexit, your order could be delayed up to 2 days.

Order by: Today 17:00
Receive by:

Mon, 30 Aug	Fri, 3 Sep	Mon, 6 Sep	Fri, 10 Sep	Mon, 13 Sep	Fri, 17 Sep
+ €1,295.00	+ €548.00	+ €544.00	+ €324.00	+ €220.00	



Part 3

1291-8812-001

Current Revision: 1

Mould Life: Limited

1 Cavity

ABS : Polytec PA-717C (Black)

Black (Original Material Colour)

Cosmetic: PM-F0

Non-Cosmetic: PM-F0

X: 48.38mm Y: 9.40mm Z: 50.33mm

Machining Tolerance: +/- 0.003 in. (0.0...

Material Tolerance: +/- 0.002 in./in. (0...

View analysis details & approve

Sample Quantity

500

[See volume pricing as low as €0.38](#)

500 Parts @ €2.10	€1,050.00
Mould	€1,425.00
Total	€2,475.00

Due to shipping uncertainties from Brexit, your order could be delayed up to 2 days.

Order by: Today 17:00

Receive by:

Mon, 30 Aug	Fri, 3 Sep	Mon, 6 Sep	Fri, 10 Sep	Mon, 13 Sep	Fri, 17 Sep
+ €1,425.00	+ €712.00	+ €698.00	+ €356.00	+ €242.00	



Part 4

1302-1301-001

Current Revision: 1

Mould Life: Limited

1 Cavity

ABS : Polytec PA-717C (Black)

Black (Original Material Colour)

Cosmetic: PM-F0

Non-Cosmetic: PM-F0

X: 45.45mm Y: 46.70mm Z: 15.72mm

Machining Tolerance: +/- 0.003 in. (0.0...

Material Tolerance: +/- 0.002 in./in. (0...

This part needs your attention

Sample Quantity

500

[See volume pricing as low as €0.44](#)

500 Parts @ €2.20	€1,100.00
Mould	€3,495.00
Total	€4,595.00

Order by: Today 17:00

Receive by:

Fri, 3 Sep	Mon, 6 Sep	Fri, 10 Sep	Mon, 13 Sep	Fri, 17 Sep
+ €1,745.00	+ €1,468.00	+ €874.00	+ €594.00	



Part 5

1270-8073-001

Current Revision: 1

Mould Life: Limited

1 Cavity

ABS : Polytec PA-717C (Black)

Black (Original Material Colour)

Cosmetic: PM-F0

Non-Cosmetic: PM-F0

X: 62.90mm Y: 16.09mm Z: 101.00mm

Machining Tolerance: +/- 0.003 in. (0.0...

Material Tolerance: +/- 0.002 in./in. (0...

This part needs your attention

Sample Quantity

500


[See volume pricing as low as €0.59](#)

500 Parts @ €2.48	€1,240.00
Mould	€2,940.00
Total	€4,180.00

Order by: Today 17:00

Receive by:

Fri, 3 Sep	Mon, 6 Sep	Fri, 10 Sep	Mon, 13 Sep	Fri, 17 Sep
+ €1,470.00	+ €1,235.00	+ €735.00	+ €500.00	



Part 6

1767-6053-001

Current Revision: 1

Mould Life: Limited

1 Cavity

ABS : Polytec PA-717C (Black)

Black (Original Material Colour)

Cosmetic: PM-F0

Non-Cosmetic: PM-F0

X: 50.75mm Y: 6.80mm Z: 101.00mm

Machining Tolerance: +/- 0.003 in. (0.0...

Material Tolerance: +/- 0.002 in./in. (0...

Sample Quantity

500


[See volume pricing as low as €0.45](#)

500 Parts @ €2.23	€1,115.00
Mould	€2,290.00
Total	€3,405.00

⚠ This part needs your attention ⓘ

Due to shipping uncertainties from Brexit, your order could be delayed up to 2 days.

Order by: Today 17:00	Mon, 30 Aug	Fri, 3 Sep	Mon, 6 Sep	Fri, 10 Sep	Mon, 13 Sep	Fri, 17 Sep
Receive by:	+ €2,290.00	+ €1,145.00	+ €962.00	+ €672.00	+ €389.00	



Part 7

1100-8826-001

Current Revision: 1

Mould Life: Limited

1 Cavity

ABS : Polytec PA-717C (Black)

Black (Original Material Colour)

Cosmetic: PM-F0

Non-Cosmetic: PM-F0

X: 14.40mm Y: 8.00mm Z: 39.90mm

Machining Tolerance: +/- 0.003 in. (0.0...

Material Tolerance: +/- 0.002 in./in. (0...

Sample Quantity

500

[See volume pricing as low as €0.35](#)

500 Parts @ €2.04	€1,020.00
Mould	€3,060.00
Total	€4,080.00

⚠ This part needs your attention ⓘ

Due to shipping uncertainties from Brexit, your order could be delayed up to 2 days.

Order by: Today 17:00	Fri, 3 Sep	Mon, 6 Sep	Fri, 10 Sep	Mon, 13 Sep	Fri, 17 Sep
Receive by:	+ €1,530.00	+ €1,285.00	+ €765.00	+ €520.00	

Shipping to

3035GN

Use My Carrier Account

No account selected

Order Summary

Quantity	500
Shipping	€0.00
Taxes	€0.00
Your part(s) need your attention.	
Total	€3,405.00

Terms and Conditions of Sale
<https://www.protolabs.co.uk/legal-notices/quotequote>

Thank you for the opportunity to quote your project. Have questions?
 Contact Customer Service at +44 (0) 1952 683047 or customerservice@protolabs.co.uk

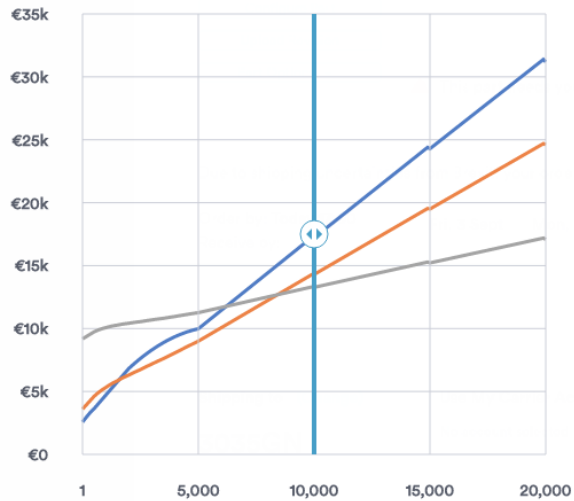
Part 1



Total Price

Part Price

Service Level



Prototype

On-Demand Manufacturing

Chart Colour

Limited

Mould Life

Unlimited

Cavities

Unlimited

Quantity

1

Mould

10,000

Part Price

€2,065.00

Total Price

€1.47

Preferred Option

€3,095.00

Unlimited

Unlimited

1

8

10,000

10,000

€8,675.00

€0.41

€13,795.00

€12,775.00

Select

Select

Add €499.50 setup charge for each production run.

Return to Quote

Part 2

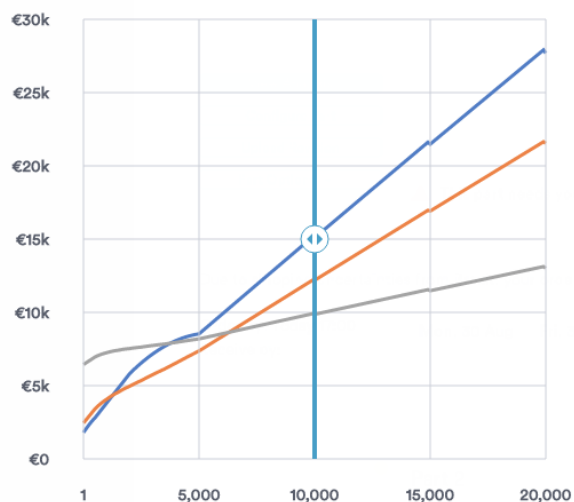
Part 2



Total Price

Part Price

Service Level



Prototype

On-Demand Manufacturing

Chart Colour

Limited

Mould Life

Unlimited

Cavities

Unlimited

Quantity

1

Mould

10,000

Part Price

€1,295.00

Total Price

€1.33

Preferred Option

€3,945.00

Unlimited

Unlimited

1

8

10,000

10,000

€5,940.00

€0.34

€11,645.00

€9,340.00

Select

Select

Add €499.50 setup charge for each production run.

Return to Quote

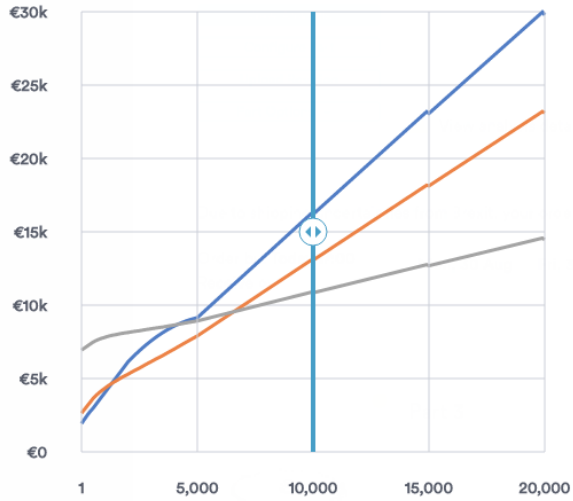
Part 3



Total Price

Part Price

Service Level



Prototype

On-Demand Manufacturing

Chart Colour

Limited

Mould Life

Unlimited

Cavities

Unlimited

Quantity

1

Mould

10,000

Part Price

€1,425.00

Total Price

€1.43

Preferred Option

€2,135.00

1

10,000

€2,135.00

€12,535.00

Select

€6,435.00

Select

8

10,000

€6,435.00

€10,335.00

Select

Select

Add €499.50 setup charge for each production run.

Return to Quote

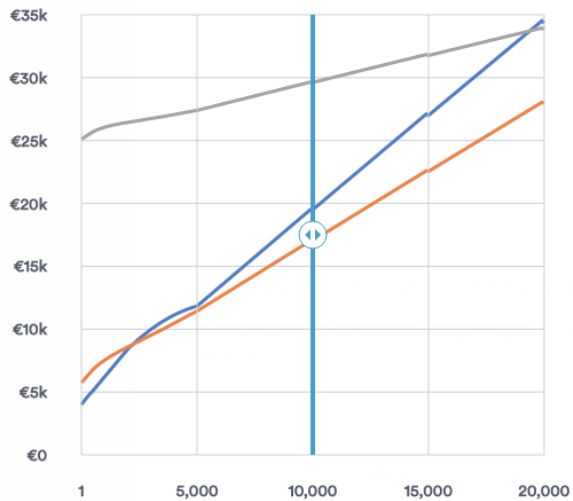
Part 4



Total Price

Part Price

Service Level



Prototype

On-Demand Manufacturing

Chart Colour

Limited

Mould Life

Unlimited

Cavities

Unlimited

Quantity

1

Mould

10,000

Part Price

€3,495.00

Total Price

€1.55

Preferred Option

€5,240.00

1

10,000

€5,240.00

€16,540.00

Select

€24,600.00

Select

8

10,000

€24,600.00

€29,100.00

Select

Select

Add €499.50 setup charge for each production run.

Return to Quote



Part 7



Total Price Part Price Service Level

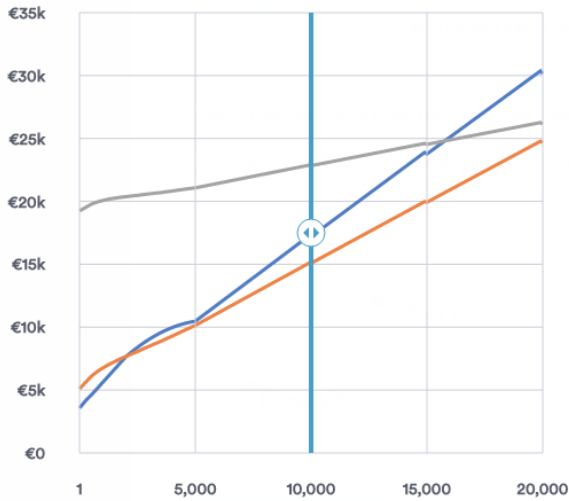


Chart Colour

Prototype

Mould Life

Limited

Cavities

1

Quantity

10,000

Mould

€3,060.00

Part Price

€1.36

Total Price

€16,660.00

Preferred Option

Selected

On-Demand Manufacturing

Unlimited

Unlimited

1

8

10,000

10,000

€4,595.00

€18,740.00

€1.00

€0.36

€14,595.00

€22,340.00

Select

Select

Add €499.50 setup charge for each production run.

Return to Quote

Appendix J – DropAdjust pincher force experiment

Purpose

Identify the needed force to fully close the tubing using the DropAdjust's pincher shape.

Method and setup

The same method and setup as described in Appendix E were used.

Measurement protocol

1. Execute the measurement preparations step 1-6 of Appendix E.
2. Attach the DropAdjust pincher (Figure 82).
3. Set the loop time to 50 ms.
4. Fill the reservoir with 7 litres of (recycled) purified water; up to the marking on the reservoir.
5. Empty the measuring cup and set the offset of the load cell attached to the pinching setup.
6. Open the ball valve.
7. Start saving the LabVIEW data.
8. Turn the linear stage towards the tube until no fluid is entering the drip chamber.
9. Wait a few seconds and loosen the pincher again.
10. Stop the LabVIEW script.
11. Close the ball valve.
12. Repeat steps

Results

Figure 83 shows the pincher forces when closing the tube entirely. The maximum force for each run was:

Run 1: 59.1 N

Run 2: 41.1 N

Run 3: 61.3 N

Run 4: 55.9 N

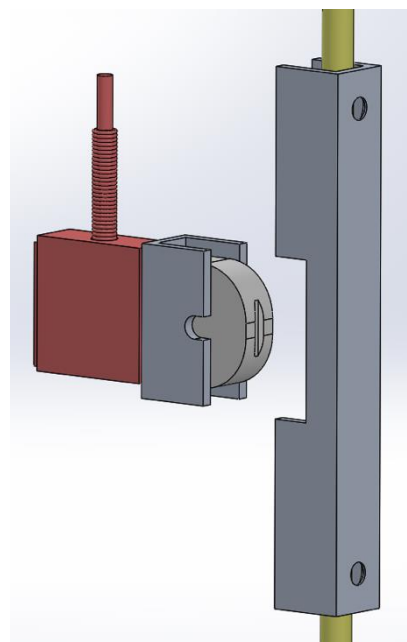


Figure 82 – SolidWorks model of the DropAdjust pincher (light grey) attached to the load cell (red). The infusion line (yellow) is guided by a housing (grey). This is part of Figure 56.

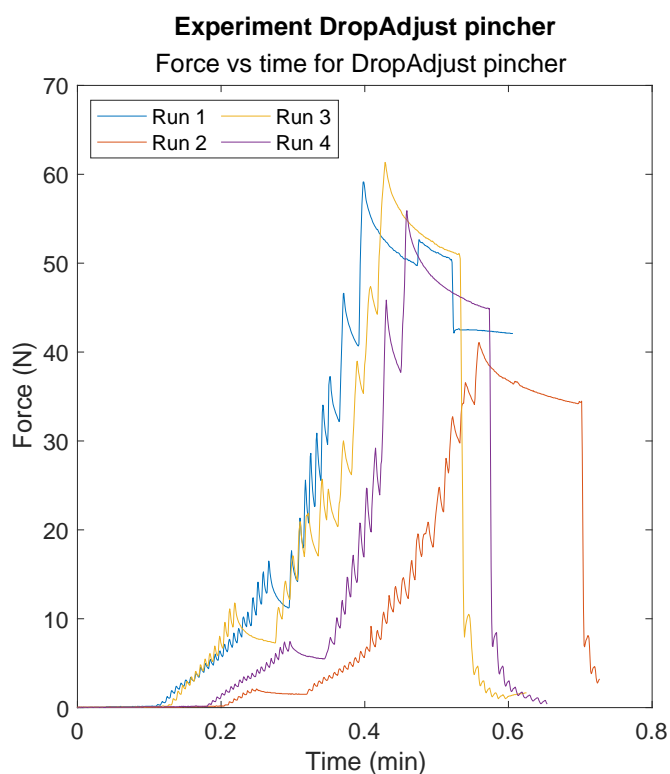


Figure 83 – DropAdjust pincher force experiment: force (N) vs time (min) for four runs.

Appendix K – Formlabs Grey Photopolymer Resin

Material Properties Data

The following material properties are comparable for all Formlabs Standard Resins.

	METRIC ¹		IMPERIAL ¹		METHOD
	Green ²	Post-Cured ³	Green ²	Post-Cured ³	
Tensile Properties					
Ultimate Tensile Strength	38 MPa	65 MPa	5510 psi	9380 psi	ASTM D 638-10
Tensile Modulus	1.6 GPa	2.8 GPa	234 ksi	402 ksi	ASTM D 638-10
Elongation at Failure	12 %	6.2 %	12 %	6.2 %	ASTM D 638-10
Flexural Properties					
Flexural Modulus	1.25 GPa	2.2 GPa	181 ksi	320 ksi	ASTM C 790-10
Impact Properties					
Notched IZOD	16 J/m	25 J/m	0.3 ft-lbf/in	0.46 ft-lbf/in	ASTM D 256-10
Temperature Properties					
Heat Deflection Temp. @ 264 psi	42.7 °C	58.4 °C	108.9 °F	137.1 °F	ASTM D 648-07
Heat Deflection Temp. @ 66 psi	49.7 °C	73.1 °C	121.5 °F	163.6 °F	ASTM D 648-07

¹ Material properties can vary with part geometry, print orientation, print settings, and temperature.

² Data was obtained from green parts, printed using Form 2, 100 µm, Clear settings, washed and air dried without post cure.

³ Data was obtained from parts printed using Form 2, 100 µm, Clear settings, and post-cured with 1.25 mW/cm² of 405 nm LED light for 60 minutes at 60 °C.

Solvent Compatibility

Percent weight gain over 24 hours for a printed and post-cured 1 x 1 x 1 cm cube immersed in respective solvent:

Solvent	24 Hour Weight Gain (%)	Solvent	24 Hour Weight Gain (%)
Acetic Acid, 5 %	< 1	Hydrogen Peroxide (3 %)	< 1
Acetone	sample cracked	Isooctane	< 1
Isopropyl Alcohol	< 1	Mineral Oil, light	< 1
Bleach, ~5 % NaOCl	< 1	Mineral Oil, heavy	< 1
Butyl Acetate	< 1	Salt Water (3.5 % NaCl)	< 1
Diesel	< 1	Sodium hydroxide (0.025 %, pH = 10)	< 1
Diethyl glycol monomethyl ether	1.7	Water	< 1
Hydraulic Oil	< 1	Xylene	< 1
Skydrol 5	1	Strong Acid (HCl Conc)	distorted

Appendix L – Design evaluation experiments

Purpose

One experiment was conducted with the following purpose:

Examine the flow rate deviation [ml/h] over 1 hour for both the DropAdjust and the conventional roller clamp, without settling time.

Additionally, also a pilot experiment was executed with the purpose:

Examine the flow rate deviation [ml/h] over 6 hours after 15 minutes of settling time for both the DropAdjust and the conventional roller clamp. Furthermore, the flow rate regulation step size will be examined.

Method

Almost the same setup and process used in the earlier experiments (Appendix E) were used for these (pilot) experiments. The only difference was that the pinching setup was redundant because of the use of the DropAdjust and conventional roller clamp instead.

Measurement protocol DropAdjust experiment

DropAdjust

1. Execute the earlier mentioned list of 'measurement preparations' of Appendix E.
2. Attach the DropAdjust (Figure 38).
3. Set the offset of the pinching load cell in LabVIEW.
4. Set the loop time to 1000ms.
5. Open the ball valve.
6. Put the DropAdjust in the 'Flow'-mode and turn the DropAdjust's regulation knob clockwise until no fluid is enters the drip chamber.
7. Fill the reservoir with 7 litres of (recycled) purified water; up to the marking on the reservoir.
8. Empty the measuring cup and set the offset of the scale load cell in LabVIEW.
9. Make sure the tube is exactly above the middle of the scale load cell.
10. Turn the regulation knob counterclockwise until the Monidrop displays a value of 100 mL/h for 10 seconds.
11. Start saving the LabVIEW data.
12. Let the experiment run for a minimum of 60 minutes without additional actions.
13. Stop the LabVIEW script.
14. Close the ball valve.
15. Put the DropAdjust in 'Open'-mode.
16. Mark the used part of the tube, let it recover for 10 minutes and shift it so a new run (N) on a new tubing part can be started.
17. Repeat steps 5-16 for four times (N=4).

Measurement protocol pilot DropAdjust experiment

Conventional roller clamp

1. Execute the earlier mentioned list of 'measurement preparations' of Appendix E.
2. Attach the conventional roller clamp (Figure 63).
3. Set the offset of the pinching load cell in LabVIEW.

4. Set the loop time to 6000ms.
5. Open the ball valve.
6. Turn the roller clamp wheel towards the tube until no fluid is entering the drip chamber.
7. Fill the reservoir with 7 litres of (recycled) purified water; up to the marking on the reservoir.
8. Empty the measuring cup and set the offset of the scale load cell in LabVIEW.
9. Make sure the tube is exactly above the middle of the scale load cell.
10. Turn the roller clamp wheel away from the tube until 21 mL/h is displayed on the Monidrop for 10 seconds.
11. Wait 15 minutes and again set the displayed value at 21 mL/h.
12. Start saving the LabVIEW data.
13. Let the experiment run for 6 hours.
14. Stop the LabVIEW script.
15. Close the ball valve.
16. Turn the roller clamp wheel away from the tube until there is no contact anymore.

DropAdjust

17. Attach the DropAdjust (Figure 38).
18. Repeat steps 5-16.

Additional Matlab results

Figure 84 shows an additional graph to support the results presented in Section 5.2.2.

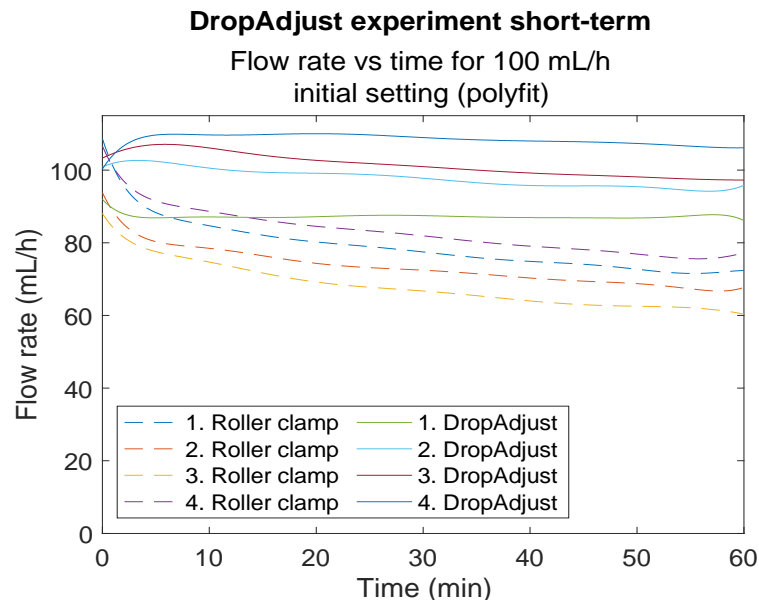


Figure 84 – DropAdjust experiment short-term: Flow rate [mL/h] versus time [min] at an initial setting of 100 mL/h using a roller clamp and the DropAdjust. The data of the roller clamp is coming from the contact area experiment.